REAL TIME LONG RANGE (LORA) BASED INDOOR POSITIONING SYSTEM USING DEEP GAUSSIAN PROCESS (DGP) ALGORITHM

NG TARNG JIAN

FACULTY OF ENGINEERING
UNIVERSITI MALAYA
KUALA LUMPUR

2025

Universiti Malaya

REAL TIME LONG RANGE (LORA) BASED INDOOR POSITIONING SYSTEM USING DEEP GAUSSIAN PROCESS (DGP) ALGORITHM

NG TARNG JIAN

DISSERTATION SUBMITTED IN FULFILMENT OF THE REQUIREMENTS FOR THE DEGREE OF MASTER OF ENGINEERING SCIENCE

FACULTY OF ENGINEERING
UNIVERSITI MALAYA
KUALA LUMPUR

2025

Universiti Malaya

UNIVERSITI MALAYA
ORIGINAL LITERARY WORK DECLARATION

Name of Candidate: Ng Tarng Jian
Matric No: 17181437/2
Name of Degree: Master Of Engineering Science
Title of Project ~~Paper/Research Report~~/Dissertation/Thesis ("this Work"):
Real Time LoRa Based Indoor Postioning System Using Machine Learning

Field of Study:
Engineering And Engineering Trades (Electronics And Automation)
I do solemnly and sincerely declare that:

(1) I am the sole author/writer of this Work;
(2) This Work is original;
(3) Any use of any work in which copyright exists was done by way of fair dealing and for permitted purposes and any excerpt or extract from, or reference to or reproduction of any copyright work has been disclosed expressly and sufficiently and the title of the Work and its authorship have been acknowledged in this Work;
(4) I do not have any actual knowledge nor do I ought reasonably to know that the making of this work constitutes an infringement of any copyright work;
(5) I hereby assign all and every rights in the copyright to this Work to the Universiti Malaya ("UM"), who henceforth shall be owner of the copyright in this Work and that any reproduction or use in any form or by any means whatsoever is prohibited without the written consent of UM having been first had and obtained;
(6) I am fully aware that if in the course of making this Work I have infringed any copyright whether intentionally or otherwise, I may be subject to legal action or any other action as may be determined by UM.

Date: 27/02/2025

Subscribed and solemnly declared before,

Witness's Signature Date: 27/02/2025

Name:

Designation:

Universiti Malaya

Real Time Long Range (LoRa) Based Indoor Positioning System Using Deep Gaussian Process (DGP) Algorithm

ABSTRACT

This thesis explores the development of a real-time LoRa-based indoor positioning system in industrial production lines. Recognizing the limitations of traditional GPS and other indoor positioning technologies, this research investigates the feasibility of LoRa and proposes a hybrid machine learning approach for accurate and reliable positioning. The study addresses challenges posed by signal fluctuations, non-line-of-sight propagation, and the need for continuous positioning estimation in dynamic environments. Through experimental evaluation and comparison of various machine learning algorithms, including Deep Gaussian Process (DGP) regression, the research demonstrates the effectiveness of DGPs in achieving precise single-point estimation, by keeping the mean absolute error to below 5 meters. Furthermore, the thesis introduces enhancement techniques such as Temporal-Weighted RSSI averaging, Kalman filtering, and lane constraints to improve the system's performance further. The experimental results, conducted in a real industrial environment, demonstrate that the proposed system achieves a mean absolute error of 1.58 meters and a root mean square error of 1.90 meters. These findings highlight the potential of combining LoRa technology with advanced machine learning algorithms and filtering techniques to achieve precise and reliable indoor tracking.

Keywords: Indoor Positioning System, LoRa, Machine Learning, Deep Gaussian Process, Continuous Positioning

Universiti Malaya

SISTEM PENENTUDUDUKAN DALAMAN MASA NYATA BERASASKAN LORA MENGGUNAKAN ALGORIMA PROSES GAUSSIAN MENDALAM

ABSTRAK

Tesis ini meneroka pembangunan sistem penentuan kedudukan dalaman bangunan berasaskan LoRa masa nyata dalam kawasan industri. Batasan daripada teknologi tradisional untuk penentuan kedudukan seperti GPS telah memberi ruang untuk penyelidikan kemungkinan penggunaan teknologi LoRa dalam sistem penentuan kedudukan dalaman bangunan dan mencadangkan pembelajaran mesin hibrid untuk penentuan kedudukan yang tepat. Kajian ini menangani cabaran yang ditimbulkan oleh turun naik isyarat, penyebaran bukan garis penglihatan, dan keperluan untuk anggaran kedudukan berterusan dalam persekitaran dinamik. Melalui penilaian eksperimen dan perbandingan pelbagai algoritma pembelajaran mesin, termasuk regresi Proses Gaussian Mendalam (DGP), penyelidikan ini menunjukkan keberkesanan DGP dalam mencapai anggaran titik tunggal yang tepat, dengan mengekalkan ralat mutlak purata di bawah 5 meter. Selain itu, tesis ini memperkenalkan teknik penambahbaikan bagi keputusan peruntukan kedudukan seperti purata RSSI berwajaran masa, penapisan Kalman, dan kekangan lorong untuk meningkatkan lagi prestasi sistem. Keputusan eksperimen, yang dijalankan dalam persekitaran industri sebenar, menunjukkan bahawa sistem yang dicadangkan mencapai ralat mutlak purata 1.58 meter dan ralat kuasa dua purata 1.90 meter. Penemuan ini menyerlahkan potensi penggabungan teknologi LoRa dengan algoritma pembelajaran mesin canggih dan teknik penapisan untuk mencapai penentuan kedudukan dalaman bangunan yang tepat.

Keywords: Sistem Penentuan Kedudukan Dalaman Bangunan, LoRa, Pembelajaran Mesin, Proses Gaussian Mendalam, Penentuan Kedudukan Berterusan

Universiti Malaya

ACKNOWLEDGEMENT

I would like to extend my heartfelt gratitude to my supervisor, Associate Prof. Dr. Narendra Kumar, for providing me with the invaluable opportunity to work under his guidance. His extensive knowledge and industry experience were pivotal in steering my research. I am also deeply appreciative of the chance he provided for me to collaborate with NXP Semiconductors Malaysia, which greatly enhanced my research journey.

My thanks also go to my co-supervisor, Dr. Mohamadariff bin Othman, for his unwavering support and consistent advice throughout my studies. I am especially thankful for his guidance during the publication process.

I am sincerely grateful to NXP Semiconductors Malaysia, for their role as an industrial collaborator. I would like to express my deepest appreciation to all the employees of NXP Semiconductors Malaysia, particularly those in the Test and Backend department, for their warm hospitality and assistance. Special thanks to Ms. Ong Lan Yit for her time, guidance, and support throughout this project. I would also like to acknowledge Sabrina, Chiah, Daniel Liew, Kumaran, Jesro, and other members of NXP Semiconductors Malaysia, who made my experience more enjoyable.

Lastly, I am profoundly thankful to my family for their unwavering support, motivation, and guidance throughout my studies and life. I am certain that I would not have reached this point without their sacrifices and encouragement.

To all those mentioned and to those whose names I may have unintentionally omitted, I offer my sincere thanks. Your contributions have been instrumental in the successful completion of this work.

Universiti Malaya

TABLE OF CONTENTS

Universiti Malaya

Universiti Malaya

Universiti Malaya

LIST OF FIGURES

Universiti Malaya

Universiti Malaya

Universiti Malaya

LIST OF TABLES

Universiti Malaya

LIST OF SYMBOLS AND ABBREVIATIONS

ANN	:	Artificial Neural Network
AP	:	Access Point
BLE	:	Bluetooth Low Energy
BPSK	:	Binary Phase Shift Keying
BS	:	Base Station
BSE	:	Bayes Static Estimation
CSS	:	Chirp Spread Spectrum
DNN	:	Deep Neural Network
DT	:	Decision Trees
DGP	:	Deep Gaussian Process
DGPR	:	Deep Gaussian Process Regression
DFC	:	Dynamic Fingerprinting Combination
ERP	:	Enterprise Resource Planning
FHSS	:	Frequency-Hopping Spread Spectrum
GFSK	:	Gaussian Frequency-Shift Keying
GNSS	:	Global Navigation Satellite System
GPS	:	Global Positioning System
GP	:	Gaussian Process
GPR	:	Gaussian Process Regression
ISM	:	Industrial, Scientific, and Medical
IoT	:	Internet of Things
IPS	:	Indoor Positioning System
KNN	:	k-Nearest Neighbour
KF	:	Kalman Filter

Universiti Malaya

LC	:	Lane Constraint
LOS	:	Line-of-Sight
LPWAN	:	Low-Power Wide Area Network
LSTM	:	Long Short-Term Memory
MAE	:	Mean Absolute Error
MAC	:	Media Access Control
MIMO	:	Multiple-Input Multiple-Output
MLP	:	Multi-Layer Perceptron
NB-IoT	:	Narrowband Internet of Things
NFC	:	Near-Field Communication
NLOS	:	Non-Line-of-Sight
NN	:	Nearest Neighbour
PKF	:	Point Kalman Filter
RF	:	Random Forest
RFID	:	Radio Frequency Identification
RMSE	:	Root Mean Square Error
RNN	:	Recurrent Neural Network
RSSI	:	Received Signal Strength Indicator
RTLS	:	Real-Time Location System
RToF	:	Round Trip Time of Flight
SVD-LS	:	Singular Value Decomposition-Least Squares
SVD-MV	:	Singular Value Decomposition-Minimum Variance
SF	:	Spreading Factor
Seg-NN	:	Segmentation Nearest Neighbour
SVM	:	Support Vector Machine
ToA	:	Time of Arrival

Universiti Malaya

ToF	:	Time of Flight
TDoA	:	Time Difference of Arrival
TWA	:	Temporal-Weighted Average
UWB	:	Ultra-Wideband
WKNN	:	Weighted k-Nearest Neighbour

Universiti Malaya

CHAPTER 1: INTRODUCTION

1.1 Background

In recent years, the concept of smart factory and digital manufacturing has emerged as a transformative paradigm in the industrial landscape. Digital manufacturing includes aspects such as smart networking, flexibility, mobility and interoperability of industry (Barreto et al., 2017). Handling and logistics controls of products are designed as a part of digital manufacturing (Holmström et al., 2017). In the age of Industrial 4.0, traceability, transparency (supply chain visibility), integrity control (incurring the right cost by considering appropriate time, place. quantity, and condition), robustness, agility, resilience and flexibility are the important aspects that needed attention when designing a logistic system (Kirch et al., 2017). The integration of digital technologies in manufacturing is revolutionizing traditional production methods, leading to improved productivity, streamlined workflows, and data-driven decision-making.

Despite the remarkable benefits of smart factories and digital manufacturing, companies still rely on Enterprise Resource Planning (ERP) systems and manual processes to manage their resource flow. ERP systems have long served as the backbone of operational management, facilitating data integration, resource planning, and process coordination. Despite their ability to standardize operations, ERP systems frequently struggle with agility and adaptability in manufacturing due to customization challenges, slow real-time data processing, and reliance on workarounds when responding to dynamic production demands (Yılmaz Börekçi et al., 2020). Moreover, reliance on manual processes can introduce inefficiencies and increase the likelihood of errors. Human intervention in data entry, process monitoring, and quality control can be time-consuming and prone to inaccuracies, leading to delays, disruptions, and quality issues in the production line. An accurate indoor positioning system provides both management and operators with clear visibility of ongoing operations and assets' positions.

Universiti Malaya

Indoor positioning plays a pivotal role in meeting this demand by providing real-time and precise location information within the spaces of the manufactory. The importance of indoor positioning in manufacturing floors rests in its capacity to support an extensive variety of crucial applications. Asset monitoring makes it possible to quickly locate finished goods, work-in-progress items, and raw materials, reducing manufacturing delays and improving supply chain management. Personnel tracking maximizes personnel deployment to increase productivity while also enhancing safety by keeping track of workers' presence in forbidden or dangerous areas. The use of equipment tracking guarantees effective maintenance programs, which save downtime and increase the life of important machinery.

The reliance on indoor positioning system (IPS) solutions has grown due to the limitations of traditional outdoor-based positioning technologies, the Global Navigation Satellite System (GNSS) (Manzoni et al., 2019) such as GPS (https://www.gps.gov/), GLONASS (https://www.glonass-iac.ru/en/), Galileo (https://www.usegalileo.eu/) or BeiDou (http://en.beidou.gov.cn/) system. GNSS is well-established for outdoor positioning and can be used in most outdoor environments. GNSS systems give sub-meter accuracy but they cannot well work indoors as GNSS systems require a distinctive line of sight (LOS) between satellites and device (Henriksson, 2016). Moreover, GNSS devices used are more complex, costly and power inefficient (Manzoni et al., 2019).

Therefore, various technologies are being researched and implemented for indoor localization. Primarily some widely used technologies are WiFi, Bluetooth, ZigBee, RFID, UWB, Visible Light, Acoustic Signals and ultrasound (Zafari et al., 2019). In order to determine the target positions, several parameters are utilized (Kim Geok et al., 2020). The fundamental parameters used in indoor positioning systems are Received Signal Strength Indicator (RSSI), Time of Arrival (ToA) and Angle of Arrival (AoA).

Universiti Malaya

Furthermore, Time Difference of Arrival (TDOA), Round Trip Time (RTT), Angle Difference of Arrival (ADOA), Phase of Arrival (POA), Phase Difference of Arrival (PDOA) and Channel State Information (CSI) are used to overcome improve accuracy and reduce complexity. These signal characteristics alone do not define the position estimates. Hence, the parameters have to be fitted into positioning algorithms to define the location coordinates (Kim Geok et al., 2020). Positioning algorithms can be classified by four basic aspects distance-based, direction-based, connectivity-based and signal-based.

The rise of the Internet of Things (IoT) (Zafari et al., 2019) has brought much attention to researching indoor localization using low power IoT devices. Low-power wide-area networks (LPWANs) are an emerging technology due to their characteristics of low power consumption and low bandwidth (Islam et al., 2017). These characteristics are a perfect fit for IoT data traffic which requires a high number of devices with low data rates and deep penetration of signals in noisy urban environments (Gu et al., 2018). The low power and long range characteristics of LPWANs have attracted much attention in the field of indoor positioning systems such that mobile tags can operate using batteries without a static power supply and reduce infrastructure costs by decreasing the number of access points.

LoRa was chosen as the positioning technology in this research due to its relatively open ecosystem among other LPWANs such as Sigfox and NB-IoT. LoRa defines the physical layer technology functioning in the sub-GHz band, operating in a frequency band less than 1 GHz (923 MHz, 915 MHz, 433 MHz), which is widely used in numerous IoT applications including smart metering, smart parking, road traffic monitoring, environment monitoring, street lighting, facility management, waste management, and precision agriculture (Islam et al., 2019). LoRa's long-range communication capability

Universiti Malaya

minimizes the need for dense deployment of access points or beacon nodes. Just a small amount of LoRa gateways is needed to cover a large area (Gu et al., 2018). LoRa is robust against multipath, Doppler effect and interference on account of its unique Chirp Spread Spectrum (CSS) Modulation scheme (Islam et al., 2017) which makes it a strong competitor for being an indoor positioning technology.

Due to the robust conditions in indoor environments, fingerprinting technique has gained much attention in the field of indoor positioning systems. The fingerprinting technique collects radio characteristics and produce radio maps. In the online phase, radio signals are matched to the radio map to predict the locations of the object. To further improve the accuracy of conventional fingerprinting method, deep learning methods such as Artificial Neural Network (ANN) (Belmonte-Hernández et al., 2019), Recurrent Neural Network (RNN) (Pichaimani & Manjula, 2022) and Deep Gaussian Processes (DGP) (Wang et al., 2020) are used. They can learn the underlying patterns and relationships within these fingerprints, enabling them to predict the location of the object even in areas with slightly different signal characteristics.

This thesis delves into the implementation of indoor positioning system with LoRa technology, employing RSSI-based fingerprinting method with a hybrid machine learning approach. DGP, a machine learning technique that learns complex relationships between the signal fingerprints and actual locations was leveraged for static point estimation. This allows more precise positioning in challenging locations such as non-line-of-sight (NLOS) and non-linear positions. Furthermore, we incorporate a maximum distance filter in correlation to time to eliminate outliers and enhance the reliability of position estimates. Additionally, a lane correction method is implemented to correct the position of the trolleys and ensure accurate positioning within production lines.

Universiti Malaya

1.2 Problem Statement

The problems to be addressed by this study are as followed:

1. Traditional methods like GPS are ineffective indoors due to signal attenuation and multipath interference, while existing technologies like WiFi, BLE, and UWB have drawbacks related to accuracy, scalability, and cost-effectiveness. This necessitates the investigation of alternative technologies, such as LoRa, for its long range and robustness against multipath, to address these limitations and enable efficient and reliable indoor positioning in industrial settings.
2. The dynamic and complex nature of industrial production lines presents significant challenges for achieving accurate and reliable indoor positioning using LoRa technology. Signal fluctuations, often caused by moving machinery and equipment, can lead to inconsistent and unreliable RSSI measurements. NLOS propagation, due to obstacles and the layout of production lines, can further degrade the accuracy of position estimates. These challenges collectively impact the performance and effectiveness of LoRa-based positioning systems, hindering their widespread adoption in industrial applications.
3. While existing research on LoRa-based indoor positioning has demonstrated its feasibility, there remains a gap in addressing the challenges of continuous positioning estimation for objects in movement within complex industrial environments. The focus has primarily been on single-point estimation, which does not fully capture the dynamic nature of objects within production lines.

Universiti Malaya

1.3 Research Objectives

The research aims to explore the potential of an accurate LoRa-based indoor positioning system in industrial production line. This research will focus on the following objectives.

1. To investigate the feasibility of implementing a LoRa-based indoor positioning system as an alternative to conventional methods in the industrial production line.
2. To evaluate and compare the effectiveness of different machine learning algorithms, particularly focusing on the potential superiority of Deep Gaussian Process (DGP), for accurate and reliable single-point estimation using LoRa technology by assessing positioning mean absolute error of below 5 meters.
3. To develop and implement a novel hybrid approach for LoRa-based indoor positioning that combines single-point estimation with enhancement techniques, addressing the gap in existing research and enabling accurate tracking of objects in movement within complex industrial environments by achieving a mean localization accuracy of less than 2 meters and 90^{th} percentile error of 5 meters.

1.4 Novelty and Contributions

The following list portrays the novelty and contributions of this research.

1. Demonstrated the feasibility of LoRa technology for indoor positioning in dynamic industrial environments.
2. Unlike many existing studies, this research specifically focuses on positioning in dynamic industrial environments with moving objects.
3. The proposed system uniquely combines LoRa technology with a hybrid approach of a two-layer Deep Gaussian Process Regression model together with spatial-temporal enhancement techniques achieving high positioning accuracy.

Universiti Malaya

1.5 Thesis Outline

The subsequent chapters of this thesis are organized to provide a comprehensive and detailed exploration of the research topic. Here's a brief overview of the chapters:

Chapter 2, Literature Review offers a thorough examination of existing research on indoor positioning systems, with a particular emphasis on LoRa-based solutions. It delves into various techniques, algorithms, and methodologies employed in the field, highlighting their strengths and limitations. The chapter also explores the application of machine learning and deep learning techniques for enhancing positioning accuracy.

The following chapter, Methodology, outlines the research methodology adopted for the study. It details the experimental setup, including the selection and configuration of hardware components, the design of the testbed, and the data collection process. The chapter also describes the data preprocessing steps undertaken to ensure data quality and prepare it for analysis. Moreover, the chapter discuss the adaptation of various machine learning techniques for single point estimation. Besides that, the chapter elaborates on the DGP architecture, model design, hyperparameter selection, and training process. To further enhance the accuracy of single-point estimation, several techniques were explored.

The Results and Discussion chapter presents the experimental results obtained from the implementation of the LoRa-based indoor positioning system. It evaluates the performance of different machine learning algorithms for single-point estimation and assesses the effectiveness of the proposed hybrid approach for continuous positioning estimation. The chapter also discusses the accuracy, reliability, and limitations of the implemented system, drawing insights from the experimental findings.

Finally, the Conclusion and Future Work chapter summarizes the key contributions of the research, highlighting the achievements and insights gained from the investigation of

Universiti Malaya

LoRa-based indoor positioning. It also discusses potential avenues for future research, identifying areas where further improvements or extensions can be made to enhance the system's performance or applicability.

Universiti Malaya

CHAPTER 2: LITERATURE REVIEW

An indoor positioning system (IPS) is a system that obtains a device or user location in an indoor environment or setting. The wide-scale adoption of mobile devices with wireless communication capabilities have made the localization and tracking of devices possible and with ease. Real world applications of the indoor positioning system are many and are mainly used by smart homes (Kim et al., 2021), museums (Dahlgren & Mahmood, 2014), healthcare centres (Dahlgren & Mahmood, 2014), shopping malls, parking lots (Anjum et al., 2020) and warehouses (Batalla et al., 2020; Silva et al., 2021) .

Presently, the most popular real-time location system (RTLS) is the Global Navigation Satellite System (GNSS). GNSS is well established for outdoor environments mainly used for vehicle navigation and missile guidance. However, GNSS does not work well indoors due to a lack of distinct line-of-sight (LOS) between the device and satellites(Henriksson, 2016). For that reason, it has attracted attention of the academia to research on simple, low-cost design indoor positioning systems that can provide accurate localization in the indoor environments. However, indoor signal patterns are more complicated than those in outdoor environment due to fading, reflecting, multipath and deep shadowing effect (Kim Geok et al., 2020). Therefore, a variety of technologies and positioning techniques were introduced to minimize the effect of the robust signal characteristics. Moreover, indoor positioning systems should be evaluated in terms of cost, availability, energy efficiency, reception range, tracking accuracy and scalability (Hayward et al., 2022).

2.1 Indoor Positioning Technologies

Positioning technologies can be categorized into non-radio-based positioning and radio-based positioning. As in Figure 2.1, Non-radio-based positioning includes infrared, ultrasound, audible sound, magnetic, vision, visible light and dead reckoning (Sakpere et

Universiti Malaya

al., 2017). Meanwhile, radio-based technologies for indoor positioning comprises of WiFi, Bluetooth, RFID, UWB, NFC, cellular, and low power wide area network (LPWAN) technologies namely, LoRa and Sigfox (Zafari et al., 2019).

Most non-radio-based positioning such as light-based and sound-based systems are short and medium range communications. They have high accuracy in room-level localization but does not perform well in non-line of sight (NLOS) conditions due to low penetration through walls. Hence, more beacons or receivers would be needed to improve accuracy in large scale application.

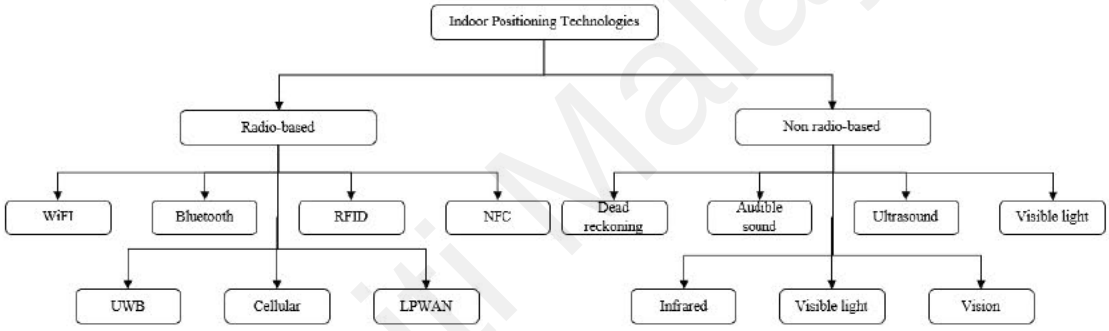

Figure 2.1: Types of indoor positioning technologies.

2.1.1 Radio-based Positioning Technology

Radio-based positioning system is the positioning technology that utilizes radio frequency signals and infrastructures to determine the position of a person or object for tracking and navigation purposes. Radio-based positioning is widely used and studied as a result of its ability to penetrate walls and obstacles leading to a wider coverage area (Sakpere et al., 2017).

WiFi, also known as the IEEE 802.11 standard, operates in the Industrial, Scientific, and Medical (ISM) band and is widely used for providing networking capabilities in private, public and commercial environments. WiFi operates on the 2.4GHz and 5.0GHz spectrum and with typical channel widths of 20MHz, 40MHZ and 80 MHZ. WiFi

Universiti Malaya

positioning is popular due to the common use of WiFi-enabled mobile devices such as smartphones and laptops and also presence of existing infrastructure would reduce the cost and complexity of deployment (Mendoza-Silva et al., 2019).

Bluetooth (or IEEE 802.15.1) consists of the physical and MAC layer specifications for connecting different fixed or moving wireless devices within a certain personal space. The latest version of Bluetooth is Bluetooth Low Energy (BLE). Most of the BLE based localization techniques were based on RSS based inputs as they are less complex. Due to medium communication range of BLE, number of beacons is needed for a large scale deployment (Mendoza-Silva et al., 2019). BLE is often chosen in indoor positioning systems because of its small, low cost, low complexity and low energy consumption compared to other technologies (Kim Geok et al., 2020).

Recent study suggest combination of WiFi and BLE can improve localization accuracy. (Molina et al., 2018) concluded that Wi-Fi alone is insufficient for precise indoor location tracking. While it can provide reasonable estimates in specific areas, its accuracy deteriorates significantly in large spaces with dynamic conditions, often requiring manual adjustments. To enhance location precision and mitigate the impact of fluctuating signal strengths, it's crucial to integrate additional technologies like Bluetooth Low Energy (BLE) and GPS, when feasible.

Ultra-Wideband (UWB) is an attractive technology in indoor localization for its immunity to interference from other signals due to its drastically different signal type and radio spectrum. The short pulse with time period of lesser than 1 nanosecond (ns) over a large bandwidth (>500MHz) make them less sensitive to multipath effects, allowing accurate position estimation in the time domain. UWB also has relatively low power consumption due to its low duty cycle. It has been shown that UWB can achieve localization accuracy up to 10cm (Zafari et al., 2019). Despite offering high precision,

Universiti Malaya

UWB's technology is incompatible with current standards, hindering its widespread public adoption. Furthermore, the high cost of implementing UWB infrastructure on a large scale due to increase in UWB sensors deployment presents a significant barrier to its broader use. (Sakpere et al., 2017).

Radio Frequency Identification (RFID) is one of the commonly used technologies for indoor positioning. There are two basic types of RFID systems, passive RFID and active RFID. Passive RFID do not have their energy source, the detection range is short (1-2m), and receivers require external high power supply. Hence, it is generally used in geo-fencing applications and not suitable for large scale localization. On the other hand, active RFID operate in the Ultra High Frequency (UHF) and microwave frequency range. The characteristics of active RFID having a reasonable range, low cost and can be easily embedded in the tracking objects makes it a reasonable choice for localization and object tracking. However, the active RFID technology cannot achieve sub-meter accuracy and it is not readily available on most portable user devices (Zafari et al., 2019). Moreover, random moving objects in the domain can reduce its accuracy due to multipath effect and signal fluctuations. (Kim Geok et al., 2020).

2.1.2 LPWAN Positioning Technology

The rise of internet of things (IoT) has supported the research of LPWANs in the field of indoor localization. LPWAN has the following advantages, long range, low power consumption, low cost, massive connections and communication capability. Some of the popular LPWANs are NB-IoT, LTE-M, LoRaWAN and Sigfox (Li et al., 2020).

NB-IoT and LTE-M follows the 3GPP standard and fall in the licensed LTE frequency band. Hence, the base stations and network are deployed by telecommunication operators. They have the advantage of having operator-level security and quality assurance.

Universiti Malaya

However, it is difficult for independent companies to setup their own private network. (Li et al., 2020).

Sigfox uses the 862-928 MHz ISM band and has a bandwidth of 100Hz and data rate of 600bps. Given its low bandwidth and data rate, it can accommodate 1 million nodes per gateway. Sigfox uses a proprietary Ultra Narrow Band (UNB) radio technology and binary-phase-shift- keying (BPSK) based modulation. By using UNB radio, the noise floor is reduced compared to classical narrow, medium or wideband systems. However, it is not recommended for real-time localization because of its limitations in messages per day and high latency time. Besides, the narrowband nature makes Sigfox radio susceptible to multipath and fast fading.

LoRaWan is an open Medium Access Control (MAC) protocol which is built on top of the LoRa physical layer. Typical LoRaWan bandwidth values are 125, 250 and 500kHz. LoRa is unique compare to other IoT technologies for the use of Chirp Spread Spectrum (CSS) modulation scheme, a spread spectrum technique where the signal is modulated by frequency varying sinusoidal pulses, which provides resilience against multipath, interference and Doppler effect, making LoRa a preferable technology for localization (Zafari et al., 2019).

Table 2.1 summarizes the advantages and disadvantages of radio-based positioning technology together with positioning metrics, range, power consumption, accuracy and cost.

Universiti Malaya

Table 2.1: Summary and comparison of radio-based indoor positioning technologies

Technologies	Range	Power consumption	Accuracy	Cost	Advantages	Disadvantages
WiFi	35 m	Medium	Low	Medium (Very low if using deployed infrastructures and smartphones)	No extra hardware Easy deployment Cover large regions	Time-varying RSS Accuracy depends on number of access points
Bluetooth	10 – 20 m	Very Low	Low	Low	Low power Easy deployment Small size	Requires extra hardware Prone to noise Interference with the same frequency band Require large number of access points to achieve better accuracy
UWB	10 – 20 m	Medium	High	Medium	High accuracy Negligible effect from interference and multipath	Needs extra hardware Short range, high cost Challenges in NLoS
RFID	200 m	Low	Low	Medium	Larger range than WiFi and BLE Medium power consumption	Needs extra hardware Multipath and signal fluctuations Large error with more target tags to locate
LoRa	20 km	Very Low	Low	Low	Low power Covers large area	Needs extra hardware Signal attenuation and multipath
Sigfox	40 km	Very Low	Low	Low	Low power Covers large area	Needs extra hardware Signal attenuation and multipath

Universiti Malaya

2.2 Indoor Positioning Techniques

Generally, indoor positioning techniques can be identified as two classes: range-based and range-free. Range-based techniques use distance or angle estimates such as Received Signal Strength Indicator (RSSI) (Anjum et al., 2020), Time of Arrival (ToA) (Ha et al., 2019), Time Difference of Arrival (TDoA) (Azmi et al., 2018), and Angle of Arrival (AoA) (Kułakowski et al., 2010) as the basis of calculation. However, range-free techniques use connectivity information between nodes and landmarks.

TOA calculates the distance between transmitter and receiver by taking account of the propagation time using the speed of light formula $c = 3 \times 10^8$ m/sec. A minimum of three reference nodes is used to estimate the coordinate of the device. TOA provides high accuracy but the require high cost and complexity of hardware because precise time synchronisation and high resolution timestamp is needed to obtain the accurate results.

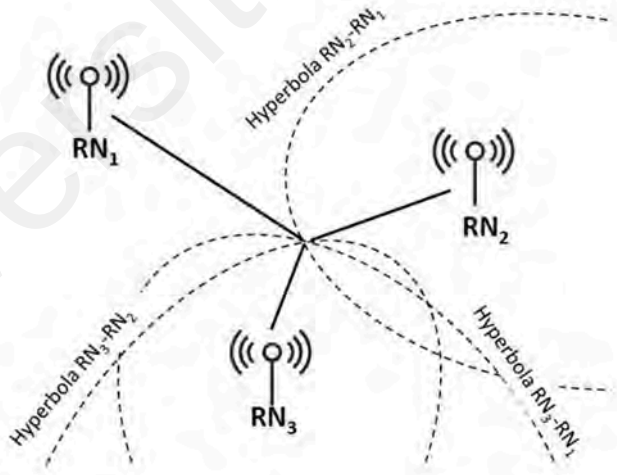

Figure 2.2: TDOA positioning method.

(Zafari et al., 2019)

TDOA is developed to mitigate the need for complex hardware required for TOA. TDOA applies the flight-time difference to a radio wave by comparing TOA at two

Universiti Malaya

different sensors and thus the absolute TOA is not needed (Laaraiedh et al., 2011; Sakpere et al., 2017). Figure 2.2 shows the TDOA positioning technique.

AoA estimates the position of the target object by calculating the angle and distance and the intersection of direction lines between two or more reference points. AoA use antennae arrays to estimate the angle at which the transmitted signal impinges on the receiver. AoA can provide accurate location estimation when transmitter-receiver distance is small or in room level. However, in NLOS conditions AoA performs poorly. Moreover, more complex hardware and precise calibration is needed. Figure 2.3 depicts how angles of signals received by antenna array reflects to user location.

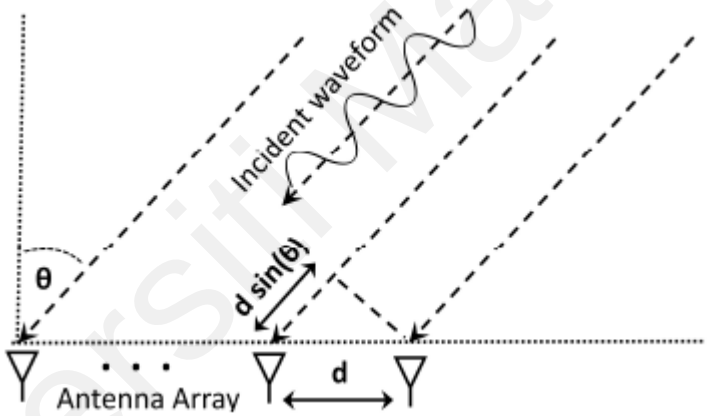

Figure 2.3: AoA based positioning.

(Zafari et al., 2019)

RSSI uses the measured signal strength intensity at the receiver side. RSSI method is popular in position tracking as the implementation is much easier comparing to ToA or TDoA which requires clock synchronisation between devices or AoA that needs special and costly antennas. However, in indoor environment RSS is greatly affected by multipath and shadowing henceforth is relatively inaccurate. RSSI uses a simple path-loss propagation model to calculate the distance between transmitter and receiver. The

Universiti Malaya

log-distance path loss model relates the received signal power $P_r(d)$ at distance d from the transmitter to the transmitted power P_t as equation 2.1:

$$PL(d) = P_t - P_r(d) = PL(d_0) - 10n\, log_{10}\left(\frac{d}{d_0}\right) + X_\sigma \quad \textbf{(2.1)}$$

where n is the path loss exponent, d_0 is a reference distance, and X_σ is a zero-mean Gaussian random variable (in dB) with standard deviation σ that models the shadowing effect.

The position of the object can then be calculated by using trilateration, multilateration, min-max and maximum likelihood algorithms. RSSI is susceptible to noise and multipath effects which significantly decreases its localization accuracy (Kim Geok et al., 2020). Table 2.2 summarises advantages and disadvantages of the positioning techniques.

Table 2.2: Summary of different positioning techniques

Positioning technique	Advantages	Disadvantages
ToA	Provide high accuracy Does not require fingerprinting	Require precise time synchronisation and high resolution timestamps LoS is needed for accurate performance Difficult to implement in narrow bandwidth
TDoA	Does not require time synchronisation between device and received nodes	Require high resolution timestamps Difficult to implement in narrow bandwidth Time synchronisation required between received nodes
AoA	Can provide high localization accuracy in room level	High device complexity with multiple directional antennas Performance deteriorates with increase in distance between transmitter and receiver
RSSI	Easy to implement Cost efficient	Prone to multipath, fading and noise Lower localization accuracy

Universiti Malaya

2.3 LoRa-based Positioning System

2.3.1 LoRa Physical Layer

LoRa defines the physical layer technology that offers long distances low data rate wireless communication with low power consumption (Islam et al., 2017). It functions in the sub 1 Gigahertz band which are 433MHz (in Asia), 868MHz (in Europe) or 916MHz (in America) license-free ISM bands.

According to Gu et al. (2018), LoRa-based positioning systems offer several advantages compared to other wireless technologies. Firstly, LoRa's long-range communication capability minimizes the need for dense deployment of access points or beacon nodes. Just a small amount of LoRa gateways is needed to cover a large area. Moreover, LoRa working at sub-gigahertz frequencies and unique modulation scheme reduces the constrain of LOS communication, attenuation from walls and obstacles and interference (Manzoni et al., 2019).

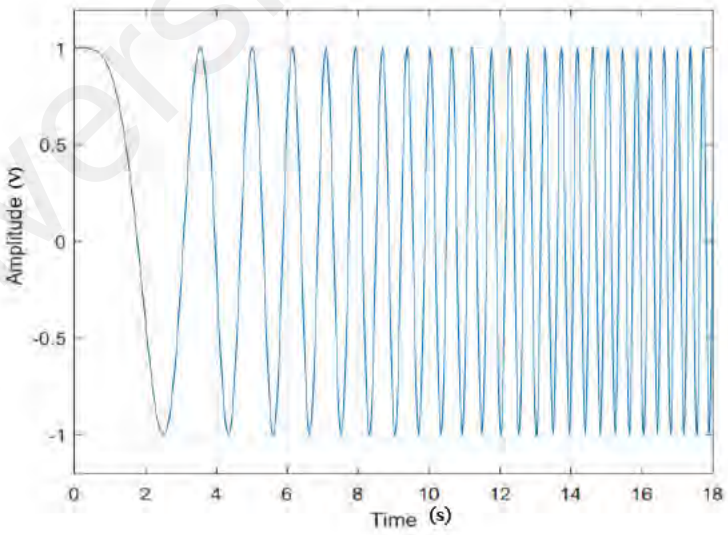

Figure 2.4: LoRa CHIRP spread spectrum modulation waveform. (Henriksson, 2016)

The LoRa physical layer utilizes a special type of spread spectrum modulation technique known as CHIRP Spread Spectrum (CSS). Information is encoded as frequency

chirps (frequency varying sinusoidal pulses) to improve its robustness against signal loss particularly interference, such as Doppler effect and multipath fading (Islam et al., 2017). These chirps have chip rates equivalent to the spectral bandwidth of signals, typically 125, 250 or 500kHz of bandwidth. Figure 2.4 shows the visualisation of the up chirps used in LoRa modulation. To further mitigate interference, Frequency-Hopping Spread Spectrum (FHSS) scheme is used. FHSS switches available channels according to pseudo-random distribution.

Each symbol is encoded with 2^{SF} chirps, where SF is the spreading factor. SF sits in the range of between 7 to 12, chirps with different values of SF are orthogonal to each other, so multiple data packets can be sent in parallel by using different values of SF. The higher the spreading factor value, the longer the time for each symbol transmission and produce farther communication range.

2.3.2 Feasibility of LoRa Positioning

Islam et al. (2017) has discussed the feasibility of LoRa for indoor localization. WiFi and Bluetooth Low Energy (BLE) were chosen as the comparison baselines because of their popularity in indoor positioning and low power consumption. The author compared the stability of the three technologies in terms of variance, median, mean and mode of their RSSI. LoRa has a lower variance compared to WiFi and BLE. Furthermore, LoRa shares similar behaviour with WiFi in terms of median and mean but LoRa outperforms WiFi in mode comparison. The author also did ranging tests in both line of sight (LOS) and non-line of sight (NLOS) conditions. Mean errors of 1.19 m in LOS and 1.72 m in NLOS were obtained respectively by using unfiltered RSSI values.

The author did a continuation of the research in (Islam et al., 2019). The comparisons between the three technologies were done in different test environments, long corridor (23 m), open room (25 m x 23 m), single floor (25.29 m with four rooms of different sizes)

Universiti Malaya

and multiple floor (four and eight stories). LoRa outperforms WiFi and BLE in terms of wireless coverage, stability, path loss trend, cost and power consumption. Therefore, LoRa is a feasible choice for indoor positioning systems especially for large spaces such as warehouses and multi-storeyed buildings.

Podevijn et al. (2018) preferred BLE over LoRa due to its lower cost and averaging capabilities. However, the results obtained were not satisfying as a median accuracy of 15m was obtained in a 69 m x 69 m environment. (Sadowski & Spachos, 2018) compared indoor positioning performance of WiFi, BLE, ZigBee and LoRaWan by applying trilateration within a range of 1 – 5 m. It was concluded that WiFi has the highest accuracy of 0.664m on average but with the most power consumption. BLE used the least amount of power. LoRaWan has the furthest transmission range but delivers the largest error of 1.19m. Therefore, optimisation in power consumption and positioning algorithm has to be done in order to have a well-performing LoRa-based positioning system. (Committee, 2018) mentioned that Kalman filtering of noisy data can improve localization performance.

Anjum et al. (2019) investigates the potential of LoRa technology for indoor positioning using RSSI fingerprinting. The study involves real-world testing in both unobstructed (LOS) and obstructed (NLOS) environments to optimize LoRa packet settings for accurate distance estimation based on signal strength. To enhance positioning precision, environmental factors are considered. The researchers conducted extensive experiments across different LoRa spreading factors, analysing signal attenuation (path loss exponent) and signal variability (shadowing) in each environment.

Khan et al. (2021) compared LoRaWAN with WiFI and BLE in three different environments, the graduate lab (24 x 24 square feet), corridor (23 x 23 square feet) and classroom (50 x 30 square feet). RSSI (trilateration) is used to calculate the coordinates

Universiti Malaya

of a sensor node. The experimental results show that Wi-Fi produces the most accurate result with an average error of 0.54 m. LoRa came in second with an average error of 0.62 m and BLE is the show the lowest accuracy with an average error of 0.82 m. The authors propose LoRa as the best suited technology for indoor localization as it has significantly lower power consumption than WiFi although it has slightly lower accuracy.

Bornholdt et al. (2021) presents a multi-step-approach with a dynamic optimal algorithm selection for LoRaWAN networks with a modified stack for direct peer communication. To minimize the influence of measurement errors, the authors examined several filtering and compensation, and selection algorithms. A key benefit of this method is the reduced need for anchor nodes due to the LoRa transmitters' extended range. The relatively low initial and ongoing costs of LoRa transmitters make this approach attractive for large-scale applications where an accuracy of approximately ten meters is acceptable. The authors conducted a series of conducted experiments to demonstrate the potential of the proposed method.

Research on RSSI-based indoor positioning using LoRa in the license free 2.4 GHz band has been done in Simka and Polak (2022). Measurements are conducted in three different indoor environments hall, locker room and corridor, for different signal configurations of LoRa. The system demonstrated an average localization error of less than 2.2 meters. However, LoRa's localization accuracy is significantly influenced by factors such as signal configuration, node placement, and environmental conditions.

Aside from proving the feasibility of LoRa technology in indoor positioning, Marquez et al. (2023) studies the impact of body obstruction on communication links and, therefore , on the localization system in LoRaWAN. Results show that signal strength decreases by an average of 3 dB on links with body shadowing.

Universiti Malaya

Hence, machine learning methods are used to further enhance the accuracy in LoRa-based positioning. The following section will study different methods on improving the accuracy for LoRa-based positioning.

2.3.3 Case Study of LoRa-based Positioning System

Savazzi et al. (2019) used Weiner algorithm to achieve higher ranging and localization accuracy by combining RSSI values received for different LoRa modulation configurations. The experiment resulted in the best mean localization error of more than 10 m using all modes Weiner with seven anchors. The localization error is even higher when the number of anchors decreases. A localization error of more than 10 m is not satisfactory. Hence, the accuracy can be improved by selecting a subset of modes that has filter coefficients with maximum absolute values.

Lam et al. (2019) proposed positioning algorithms that reduce the non-Gaussian noise in LoRa networks by eliminating ill-performing anchor nodes or selecting anchor nodes that have higher confidence to be more accurate. In a large-scale indoor environment, Minimum MBRE and Density-based Clustering shows the best results with median localization error of 0.9821 m and 1.0895 m respectively. These two algorithms significantly improved the traditional Linear Least Squares which has a median localization error of 4.1823 m.

RSSI Fingerprinting combined with machine learning techniques is used by Anjum et al. (2020). RSSI fingerprints were collected and fitted into different models to develop RSSI-to-Distance functions. Among some methods used by the author are the path loss model, traditional regression model and modern machine learning models such as smoothing spline, support vector regression, decision trees and random forest. Then the obtained distances were fitted in a trilateration algorithm to obtain the position estimates. In indoor environments, smoothing spline achieved a mean error of 9.38 m and 91.92 %

Universiti Malaya

accuracy. The author proved the feasibility of LoRa positioning in an indoor environment, but the error has to be reduced in order for it to be applied practically.

Kim et al. (2021) confirms the feasibility of using LoRa-based technology for indoor localization in smart homes. The authors obtained a maximum error of 3.2 m and a standard deviation of below 25 cm of stationary objects by solely using trilateration. The authors suggested that the accuracy and precision can be further improved by using filtering techniques, more anchor nodes and fingerprinting method.

Lazaro et al. (2021) proposed an interesting topic and utilizing LoRa backscatters for localization. By using backscattering, the cost and power consumption of end user devices can be further reduced. However, the author only tested out for room-level localization and the experiment can be further researched by narrowing down the precision of position estimates.

In (Hu et al., 2022), the authors proposed LTrack, a long-range tracking system based on LoRa. This system consists of a mobile rotating anchor, a LoRa tag, and a commercial robot. Due to the limitations of LoRa devices to estimate AoA of signals, the authors designed a virtual circular antenna array in the mobile rotating anchor via a lightweight hardware modification to multiplex the only radio frequency channel in the low-cost LoRa device. To estimate the target AoA, the difference of time of flight (TDoF) measured in the circular antenna array is fused with the rotating orientation. They also redesigned and optimized the primitive LoRa ranging engine based on systematic analysis. Additionally, the researchers developed a real-time algorithm to track moving targets by utilizing Doppler frequency shifts, addressing the challenge of target movement-induced uncertainty. The experiments were done in both LOS and NOLS indoor scenarios. The experiment results shows that LTrack supports robust tracking with a median error of 0.12 m and 0.45 m in a 137 m^2 lab space and a 600 m^2 corridor, respectively.

Universiti Malaya

Chen et al. (2023) introduced a Kalman filter-based LoRa positioning algorithm adaptable to various environments. Implemented using the NS-3 network simulator, their approach significantly enhanced LoRa positioning accuracy. Simulation results demonstrated the effectiveness of the improved LoRaWAN module for diverse positioning scenarios and the substantial accuracy gains achieved through Kalman filtering. Table 2.3 summarizes the methodology and findings of the LoRa-based positioning systems case studies.

Table 2.3: Summary of Case Studies of LoRa-based Positioning Systems

Study	Methodology	Findings
Savazzi et al., 2019	Used Weiner algorithm to enhance ranging and localization accuracy by combining RSSI values from various LoRa modulation configurations	Achieved best mean localization error of >10m using all modes Weiner with seven anchors; error increased when fewer anchors were used
Lam et al., 2019	Proposed positioning algorithms to reduce non-Gaussian noise in LoRa networks	Minimum MBRE and Density-based Clustering achieved best results with median localization errors of 0.9821m and 1.0895m, respectively, significantly improving traditional Linear Least Squares (median error 4.1823m)
Anjum et al., 2020	Combined RSSI fingerprinting with machine learning techniques	Developed RSSI-to-Distance functions using various models; achieved mean error of 9.38m and 91.92% accuracy in indoor environments using smoothing spline
Kim et al., 2021	Confirmed feasibility of LoRa-based indoor localization in smart homes	Obtained maximum error of 3.2m and standard deviation <25cm for stationary objects using trilateration
Lazaro et al., 2021	Utilized LoRa backscatters for localization	Demonstrated potential for reduced cost and power consumption in end-user devices; focused on room-level localization
Hu et al., 2022	Proposed LTrack, a long-range tracking system with mobile rotating anchor and LoRa tag	Designed virtual circular antenna array and optimized LoRa ranging engine; used Doppler frequency shift for real-time tracking; achieved median error of 0.12m and 0.45m in a 137 m^2 lab and 600 m^2 corridor, respectively
Chen et al., 2023	Proposed multi-scene LoRa positioning algorithm based on Kalman filter	Implemented algorithm in NS-3 simulator; used Kalman filter to improve accuracy; showed improved accuracy with Kalman filter; validated algorithm in diverse scenarios using simulation

Universiti Malaya

2.4 Fingerprinting Technique

Fingerprinting is a popular localization method, especially where line of sight propagation is not typical. Fingerprinting technique has advantages of providing promising performance and also low hardware cost (Chen et al., 2013). This technique operates based on the concept of segmenting the map into grids, typically 1 meter squared per grid.

The fingerprint-based localization process is divided into two phases, training phase or "offline phase" and online phase(Dahlgren & Mahmood, 2014). The training phase creates a fingerprint database. At training phase, each grid cell has some unique attributes to break the symmetry among them. These attributes such as RSSI, IRR or LQ are measured and assigned to each grid cell. For example, RSSI is continuously sampled at each sampling point and the average is calculated.

In the second stage, the "online phase", the estimation of the actual position of the unknown node is performed. To locate the mobile node, the mobile node collects measurements of the same attributes stored in the database and compare the values in the fingerprints in the database.

2.4.1 Pattern recognition techniques in fingerprinting positioning

However, the collected signal in indoor propagation environments could be easily affected by diffraction, reflection and scattering in indoor. Multiple pattern recognition techniques are proposed for fingerprinting based positioning (Kim Geok et al., 2020), namely, probabilistic methods, k-nearest neighbour (KNN), support vector machine (SVM), Decision Trees (DT), Random Forest (RF), artificial neural networks (ANN), Gaussian Processes (GP) and Deep Gaussian Processes (DGP).

The probabilistic approach utilizes the decision rule based on the probability that the mobile node is in the estimated location by applying filters to the Gaussian distribution

Universiti Malaya

of the received signal vector. The HORUS WLAN location determination system (Youssef & Agrawala, 2005) is one of the most referenced positioning system using the probabilistic method. Given that S = (s_1, …, s_k) as recorded RSS vector, the estimated location x is computed by maximizing the probability P(x|S) as shown in equation 2.2.

$$argmax_x P(x|S) = argmax_x \frac{P(S|x) * P(l)}{P(S)} \quad \textbf{(2.2)}$$

Assuming P(S) remains stable for a long duration and consider it as a constant, P(S) is factored out from equation 2.3 and 2.4. By using Bayes.' Theorem, the equation is equivalent to,

$$argmax_x P(x|S) = argmax_x P(S|x) \quad \textbf{(2.3)}$$

$$argmax_x P(S|x) = argmax_x \prod_{i=1}^{k} P(s_i|x) \quad \textbf{(2.4)}$$

Bayesian Fusion (BF) is proposed by using both Bayes Static Estimation (BSE) and Point Kalman filter (PKF) estimation (Dahlgren & Mahmood, 2014). BF is experimentally proved to have higher accuracy compared to using solely BSE or PKF.

The KNN sampling uses the latest RSSI to search for k-closest matches of known location formerly stored in the database using root mean square errors principle. KNN first originated as a method for estimating the nearest location in RADAR,(Bahl & Padmanabhan, 2000). However, it does not work well with environmental changes. Weighted k-Nearest Neighbour (WKNN) is an extension of KNN where values are the values are weighted to improve accuracy and deal with simple environmental changes.

SVM is one of the most popular models in Machine Learning, capable of performing linear or non-linear classification, regression and outlier detection. SVMs are powerful algorithms that find a hyperplane in an N-dimensional space that distinctly classifies the data points. Hyperplanes are decision boundaries that assist in the classification of data

Universiti Malaya

points. The dimension of the hyperplane increases with the number of features. SVMs performs best for classifying complex but small or medium-sized datasets (Géron, 2019). However, SVMs would be computationally expensive for the classification of large datasets.

DT is an algorithm that has a tree-like structure, that split data into subsets based on attribute values. RF is an ensemble of DTs trained on different subsets of data and randomly chosen features. RF is more superior than DT because it is less susceptible to overfitting and more efficient when handling large datasets.

Artificial neural networks (ANNs) have emerged in recent years as a promising technique for indoor positioning due to their ability to model complex nonlinear relationships. Deep Neural Networks (DNN) (Xingli et al., 2018) are ANNs with multiple hidden layers between the input and output layers. Their hierarchical feature learning capability makes DNNs suitable for modelling ambiguous and spatially correlated for fingerprinting-based indoor positioning by a single or multi data sources. Recurrent Neural Networks (RNN) (Hoang et al., 2019) is a class of ANN, where the output results relies not only on current inputs but also on the preceding states. Hence, RNN can correlate user to its previous locations as the user is in movement and set predicted location estimates along a continuous trajectory. Long Short Term Memory (LSTM) (Sahar & Han, 2018) is an extension of RNN that resolves its limitations of inability to learn long-term temporal relationships due to the vanishing gradient problem.

GP have emerged as a promising technique for indoor localization due to their nonparametric Bayesian modelling capability to capture complex indoor radio signal propagation characteristics (Guan et al., 2021). Hence, it can interpolate to explored areas and model RSSI uncertainty. The GP comprises of two main components, the mean function and the kernel. The mean function defines the prior knowledge of the expected

Universiti Malaya

outputs and is assumed to be zero in most works. The kernel correlates the similarity between the inputs, in the context of indoor positioning, the kernel encodes the spatial correlations between locations.

DGP offers a powerful probabilistic nonparametric approach to address complex machine learning problems while quantifying uncertainty effectively. These DGPs are multilayer hierarchical extensions of GPs and share formal equivalence with neural networks featuring infinitely wide hidden layers. DGPs retain the advantageous properties of GPs, such as nonparametric modelling capabilities and well-calibrated predictive uncertainty estimates. Moreover, they overcome the limitations of single-layer GPs, which can only represent a restricted class of functions. Generally, DGPs are richer models just like how deep networks surpass generalized linear models. Instead of highly parameterized kernel-based models, DGPs learn a nonparametric representation hierarchy with minimal hyperparameter tuning. The structural advantages of deep models enhance learning quality, especially in intricate datasets associated with abstract information (Wang et al., 2020).

DGP can be represented by a graphical model with three different types of nodes, namely the leaf nodes, the intermediate latent nodes, and the parent nodes, as shown in Figure 2.5.

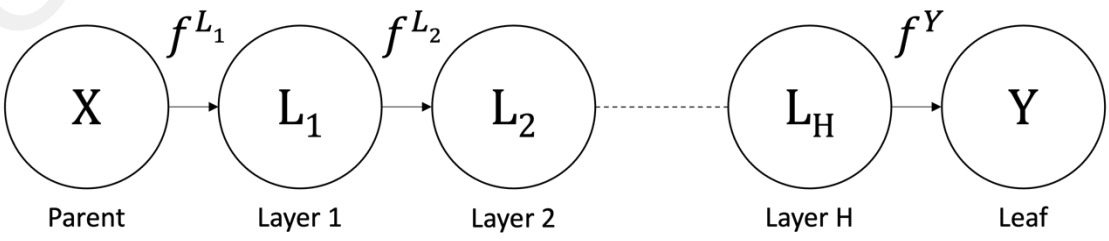

Figure 2.5: Deep Gaussian process model for RSSI radio map construction

The nodes at each layer has a input dimension of the output of the previous layer. In which where the parent node, $X \in \mathbb{R}^{N \times M}$, where N is the number of inputs and M is the

Universiti Malaya

number of input dimensions. The intermediate latent nodes $L_h \in \mathbb{R}^{N \times Q_h}$, where h = 1,2, …, H and H is the number of hidden layers and Q is the number of hidden dimensions for layer h. The leaf node is $Y \in \mathbb{R}^{N \times D}$, where D is the number of outputs. Each layer of the DGP is an individual GP function which can be formulated as equation 2.5.

$$L_{h_{nq}} = f_{q_h}^{L_h}(L_h) + \epsilon_n^{L_h}, where\ L_1 = X \quad \textbf{(2.5)}$$

$$Y_{nd} = f_D^{L_H}(L_H) + \epsilon_n^{L_H} \quad \textbf{(2.6)}$$

Such that $f_D^{L_h} \sim GP\left(\overline{L_h}, K^L\right)$ where K represents the kernel function.

The DGP process can be solved by log likelihood optimization by equation 2.7.

$$\log p(Y|X) = \log \int_{L_{H,X}} p(Y|L_H)p(L_H|L_{H-1}) \dots p(L_1|X) \quad \textbf{(2.7)}$$

2.4.2 Case Study of Indoor Positioning Using Fingerprinting Method with Machine Learning

Kodippili and Dias (2010) proposes fingerprinting technique as a pre-processing step. KNN (K=3) was used in this paper. Then, the distance between the Nearest Neighbours (NNs) and beacon node was calculated using the modified path loss model. Then the position of beacon node was estimated using trilateration. The proposed algorithm has an 44% improvement in accuracy compared to basic fingerprinting technique and is 73% better compared to basic trilateration technique.

Fang et al. (2011) proposes a dynamic fingerprinting combination (DFC) algorithm that improves mobile localization by weighting the spatial correlation dynamically from multiple location fingerprinting systems. The DFC algorithm reduces the risk of selecting poorly performing fingerprinting function. The DFC algorithm initially leverages the strengths of different fingerprinting methods to create a combined profile. Subsequently, it dynamically integrates the individual outputs based on the characteristics of the surrounding data points. DFC improves the positioning accuracy of base fingerprinting

Universiti Malaya

algorithms, including the Bayesian approach and a neural network model. The DFC was found out that it performs better than any individual fingerprinting approach. In addition, the results also demonstrated that the Bayesian approach performed better than the neural network.

Alraih et al. (2017) proposed a clustering algorithm to reduce computational time and radio map size. Fingerprinting technique was used to evaluate the performance of the proposed algorithm. Four WiFi Access Points (AP) were deployed in an area with dimension of 52 m x 22 m. The construction and materials of the building in the experiment were includes: the inner walls were made from plaster partition boards, whereas the outer walls were concrete and glass, and light wood doors with a small glass. The clustering algorithm outperformed the conventional method, reducing average distance error from 3.4 m to 2.4 m, representing a 41 % improvement in system accuracy.

Alhammadi et al. (2017) proposes a fingerprinting-based localisation algorithm with clustering technique (Signal space clustering algorithm) to estimate the user location. In the offline phase, calibration points are collected at certain places in floor to build a radio map. In the online phase, deterministic (KNN) and probabilistic Bayesian Network (BN) approaches are applied. The results have shown the proposed clustering technique has significantly reduced the size of radio map from 30 to 15 calibration points for both approaches. The accuracy in deterministic approach was slightly improved from 7.3 to 6.9 m while the probabilistic approach achieved a better average accuracy of 2.6 m.

Abdelghani and Qiang (2017) propose a hybrid algorithm that integrates KNN and Segmentation Nearest Neighbour (Seg-NN). The final estimated location will be the result of the algorithm that is closest to the previously estimated location. The mean error decreases from 83 m to 24 m after applying the hybrid algorithm. (Lu et al., 2016) exploits two algorithms adapting the singular value including a least squares estimation (SVD-LS)

Universiti Malaya

and a minimum variance technique (SVD-MV). SVD-MV reports a more powerful ability of noise reduction than SVD-LS. Under one meter accuracy, SVD-LS has 92.56 % whereas SVD-MV achieves 93.84 %.

Molina et al. (2018) integrates two different technologies (BLE and WiFi) to provide improved accuracy. Various configuration parameters are used: Positioning algorithm (WKNN), Maximum sample size, Missing MAC penalty, Candidate set size, Checks before hop, Distance algorithm, Distance algorithm arguments, and Filter sequence. The initial algorithm correctly identified the node in only 50 % of instances. To improve accuracy, three filter sequences were implemented. The refined algorithm achieved a success rate of 80% for correct node identification and 94 % for identifying an adjacent node. The resulting indoor service accuracy of approximately 5 meters surpassed the internal geolocation plugin's accuracy of around 10 meters.

Ji et al. (2021) proposes the building of a multivariable fingerprinting database by choosing ten 5G variables related to distance-power relationship. To utilize correlation among the multivariable fingerprints, Random Forest Variable Selection (RFVS) is used to sort variable importance and combinations. In three different experimental scenarios, five machine learning algorithms are used to calculate user equipment positions. Combined with RFVS, MLP shows 31.4 2%, 39.56 %, 30.54 % accuracy improvements for each respective room compared with that of only RSSI used.

Universiti Malaya

2.4.3 Case Study of Indoor Positioning Using Fingerprinting Method with Deep Learning

Teng et al. (2018) proposes an indoor positioning system that is based on the deep Gaussian process regression (DGPR) model. The nonparametric characteristics of the model and the need to measure part of the reference points, reduces time and cost for data collection. RSS values were converted into four types of characterizing values as input data and then predicts the position coordinates using DGPR model. Lastly, after reinforcement learning, the position coordinates are optimized. Several experiments were conducted which includes a simulated environment by MATLAB and in the physical environments at Tianjin University. The experiments examined positioning accuracy with different kernels and in different environments. The results showed that the proposed method achieve the results of average error of 2.28 m and maximum error of approximately 6 m.

Belmonte-Hernández et al. (2019) presents the framework SWiBluX, that integrates various technologies, WiFi, Bluetooth and Xbee technologies adopting fingerprinting for position estimation. The Neural Networks were used in combination with a novel Gaussian Outliers Filter (GOF) to improve the positioning accuracy for person tracking. The authors have compared positioning errors of several methods, deterministic and probabilistic methods, machine learning methods and deep learning methods. Deep Neural Network together with GOF, Weighted Combination and Particle Filter achieves the best result with average error of 45.41 cm.

Wang et al. (2020) propose the DeepMap system, that is the first, to construct radio maps and perform indoor localization using Deep Gaussian Process (DGP) model. The proposed DeepMap system can effectively overcome the drawbacks of the Gaussian process by generating detailed radio maps using sparse training data. The proposed

Universiti Malaya

system consisted of a two-layer deep Gaussian process model to regress the relationship between RSS samples and location. Then, the Bayesian training method is used that optimizes model parameters, and a Bayesian fusion method that boosts localization performance were designed. DeepMap achieves median error of 1.3 m and maximum error of 5.207 m as opposed to typical Gaussian Processes of 1.5 m and 6.182 m of median and maximum error respectively. Impact of number of inducing points, impact of latent nodes and impact of the number of iterations for initializing the variational distribution were also studied.

Guan et al. (2021) proposes DGP as a more informative alternative to GP for probabilistic positioning and points out the pitfall of using GP to model signal fingerprint uncertainty. In a office building, DGP produces mean error of 3.36 m compared to mean accuracy of 3.71 m by using GP. Whereas in a shopping environment, DGP produces a mean accuracy of 5.79 m while GP produces mean accuracy of 6.25 m. DGP also outperform GP in all percentiles.

Wang et al. (2021) present a geomagnetic indoor positioning algorithm based on the hierarchical LSTM. The system can jointly consider the short-term features such as divergences and anomalies as well as the long term features like the geomagnetic signal shape change characteristics to improve the position accuracy. Utilizing the advantage of LSTM which has strong learning ability on time series data, the authors utilize LSTM networks to extract temporal features. Implementing the hierarchical structure of LSTM networks enables the model to learn the short-term and long-term geomagnetic features.

Pichaimani and Manjula (2022) proposes a novel framework called Gaussian Distributive Feature Embedding based Deep Recurrent Perceptive Neural Learning (GDFE-DRPNL) that improves the accuracy of indoor positioning systems. The framework reduces the time consumption and overhead for estimating the location of

Universiti Malaya

various devices by selecting principal features and utilizing Deep Recurrent multilayer Perceptive Neural Learning to evaluate the device position with dimensionality reduced features. The experimental assessments with various factors such as positioning accuracy minimized by 70 % and 60 %, computation time minimized by 45 % and 55 % as well as overhead by 11 % and 23 % compared with Particle Filter based Reinforcement Learning (PFRL) and two-dimensional localization algorithm.

The authors, Tang et al. (2022) investigate three different methods of RSSI data augmentation based on Multi-Output Gaussian Process (MOGP), by a single floor, by neighbouring floors, and by a single building. The effectiveness of augmenting RSSI data using a MOGP model was demonstrated through experiments on an RNN-based indoor localization model trained with the UJIIndoorLoc dataset. By incorporating the entire building's RSSI data into the MOGP model for data augmentation, the RNN model achieved a mean three-dimensional positioning error of 8.42 meters, surpassing the original model's error of 8.62 meters and outperforming other augmentation methods.

Nabati and Ghorashi (2023) proposes a positioning algorithm using deep neural network (DNN) to learn the distribution of available RSS samples instead of averaging them at offline phase. Then a novel state-based positioning method is utilized to consider the previous state information of users assuming that users' movements are continuous. The proposed algorithm is tested on both benchmark and collected datasets in two different scenarios (single RSS sample and many RSS samples for each user in the online phase) and is shown to be superior to traditional regression algorithms such as Gaussian process regression, deep neural network regression, random forest, and WKNN.

Qin et al. (2021) introduces CCpos, a novel WiFi fingerprinting-based indoor positioning system that leverages a contractive denoising autoencoder (CDAE) and convolutional neural network (CNN) to improve localization accuracy. The main

Universiti Malaya

innovation lies in the combination of CDAE for denoising and feature extraction with CNN for spatial learning, enhancing the robustness of WiFi fingerprinting against environmental noise and signal fluctuations. The average positioning error is reduced to 1.46 meters, compared to 2.32 meters in conventional methods. The system achieves a 24.8% improvement in localization accuracy, demonstrating superior robustness in complex indoor environments

Nguyen et al. (2024) proposes an enhanced Wi-Fi fingerprint-based indoor localization method by integrating Truncated Singular Value Decomposition (TSVD) and a LSTM model. TSVD reduces the dimensionality of raw fingerprint data, improving signal quality, while LSTM captures temporal dependencies to refine positioning accuracy. The model achieves an average localization error of 1.25 meters, outperforming baseline techniques with errors of 1.98 meters. The proposed TSVD-LSTM model improves positioning accuracy by 37%, making it well-suited for dynamic indoor environments

Universiti Malaya

Table 2.4: Summary of Case Studies of Positioning Systems Using Fingerprinting Techniques with Machine Learning

Study	Methodology	Findings
Kodippili and Dias (2010)	Fingerprinting with KNN (K=3) and modified path loss model for distance calculation, trilateration for position estimation	44 % accuracy improvement compared to basic fingerprinting, 73 % accuracy improvement compared to basic trilateration
Fang et al. (2011)	Dynamic fingerprinting combination (DFC) algorithm with Bayesian approach and neural network model	DFC improved positioning accuracy compared to individual fingerprinting approaches, reducing 67th percentile localization errors by 19.28 % (Bayesian) and 27.78 % (neural network)
Alraih et al. (2017)	Clustering algorithm with fingerprinting using four WiFi APs	Average distance error of 2.4 m (clustering) vs. 3.4 m (non-clustering), 41 % accuracy improvement with clustering
Alhammadi et al. (2017)	Fingerprinting with signal space clustering, KNN, and Bayesian Network (BN)	Clustering reduced radio map size from 30 to 15 calibration points; KNN accuracy slightly improved from 7.3 m to 6.9 m, BN accuracy improved to 2.6 m
Abdelghani and Qiang (2017)	Hybrid algorithm integrating KNN and Segmentation Nearest Neighbour (Seg-NN)	Mean error decreased from 83 m to 24 m using the hybrid algorithm
Lu et al. (2016)	SVD-LS and SVD-MV algorithms for noise reduction	SVD-MV showed better noise reduction; under 1m accuracy, SVD-LS achieved 92.56 %, SVD-MV achieved 93.84 %
(Molina et al., 2018)	Integrated WiFi and BLE with WKNN and filter sequences	Initial accuracy of 50 % (right node), improved to 80 % (right node) and 94 % (adjacent node) after applying filter sequences; average accuracy of 5 m, outperforming internal geolocation plugin (10 m accuracy)
Ji et al. (2021)	RFVS for variable importance and combinations, MLP for position calculation using 5G variables	MLP with RFVS showed 31.42 %, 39.56 %, and 30.54 % accuracy improvements in different rooms compared to using RSSI only

Universiti Malaya

Table 2.4, continued: Summary of Case Studies of Positioning Systems Using Fingerprinting Techniques with Machine Learning

Teng et al. (2018)	Deep Gaussian Process Regression (DGPR) with RSS values as input	Average error of 2.28 m and maximum error of approximately 6 m
(Belmonte-Hernández et al., 2019)	SWiBluX framework using WiFi, Bluetooth, and Xbee with fingerprinting and neural networks	Deep Neural Network with GOF, Weighted Combination, and Particle Filter achieved best result with average error of 45.41 cm
Wang and Park (2020)	DeepMap system using Deep Gaussian Process (DGP) for radio map construction and localization	Median error of 1.3 m and maximum error of 5.207m, outperforming typical Gaussian Processes (1.5 m median error, 6.182 m maximum error)
Guan et al. (2021)	DGP for probabilistic positioning	DGP outperformed GP in office building (3.36 m mean error vs. 3.71 m) and shopping environment (5.79 m mean error vs. 6.25 m), as well as in all percentiles
Wang et al. (2021)	Hierarchical LSTM for geomagnetic indoor positioning considering short-term and long-term features	Utilized LSTM networks to extract temporal features and hierarchical structure to learn geomagnetic features; improved position accuracy compared to traditional methods
Pichaimani and Manjula (2022)	GDFE-DRPNL framework with feature selection and Deep Recurrent Perceptive	Positioning error decrease up to 70% and computational time reduced up to 55 %.
Nabati and Ghorashi (2023)	State-based deep neural network to consider the previous state information of users assuming that users' movements are continuous	Superior accuracy compared to traditional regression algorithms.
Qin et al. (2021)	Leverages a CDAE and CNN	The average positioning error is reduced to 1.46 meters, compared to 2.32 meters in conventional methods.
Nguyen et al. (2024)	Proposed the TSVD-LSTM model. TSVD reduces the dimensionality of raw fingerprint data, while LSTM captures temporal dependencies.	The model achieves an average localization error of 1.25 meters, outperforming baseline techniques with errors of 1.98 meters.

Universiti Malaya

2.5 Research Gap

Despite extensive research on indoor positioning systems, significant challenges remain, particularly in leveraging LoRa-based technology for dynamic motion tracking in industrial environments. The existing literature provides valuable insights into different aspects of positioning, including radio-based technologies (Chapter 2.1.1), LPWAN-based positioning (Chapter 2.1.2), and LoRa's feasibility for localization (Chapter 2.3.2). However, several key limitations persist.

Firstly, previous studies demonstrate the feasibility of LoRa for positioning but often focus on static or low-mobility environments. The accuracy of LoRa-based positioning systems in dynamic motion scenarios has not been explored. While machine learning and deep learning have been explored, most studies lack uncertainty quantification in their models. This is crucial for low-data and high-noise environments like industrial settings, where signal reception is highly variable. Deep Gaussian Process Regression (DGPR) has been underutilized in positioning studies, despite its potential to improve accuracy by capturing uncertainties in localization.

Moreover, many existing fingerprinting-based methods overlook the importance of time-dependent signal variations. Signal strength fluctuations due to environmental changes, device movement, and interference are often ignored, leading to inconsistent and unreliable positioning results. To address these gaps, this research proposes an enhanced LoRa-based indoor positioning system integrating DGPR and spatial-temporal enhancement techniques, aiming to improve localization accuracy in dynamic industrial environments.

Universiti Malaya

CHAPTER 3: METHODOLOGY

In this research, we equipped LoRa technology as the foundation for indoor positioning. LoRa access points and beacons were strategically deployed within a real-world industrial environment to capture and analyse radio characteristic data. This data was then used to construct machine learning pipelines for precise beacon position prediction. The result of this research saw the implementation of these models in a proof-of-concept demonstration of trolley location detection, showcasing their practical application and potential impact.

More precisely, the methodology progression involved five primary phases:

1. Configuring LoRa-enabled devices for radio fingerprint collections within the test area by using static and striding methods.
2. Evaluate and validate the feasibility of LoRa-based indoor positioning systems by comparing various machine learning models to map collected radio maps to spatial coordinates.
3. Demonstrate the effectiveness of DGPs in positioning in complex environments. Extensive parameter tuning was conducted to optimize the DGPs' internal structure, enabling them to capture the intricate nuances of spatial relationships within the environment.
4. Implementation of spatial-temporal techniques to reduce large positioning errors and show object movements.
5. Integration of hardware, process flows, system backend, database and frontend user interface to build a robust proof of concept of the real-world application of the indoor positioning system.

Universiti Malaya

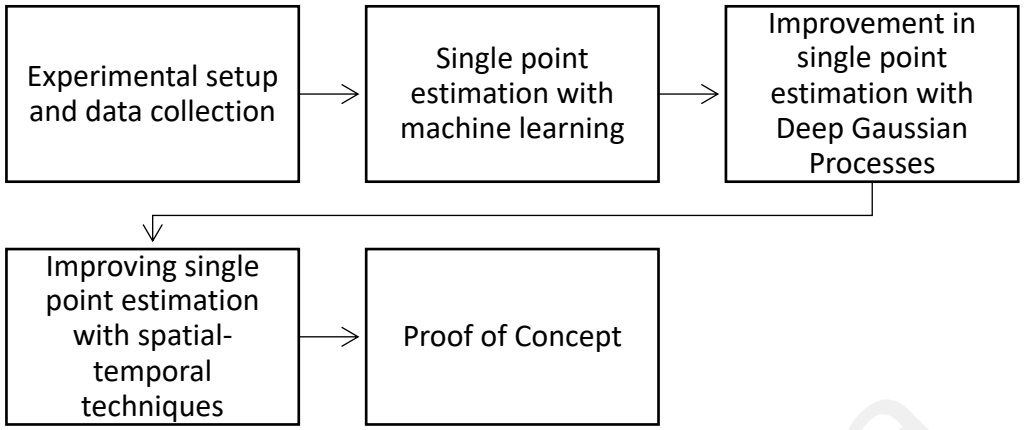

Figure 3.1: Flow diagram for the methodology section

Figure 3.2 presents the architecture of the proposed positioning system. The proposed system is a combination of the fingerprinting-based indoor positioning system with temporal-based filtering techniques for dynamic positioning (Ng et al., 2024). First, the radio packets from the mobile nodes LoRa transceivers are received by the base stations, then, the radio parameters, and necessary input information are sent to the server for processing, and stored in the radio map. Second, a Temporal Weighted RSSI filter is used to smoothen the current RSSI value with the previous RSSI values while carrying a weightage. The weight is calculated using the exponential decay function by taking the sending time difference between the current radio packet with the previous radio packet. Thirdly, a Deep Gaussian Process Regression model is trained using the radio map for single point estimation. Subsequently, the x and y coordinates from the single point estimator are inserted into the Kalman filter to simulate real dynamic movement. Since no external sensors were used to determine the acceleration and velocity, only the time difference between the sending of radio packets is used as a variable in the Kalman filter.

Universiti Malaya

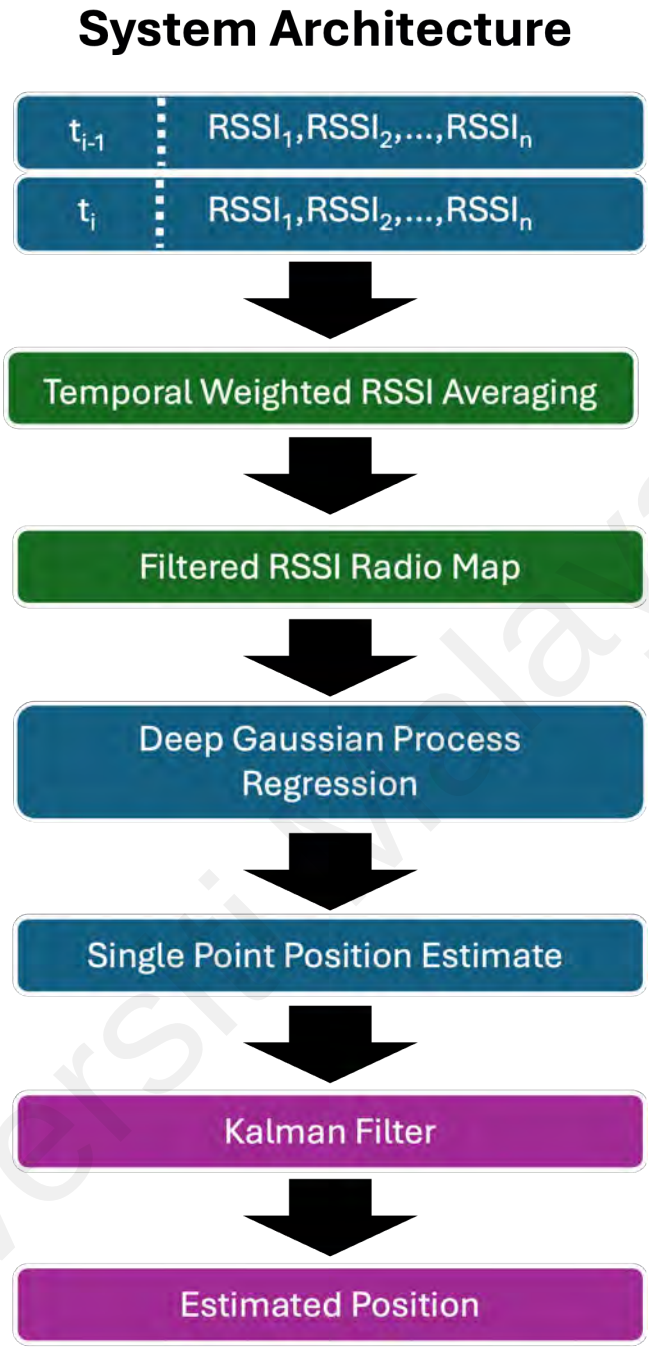

Figure 3.2: TWA-DGPR-KF overall system architecture. Temporal Weighted RSSI Averaging was applied on the current and historical RSSI vector with timestamps to form a filtered RSSI radio map. The Deep Gaussian Process Regression model was trained on the filtered RSSI radio map to produce single point position estimates. Kalman filter was applied to the single point position estimate to predict the current state which is the estimated position.

Universiti Malaya

3.1 Experimental Setup

3.1.1 System Hardware and Nodes

The TTGO LoRa32 V2.1.6 915MHz boards (Figure 3.3) were used as both beacons and base stations (BSs). The LoRa32 module is an ESP32 module integrated with another LoRa module. Since it operates at 2 different frequencies, 2.4GHz for WiFi and Bluetooth and 433/868/915MHz for LoRa, it utilizes two different antennas. Table 3.1 shows the specifications of the TTGO LoRa32 V2.1.6 module.

Table 3.1: Specifications of TTGO LoRa32 V2.1.6 module

ESP chip	ESP32 PICO-D4
Working frequency	433/868/915MHz
Modulation method	FSK, GFSK, MSK, GMSK, LoRa, OOK
LoRa RF power	+2dBm to +20dBm
LoRa antenna	SMA antenna
Number of pins	26
Power Consumption	Active state: 20mA to 120mA Idle state: 1.5µA Sleep state: 0.2µA
Operating voltage	1.8V to 3.7V
Operating temperature	-40ºC to +85ºC

The beacon nodes were configured to send LoRa radio packets at 2 dBm, and LoRa configuration of spread factor (SF) 7 and bandwidth of 125 kHz. The radio packets are sent with a constant interval of 1000 ms. The payload of the beacon node consists of the beacon number, device timestamp and packet number for data processing purposes during the data collection process. The beacon nodes are attached to a lithium battery for mobility convenience purposes.

Universiti Malaya

Figure 3.3: The TTGO LoRa32 V2.1.6 (LILYGO®, n.d.)

The anchor nodes were configured to act as both LoRa and WiFi transceivers. Each anchor node was continuously listening for incoming LoRa radio packets. Upon receiving a packet with the correct packet type, the BS would further process the data payload. In addition to the packet information, the BS recorded crucial radio signal parameters available from the LoRa module, including the RSSI, SNR and frequency error, for the received packet. The BS then compiled the packet information, RSSI, SNR, and frequency error into a JSON formatted object. This JSON object encapsulated the complete dataset for each received packet, providing a structured and standardized representation of the collected data. Subsequently, the JSON objects were transmitted from the BSs to a central server through websocket, where they were securely stored in a fingerprint database. The fingerprint database was then used for further analysis and used on various machine learning techniques as described in further sections. Figure 3.4 depicts the block diagram of the proposed IoT-based indoor positioning infrastructure and data flow.

Universiti Malaya

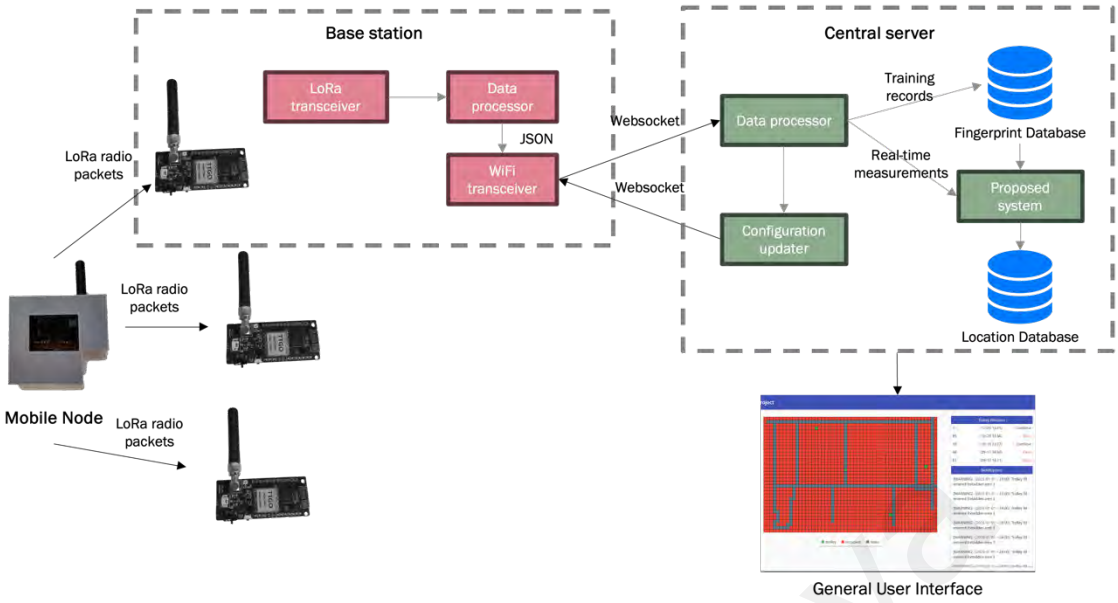

Figure 3.4: Block diagram of the proposed IoT-based indoor positioning infrastructure and data flow.

3.1.2 Testbed and node placement

The experiment was performed in a production line at the Test Backend Department in NXP Semiconductors, Malaysia. The floor plan layout of the production line is shown in Figure 3.5 with the largest length and width of 53 meters and 34 meters. The environment is filled with machines, shelves, workstations, trolleys and human movement distributed intermittently characterized the space presenting potential radio occlusion and reflection surfaces.

Five BSs were placed in locations represented by red star symbols where machines and pillars are available for installation. The dark grey sections are partitions or portioned rooms. The light grey sections are conveyor and packaging platforms. Purple, white, light blue, and neon blue are packaging machines. Dark blue areas are inspection workstations. Yellow boxes represent metallic shelves, and the orange colour represents wafer baking machines. Data collection is done along the lanes where trolleys can commute. Further details of data collection will be described in the next section.

Universiti Malaya

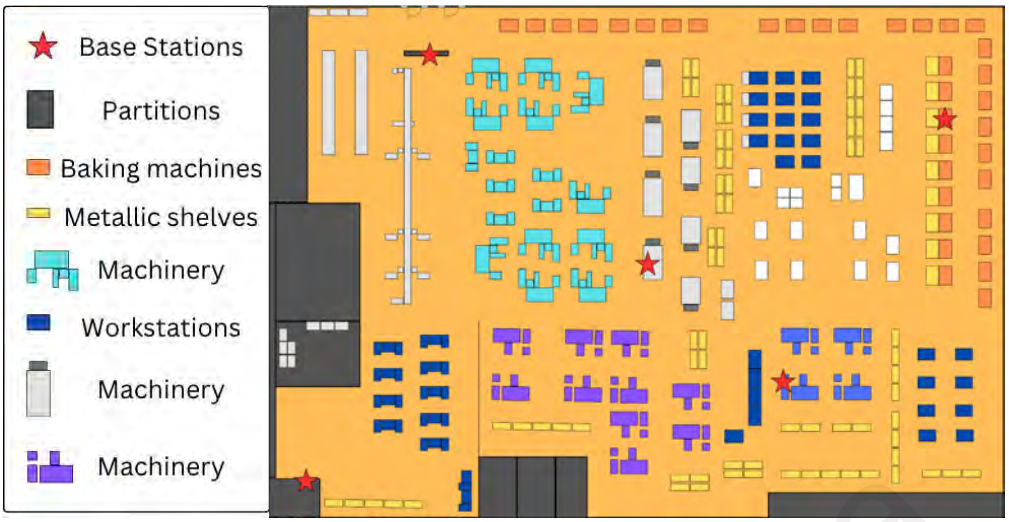

Figure 3.5: Floor plan layout of the testbed environment.

3.1.3 Data Collection

This research employed two distinct methods, static and motion, to gather data from the LoRa devices deployed within the testbed.

The static dataset involved holding the beacon node at fixed points with 1 meter intervals along the lanes where trolleys can commute (Figure 3.7). The location was first set as location information in the radio packet payload. Then, 30 radio packets were broadcasted at the location before moving on to the next predetermined point. Subsequently, the process is repeated throughout all the points. Depiction of the radio packets is shown in Figure 3.6.

For the motion dataset, the constant speed method described in (Li et al., 2017) was used to infer the location of the beacon node. The authors suggested that the method can reduce time for site surveying such as hardware configuration and precise distance interval marking, without sacrificing localization performance. The user's location loc_i at t_i can be calculated by using equation 3.1,

$$loc_i = loc_{start} + \frac{t_i - t_{start}}{t_{end} - t_{start}} \times (loc_{end} - loc_{start}) \quad \textbf{(3.1)}$$

Universiti Malaya

This experiment involved defining five lanes, including two horizontal and three vertical lanes. The movement speed was approximately 1.5 ms^{-1}. For each lane, data was collected in two batches, with the batches moving in opposite directions along the entire length of the lanes.

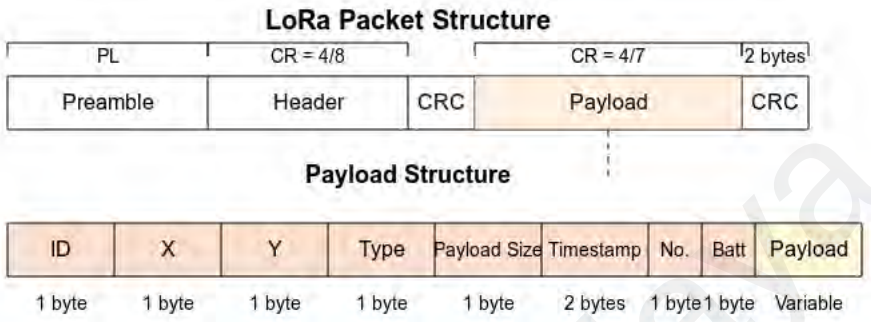

Figure 3.6: LoRa packet structure, showing its primary components of Preamble, Header with CRC, Payload, and a final CRC section. The lower portion details the Payload structure, where ID is the device ID, X and Y represents the x and y coordinates, type indicates the type of packet, timestamp is the sending timestamp, no. is the number of packet sent, batt represents the battery value, and payload for additional information.

The testing dataset is collected separately by moving around the testbed using the constant speed method. The data points collected for the static and motion datasets are shown in Figure 3.7 and Figure 3.8 respectively.

Overall, the RSSI, SNR and frequency error of the beacon nodes would be recorded in the database as (x, y, packet ID, ID, timestamp, rx_1_RSSI, rx_1_SNR, rx_1_freq, rx_2_RSSI, rx_2_SNR, rx_2_freq, … rx_5_RSSI, rx_5_SNR, rx_5_freq) from BS1 to BS5 grouped by packet ID and timestamp where x and y represents the x and y coordinates and ID represents the labelled value for each x, y coordinates pair.

Universiti Malaya

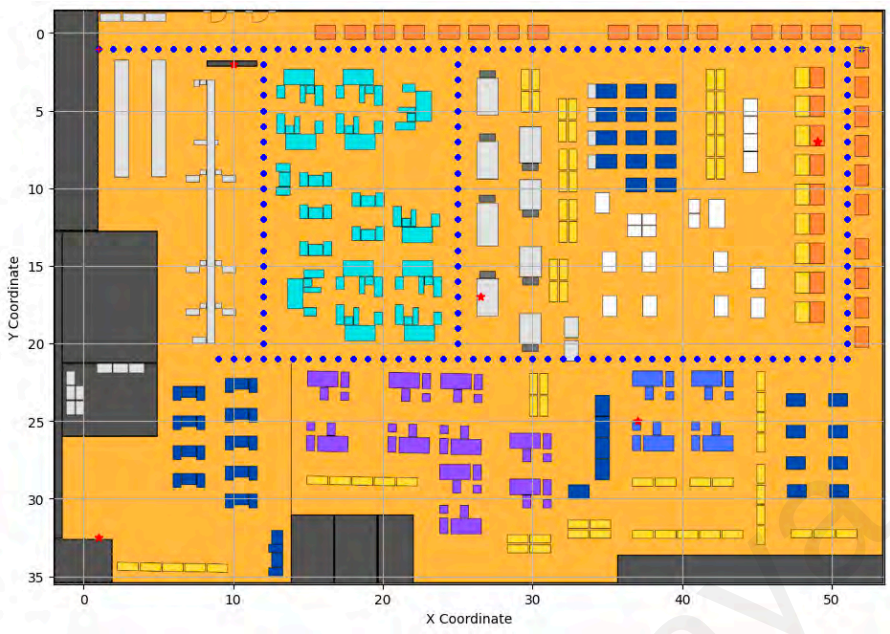

Figure 3.7: Data points collected using conventional static method

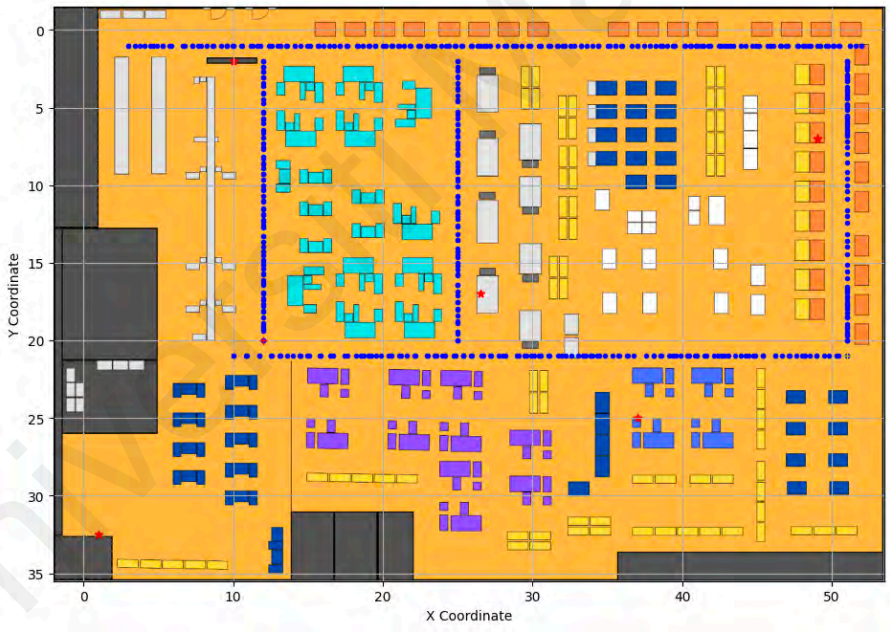

Figure 3.8: Data points collected in motion

Universiti Malaya

3.2 Data Preprocessing

Before applying machine learning algorithms for position estimation, several data preprocessing steps were performed to ensure data quality, handle missing values, and prepare the feature spaces (Figure 3.9). Proper data preprocessing is crucial for achieving accurate and reliable position estimates, as it can significantly impact the performance of the machine learning models.

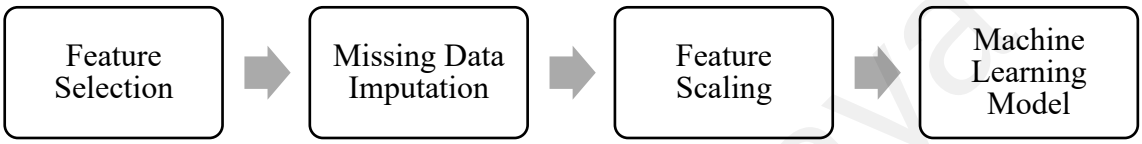

Figure 3.9: Preprocessing steps on raw data before machine learning model training

3.2.1 Feature Selection

In this research, the collected data was segmented into three distinct fingerprint databases to investigate the impact of different feature combinations on position estimation accuracy. The three fingerprint databases were:

1. RSSI, SNR, and Frequency Error (All Features). This database contained the complete set of features from all BSs, including RSSI, SNR and frequency error values.
2. RSSI and SNR. This database consisted of only the RSSI and SNR features from all BSs, excluding the frequency error.
3. RSSI only. This database consisted of only the RSSI features from all BSs, excluding the frequency error.

3.2.2 Missing Data Imputation and Feature scaling

To handle missing or incomplete data points in the collected datasets, a missing data imputation technique was employed. Specifically, the K-Nearest Neighbours Imputer

Universiti Malaya

(KNNImputer) from the scikit-learn library was utilized, with the number of neighbours (k) set to 3. To impute missing features, values from the n nearest neighbours that have a value for the feature are utilized. The neighbours' features are uniformly averaged by their distance to each neighbour. The Euclidean distance metric is used to determine the nearest neighbours.

To ensure that all features contribute equally to the position estimation models, to reduce computational resources and to prevent any potential dominance of features with larger numerical ranges, feature scaling was performed. The standard scaler was employed to standardize the feature values, where each standard score z of sample x can be calculated as shown in (3.2),

$$z = \frac{(x - \mu)}{s} \tag{3.2}$$

where μ is the mean of the training feature and s is the standard deviation of the training feature.

3.3 Machine Learning Algorithms for Single Position Estimation

This subsection describes the application of various machine learning algorithms, which leverage the collected data as mentioned in the previous section to learn patterns and relationships between the radio signal parameters and the corresponding locations. This research employed a diverse set of machine learning algorithms for position estimation, including both classification and regression techniques. All machine learning models in this subsection were trained using the scikit-learn library. Each machine learning algorithm was evaluated with the three feature datasets (All features, RSSI and SNR, RSSI only) for both motion and datasets.

The outputs of the machine learning algorithms were labelled values for classification models, whereas, for regression models, the output would be in the form of coordinates.

Universiti Malaya

The output results were then related to their corresponding coordinates on the testbed. The errors of the position estimates were calculated with the absolute Euclidean distances between the position estimate and the actual position.

The evaluation metrics for the machine learning algorithms were mean absolute error (MAE) and root mean square error (RMSE). MAE measures the average magnitude of the errors between predicted and actual values, providing a straightforward interpretation of the average error. On the other hand, RMSE provides a more comprehensive measure of the error by penalizing large errors more heavily compared to MAE. By utilizing these evaluation metrics, we were able to not only observe the average error but also compare large errors. The performance of these different models was evaluated by comparing their accuracy, and the model with the highest accuracy was selected.

3.3.1 Classification Models for Single Position Estimation

The classification models explored in this study include Random Forest (RF), Decision Tree, K-Nearest Neighbours (KNN), Weighted KNN (wKNN), Multilayer Perceptron (MLP), and Naive Bayes (NB). Each model offers unique advantages and characteristics, making them suitable for different scenarios and data distributions.

The Random Forest and Decision Tree are non-parametric supervised learning methods that recursively partition the feature space into smaller regions based on the most discriminative features. The tree-like structure consists of internal nodes representing feature tests and leaf nodes representing class labels. The Random Forest is an ensemble learning method that constructs multiple decision trees during training and combines their predictions for classification tasks. Each tree is grown using a random subset of features, and the final prediction is determined by majority voting of the individual trees. Random Forests compared to Decision Trees are robust to overfitting, can handle high-dimensional data, and are relatively insensitive to outliers.

Universiti Malaya

KNN is a non-parametric, instance-based learning algorithm that classifies new instances based on their similarity to the nearest neighbours in the training set. The algorithm computes the distances between the new instance and all training instances, selects the k closest neighbours, and assigns the class label based on the majority vote of these neighbours. WKNN is an extension of the KNN algorithm that assigns weights to the neighbours based on their distances from the new instance. Closer neighbours contribute more to the classification decision than farther neighbours. The Euclidean distance metric and k value of 3 were used in this experiment.

MLP is a type of artificial neural network that consists of multiple layers of interconnected nodes or neurons. One or more hidden layers between the input and output layers perform non-linear transformations on the data. In this experiment, the MLP consists of one hidden layer with 64 nodes, tangent hyperbolic (tanh) activation function and the Adam optimizer with adaptive learning rate.

The NB classifiers are probabilistic models based on Bayes' theorem with the “naive” assumption of conditional independence between every pair of features given the value of the class variable. Despite the strong assumption of feature independence, which is often violated in real-world data, Naive Bayes classifiers can perform surprisingly well and are computationally efficient.

3.3.2 Regression Models for Single Position Estimation

In addition to classification models, regression techniques were also explored for the position estimation task. Regression models aim to learn a mapping function that relates the input features (radio signal parameters) to continuous target variables (location coordinates).

Universiti Malaya

Similar to its classification counterpart, Random Forest Regression is an ensemble learning method that constructs multiple decision trees during training. However, instead of majority voting, the final prediction is obtained by averaging the predictions of individual trees. Next, Decision Tree Regression shares the same tree-like structure as its classification variant but predicts continuous target values at the leaf nodes instead of class labels.

WKNN Regression is an adaptation of the Weighted KNN classifier for regression tasks. Instead of majority voting, it predicts the target value by taking a weighted average of the target values of the k nearest neighbours, where closer neighbours contribute more to the prediction. Subsequently, MLP Regression is a variant of the MLP classifier, where the output layer produces continuous target predictions instead of class labels. The underlying architecture and training process remain similar, with the objective of minimizing the error between the predicted and true target values.

On top of that, Linear Regression is a classical statistical method that models the relationship between the input features and the target variable as a linear function. It assumes that the target variable can be expressed as a linear combination of the input features, weighted by coefficients learned from the training data. Linear Regression is simple and interpretable but may not capture non-linear relationships effectively.

Gaussian Processes Regression (GPR) is a non-parametric Bayesian approach that models the target variable as a Gaussian process governed by a covariance function also known as a kernel. Unlike other regression models that learn a specific mapping function, GPR directly models the distribution of the target variable, allowing for uncertainty quantification and probabilistic predictions.

Universiti Malaya

In GPR, the covariance function encodes the assumptions about the smoothness and behaviour of the target function. The choice of the kernel function plays a crucial role in the performance of the GPR model, as it determines the properties of the underlying Gaussian process. This research explored several kernel functions to capture different types of non-linear relationships in the data, namely Radial Basis Function (RBF) Kernel, Matérn kernel, sum of RBF kernel and Matérn kernel, product of RBF kernel and Matérn kernel.

The RBF kernel, also known as the Gaussian kernel or the squared exponential kernel, is a popular choice for GPR. It assumes that the target function is infinitely differentiable and has a high degree of smoothness. The RBF kernel (equation 3.3) is particularly well-suited for modelling continuous and smooth functions but may struggle with abrupt changes or discontinuities in the data.

$$k_{RBF}(x, x') = \exp\left(-\frac{\|x - x'\|^2}{2\ell^2}\right) \qquad \textbf{(3.3)}$$

The hyperparameter ℓ controls the length scale, determining how quickly the correlation decays with distance.

The Matérn kernel is a class of kernels that can model functions with varying degrees of smoothness. It is parameterized by a positive smoothness parameter that controls the differentiability of the resulting functions. Lower values of the smoothness parameter produce rougher functions, while higher values lead to smoother functions. The Matérn kernel (equation 3.4), can be useful when the target function exhibits non-smooth or discontinuous behaviour.

$$k_{\text{Matérn}}(x, x') = \sigma^2 \frac{2^{1-\nu}}{\Gamma(\nu)}\left(\sqrt{2\nu}\frac{\|x - x'\|}{\ell}\right)^{\nu} K_{\nu}\left(\sqrt{2\nu}\frac{\|x - x'\|}{\ell}\right) \qquad \textbf{(3.4)}$$

Universiti Malaya

The hyperparameter ν controls the degree of smoothness of the learned function. The smaller nu, the less smooth the approximated function is. For ν = inf, the kernel becomes equivalent to the RBF kernel and for ν = 0.5 to the absolute exponential kernel. Some of the other popular ν values are $\nu = 1.5$ and $\nu = 2.5$ as they are computationally less expensive.

In some cases, a single kernel may not be sufficient to capture the complexities of the underlying function. To address this, a combination of kernels can be used. The sum of RBF and Matérn kernels as shown in equation 3.5

$$k_{sum}(x, x') = k_{RBF}(x, x') + k_{\text{Matérn}}(x, x') \quad \textbf{(3.5)}$$

allows the model to leverage the strengths of both kernels, potentially capturing both smooth and non-smooth aspects of the target function.

Another approach to combining kernels is through the product operation (equation 3.6).

$$k_{prod}(x, x') = k_{RBF}(x, x') \cdot k_{\text{Matérn}}(x, x') \quad \textbf{(3.6)}$$

The product of RBF and Matérn kernels can be useful when the target function exhibits both smooth and non-smooth regions, and the product kernel can model these characteristics more effectively than individual kernels alone.

3.4 Deep Gaussian Process Regression

Deep Gaussian Processes (DGPs) are a hierarchical extension of the Gaussian Processes Regression (GPR) model, capable of learning rich representations from high-dimensional data. In this research, DGPs were explored as a powerful approach for indoor position estimation using LoRa technology.

Unlike traditional GPR, which models the target variable directly from the input features, DGPs introduce a series of latent variables or hidden layers. These latent

Universiti Malaya

variables are themselves modelled as Gaussian Processes, allowing for the automatic discovery of useful representations and feature abstractions from the input data.

The hierarchical nature of DGPs enables the model to capture complex non-linear relationships and patterns in the data, making it well-suited for the intricate radio signal propagation dynamics encountered in indoor environments. By learning these rich representations, DGPs can potentially improve the accuracy and robustness of position estimates (Wang et al., 2020).

3.4.1 DGP Architecture

The Deep Gaussian Processes (DGP) model employed in this research was implemented using the GPyTorch library, a flexible and efficient Gaussian Process library built on PyTorch. The DGP architecture consisted of multiple layers, with each layer being a DGP layer, capable of learning rich representations from the input data.

The foundation of the DGP architecture was the standard DGP layer with configurable input and output dimensions, number of inducing points, and kernel functions.

The DGP architecture can be visualized as a graphical model (Figure 3.10) where each node represents a GP. The input layer receives the raw data, and the output layer produces the final predictions. The hidden layers, composed of latent variables, enable the model to learn increasingly abstract and informative features from the data. This hierarchical structure allows DGPs to model complex functions that may not be well-represented by a single-layer GPR.

The model utilized a Gaussian Likelihood. This likelihood function jointly modelled the distribution of the target coordinates, allowing the DGP model to capture the dependencies and correlations between them.

Universiti Malaya

Since the log likelihood is not analytically tractable because of the nonlinearity of the GPs, sparse variational inference is used to optimise the DGP.

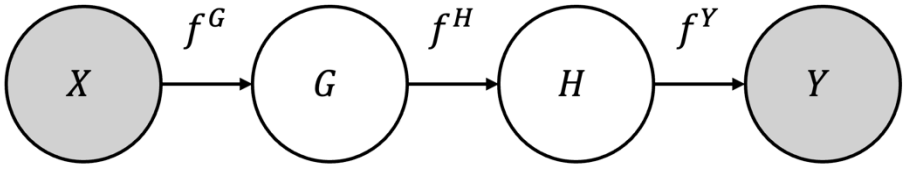

Figure 3.10: Graphical model of DGP with two hidden layers

3.4.2 Model Design and Hyperparameter Selection

3.4.2.1 Kernel Selection

The choice of kernel functions plays a crucial role in the performance of Gaussian Processes models, as it determines the characteristics of the learned function. In this study, though each layer can have varying kernels or covariance functions, the same kernel is used for each layer. Two combinations of kernels were explored: the sum of the RBF kernel and the Matérn kernel, and the product of the RBF kernel and the Matérn kernel.

To facilitate the initial exploration phase, a constant number of dimensions (5) and a fixed number of inducing points (60) were chosen. While these values were selected randomly, they provided a reasonable starting point for evaluating the performance of the different kernel combinations. The covariance function that exhibited better performance, as measured by the chosen evaluation metrics, was selected for further hyperparameter tuning.

3.4.2.2 Number of Dimensions in the Hidden Layer

The number of dimensions in the hidden DGP layer determines the complexity of the learned representations. Higher-dimensional representations can capture more intricate patterns but may also increase the risk of overfitting and computational demands.

Universiti Malaya

To find the optimal number of dimensions for the hidden layer, a range of values from 1 to 19, with an interval of 2, was explored (1, 3, 5, ..., 19). During this process, the number of inducing points was fixed at 60. The dimension that yielded the best performance, as measured by the lowest loss, was chosen as the optimal setting for the hidden layer.

3.4.2.3 Number of Inducing Points

Inducing points are a key component of Gaussian Processes models, as they act as a summary of the data, reducing computational complexity while maintaining reasonable accuracy. The number of inducing points balances computational efficiency and model performance.

With the optimal number of dimensions for the hidden layer determined, the next step involved tuning the number of inducing points. A range of values from 24 to 72, with an interval of 4, was evaluated (24, 28, 32, ..., 72). The range of values was selected empirically based on initial observations of model performance. This ensures a sufficient number of inducing points for good model performance while not overfitting the model with high number of inducing points. Moreover, the interval of 4 has been chosen empirically for showing model performance while considering computational efficiency. The number of inducing points that resulted in the best performance, considering factors such as accuracy and computational resources, was selected as the final configuration for the DGP model.

3.4.3 Model Training

For the training process, the motion dataset containing the RSSI only feature set was selected. The RSSI only feature set was chosen because of its exceptional performance in the previous section on capturing the patterns and relationships between the radio signal

Universiti Malaya

characteristics and the corresponding location coordinates when used on other machine learning methods.

The training process involved iteratively updating the model parameters to minimize the objective function in equation 2.7 over the training dataset using the Adam optimizer (Kingma & Ba, 2014). To ensure thorough convergence and optimal learning, the DGP model was trained for 3000 epochs, which represents 3000 complete passes over the entire training dataset.

The trained DGP model was subsequently evaluated on the test dataset where evaluation metrics of MAE and RMSE were used. The accuracy of the DGP model was compared to the better performing machine learning models in the previous section.

3.5 Improving Single Point Estimation

While the machine learning models in Section 3.3 and Section 3.4 provide single point position estimates, there are still some large errors in the single point estimates, especially in areas with poor signal quality or multipath propagation. The presence of large errors can be referred to Figure 4.25, where there are multiple error values that are above 10 meters. Several techniques are employed to refine these estimates and improve overall positioning accuracy and robustness.

First, a Temporal-Weighted RSSI Averaging (TWA) approach is used, where multiple RSSI samples are collected over a sliding window and exponentially weighted, giving more importance to the most recent samples. This helps mitigate the effects of RSSI fluctuations and noise. A detailed evaluation of the effects of RSSI fluctuations and noise mitigation is provided in Chapter 4.4.1.

Next, the position estimates from the machine learning models are then filtered using a Kalman filter. A linear state-space model is defined, with the state vectors representing

Universiti Malaya

the device's position and velocity. The Kalman filter recursively incorporates the position estimates as measurements to update the state estimates, leveraging the temporal correlation between consecutive positions.

Finally, a lane constraint model is applied by mapping the navigable lanes in the environment. The filtered position estimates are projected onto the nearest lane, restricting the estimated positions to only feasible locations. This compensates for errors where the raw estimates may fall outside of the walkable areas.

By combining Temporal-Weighted RSSI averaging, Kalman filtering, and lane constraints, the single point position estimates become significantly more accurate, stable, and consistent with the real-world spatial constraints of the operational environment.

3.5.1 Temporal-Weighted RSSI Averaging

Instantaneous RSSI values can be susceptible to temporal variations in RSSI readings (Youssef & Agrawala, 2005). While simple averaging of RSSI samples over a fixed window can help reduce noise, it treats all samples within the window equally, regardless of their temporal distance from the current time instant. However, in scenarios involving device movement, historical RSSI values become less correlated with the current RSSI signature as the time difference increases, due to probable changes in the device's location and surrounding environment.

To mitigate the effects of RSSI fluctuations and noise, a Temporal-Weighted RSSI Averaging (TWA) approach is employed before feeding the RSSI data into the machine learning models for position estimation.

To account for this temporal dependence, a time-weighting scheme is introduced, where RSSI samples are weighted based on their time difference from the current time, with more recent samples being given higher importance. The rationale is that RSSI

Universiti Malaya

values closer in time are more likely to be representative of the current position, while the impact of older samples diminishes as the time difference increases. The TWA for anchor node i at time t is calculated as:

$$RSSI_{n\_new} = \frac{1}{\mathrm{W}} \sum_{\mathrm{i}=0}^{\mathrm{n}} w_{\mathrm{i}} * RSSI_{\mathrm{i}} \tag{3.7}$$

Where W is the sum of the time decay weightings $w_1, w_2 \ldots w_{\mathrm{i}}$ and w_{i} is the time decay weighting for $RSSI_{\mathrm{i}}$ which can be represented by

$$\mathrm{w_i} = \mathrm{e}^{-\lambda * |t - t_i|} \tag{3.8}$$

Where t is the timestamp of the latest RSSI data point in seconds and t_i is the timestamp of the RSSI of data point i. The weighting factor λ determines the rate of decay for older samples. Values closer to 1 give more importance to recent samples, while values near 0 weight all samples within the window nearly equally, effectively reducing to a simple average.

For the TWA scheme, a lag of 1 (n=1) is employed in this experiment. This means that only the immediately preceding RSSI sample and the current sample are considered for the weighted average calculation. With n=1, the TWA for anchor node i at time t simplifies to:

$$RSSI_{n\_new} = \frac{RSSI_{\mathrm{n}} + \mathrm{e}^{-\lambda |t_n - t_{n\ 1}|} * RSSI_{\mathrm{n-1}}}{1 + \mathrm{e}^{-\lambda |t_n - t_{n\ 1}|}} \tag{3.9}$$

3.5.2 Kalman Filtering

To further refine the single point position estimates obtained from the machine learning models, a Kalman filter is applied. The Kalman filter is a recursive algorithm that optimally estimates the state of a dynamic system from a series of noisy measurements and a theoretical model of the system dynamics.

Universiti Malaya

The Kalman filter implementation used in this work is based on the standard linear Kalman filter formulation. The filter maintains an estimate of the current state vector x_t and its associated covariance matrix P_t. At each time step t, the filter performs two main operations:

1. **Prediction Step**: The state vector and covariance are projected forward in time using the system's transition model.
2. **Update Step**: The projected state and covariance are updated based on the current measurement, incorporating the new information while accounting for the measurement noise.

In the context of position tracking, the state vector x_t typically consists of the device's position and velocity components $x_t = \{x_t, y_t, v_{x,t}, v_{y,t}\}$. Where (x_t, y_t) represents the position coordinates, and $(v_{x,t}, v_{y,t})$ are the velocity components in the x and y directions, respectively.

The transition model describes the evolution of the state vector over time, assuming a constant velocity motion model:

$$\mathbf{P} = \mathbf{A}\mathbf{x_t} + \mathbf{w_t} \quad \textbf{(3.10)}$$

Where A is the state transition matrix, and $\mathbf{w_t}$ is the process noise, assumed to be zero-mean Gaussian with covariance Q.

The measurement vector **S** consists of the position estimates obtained from the machine learning models at each time step. The measurement model relates the state vector to the measurement vector:

$$\mathbf{S} = \mathbf{H}\mathbf{x_t} + \mathbf{v_t} \quad \textbf{(3.11)}$$

Universiti Malaya

Where H is the measurement matrix, and $\mathbf{v_t}$ is the measurement noise, assumed to be zero-mean Gaussian with covariance R.

At each time step, the Kalman filter incorporates the new position estimate as a measurement update, combining the prediction from the transition model with the measurement information to obtain an optimal estimate of the state vector and its associated uncertainty.

3.5.3 Lane Constraint

While the regression model provides position estimates, these estimates may still deviate from the actual traversable paths or lanes within the environment. To account for this, a lane constraint and correction step is applied to ensure that the estimated positions adhere to the spatial constraints of the operational area.

The indoor environment is divided into a grid of tiles, with each tile representing a specific location or area. A list of traversable lanes is predefined, which consists of a sequence of connected tiles that correspond to the walkable or drivable paths within the environment. To map the traversable lanes, each lane is represented as an ordered list of tile coordinates.

Let (x, y) be the position estimate, the tile coordinate $(\mathrm{x_i}, \mathrm{y_i})$ in the lane list that minimizes the Euclidean distance to (x, y) is found using the following formula:

$$(x_i, y_i) = \boldsymbol{argmin_j}\sqrt{\left(\boldsymbol{x - x_j}\right)^2 + \left(\boldsymbol{y - y_j}\right)^2} \quad \textbf{(3.12)}$$

Where (x_j, y_j) are the tile coordinates in the lane list, and j is the index iterating over all tile coordinates.

Universiti Malaya

By applying the lane constraints technique, the position estimates become more consistent with the spatial layout of the environment, reducing the likelihood of erroneous estimates falling outside of traversable areas and ensuring smooth transitions between lanes during device movement.

This chapter outlined the methodology used in developing the LoRa-based indoor positioning system for dynamic motion in industrial environments. The experimental setup was described in detail, including the system hardware, node placements, and the data collection process. The data preprocessing steps, such as feature selection, missing data imputation, and feature scaling, were then discussed to ensure data quality and consistency.

For single position estimation, various machine learning models, including classification and regression-based approaches, were explored, followed by the introduction of DGPR model. The DGPR model architecture, hyperparameter selection, and training process were elaborated to demonstrate its adaptability in capturing complex spatial relationships.

To further enhance localization accuracy, several spatial-temporal techniques were integrated, including temporal-weighted RSSI averaging, Kalman filtering, and the lane constraint method. These techniques aim to reduce positioning errors by leveraging temporal dependencies and motion constraints, addressing the limitations of conventional machine learning models in dynamic environments.

Universiti Malaya

CHAPTER 4: RESULTS

This section presents the findings from the research on developing a LoRa-based indoor positioning system that utilizes Deep Gaussian Processes (DGP) for localization. The results are organized into the following subsections:

1. LoRa Signal Characterization

   Analysis of LoRa signal propagation characteristics, including path loss modelling, multipath effects, and small-scale fading observed in the indoor test environment.

2. Machine Learning Algorithms for indoor positioning

   Details on the development and implementation of machine learning algorithms to improve indoor positioning accuracy. The process covers datasets collection and application of various machine learning pipelines. The results of the machine learning pipelines were compared on the static set and motion set with multiple feature sets.

3. Deep Gaussian Processes Positioning Algorithm

   The particulars on the development of the DGP-based positioning algorithm, covering hyperparameter tuning of model architecture. The algorithm was then evaluated with other machine learning methods in the previous section.

4. Enhancement to Single Point Estimations

   Implementation of techniques by taking historical RSSI inputs and DGP output coordinates into account by using correlation and filtering technique. The different combinations of enhancement techniques were benchmarked against the DGP single point estimation model.

Universiti Malaya

4.1 LoRa Signal Characterization

Understanding the characteristics of the LoRa signal propagation in the indoor environment was crucial for developing accurate positioning systems. The RSS measurements, which form the basis for many positioning techniques, were influenced by various propagation phenomena. In this subsection, the key signal characteristics observed in our experimental data were analysed, including the path loss model, path loss exponent, multipath fading, and small-scale fading effects. The experimental data was collected from the longest row with line-of-sight available in the manufacturing line (53 m).

4.1.1 Log-Distance Path Loss Model and Path Loss Exponent

In this section, the path loss characteristics of the LoRa signals were analysed using the log-distance path loss model. The path loss model captures the signal decay as a function of the distance between the transmitter and receiver. We consider the following log-distance path loss model in equation (2.1). To estimate the path loss exponent, the graphs of RSS values against the corresponding distances in a log scale are plotted. The linear scale representation shows the absolute variation of RSSI with increasing distance, which helps visualize the direct relationship between distance and signal strength in real-world scenarios. While the logarithmic scale helps highlight how signal attenuation follows a power-law decay, making it easier to compare with theoretical models and fit empirical data.

Two sets of data were collected, where the first dataset was collected moving away from the receiver from 1 m to 52 m, whereas the second dataset was collected moving towards the receiver from 50 m to 1 m, where both datasets consisted of a batch of around 25 to 30 radio packets at each location with a distance interval of 1 m. Figure 4.1 to Figure 4.4 shows the log-distance path loss model with the available data.

Universiti Malaya

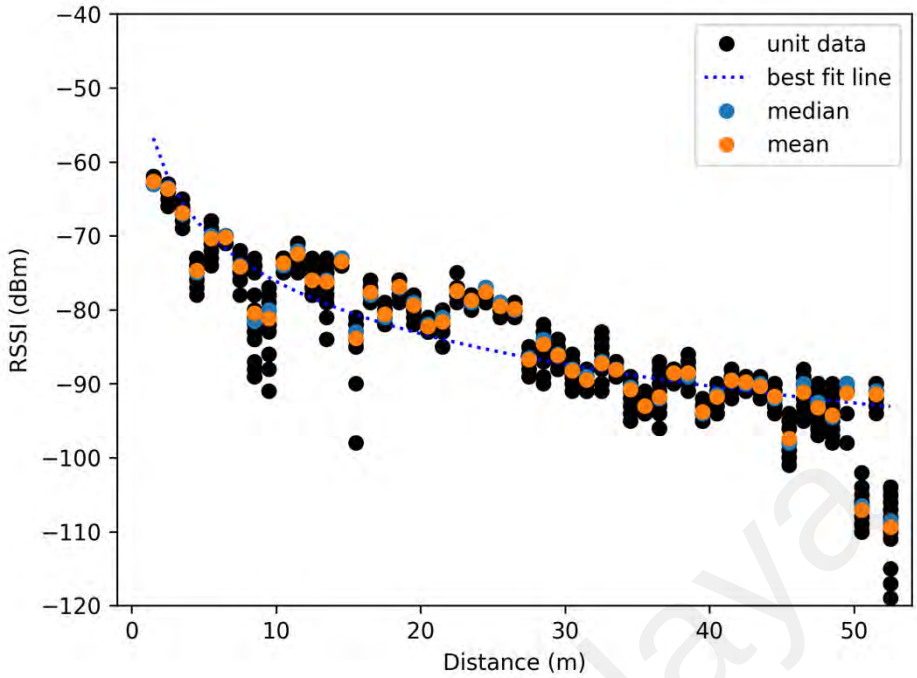

Figure 4.1: Log distance path loss model of the RSSI data collected moving away from the receiver, with x-axis in linear scale

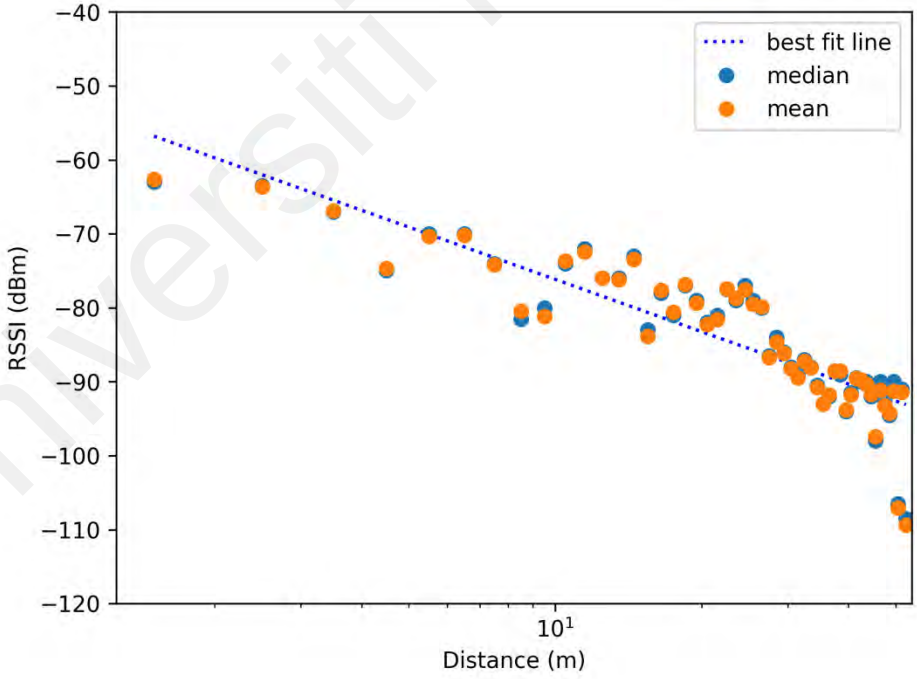

Figure 4.2: Log distance path loss model of the RSSI data collected moving away from the receiver, with x-axis in log scale

Universiti Malaya

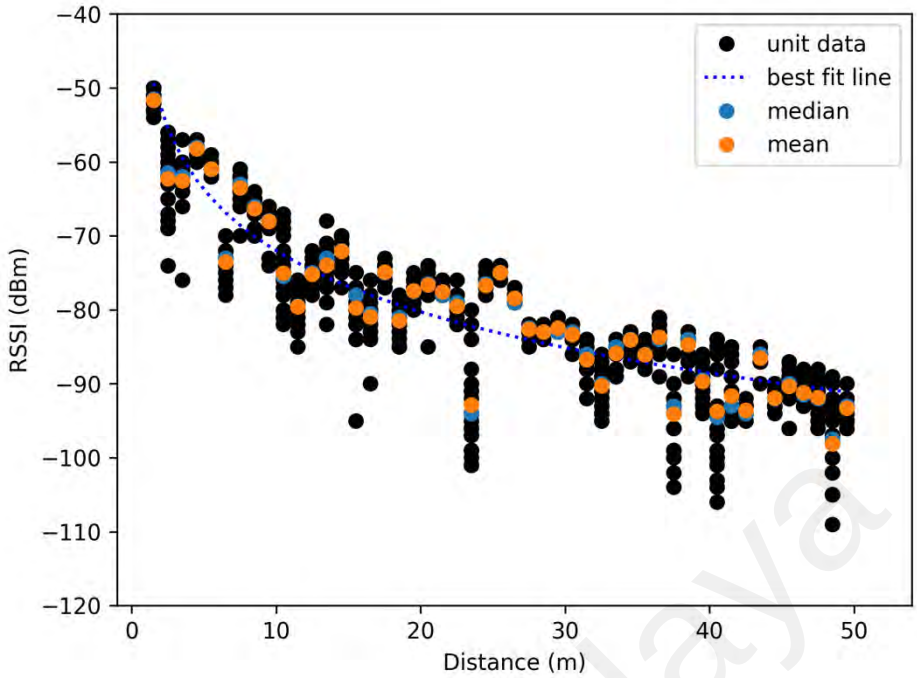

Figure 4.3: Log distance path loss model of the RSSI data collected moving towards the receiver, with x-axis in linear scale

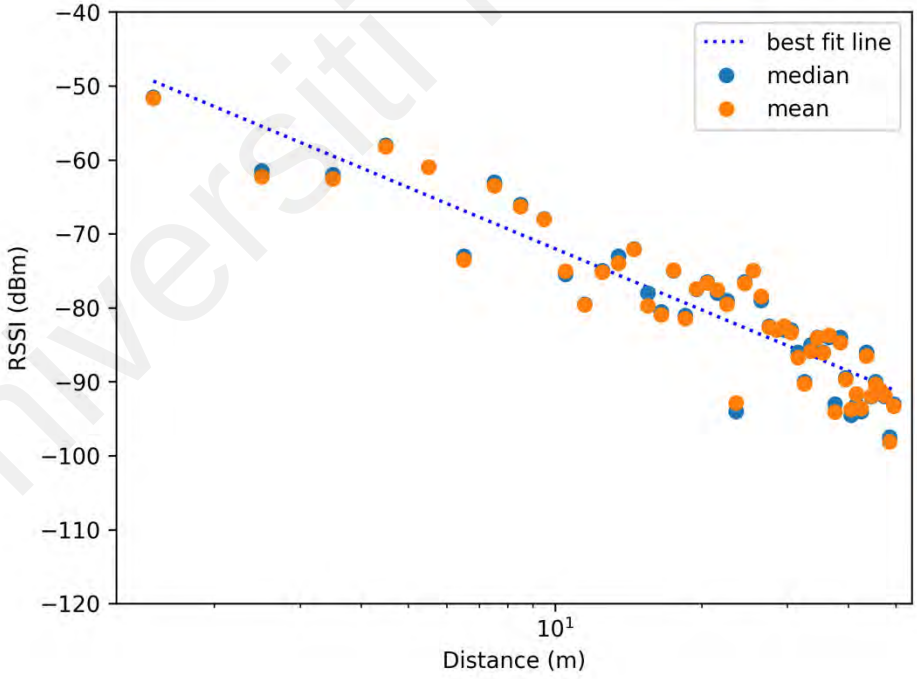

Figure 4.4: Log distance path loss model of the RSSI data collected moving towards the receiver with, x-axis in logarithmic scale

Universiti Malaya

From the graphs, we can observe a linear relationship between the RSS and the log of the distance, proving the log-distance path loss model. In Figure 4.1 and Figure 4.2, for the first dataset, with the beacon moving away from the receiver, the estimated path loss exponent was approximately 2.35 and the estimated path loss at 1 m (d_0), was approximately 52.65 dB. Figure 4.3 and Figure 4.4, for the second dataset, with the beacon moving towards to the receiver, the estimated path loss exponent was approximately 2.75 and the estimated path loss at 1 m (d_0), was approximately 44.51 dB.

As observed from Figures 4.1 to 4.4, the second dataset shows a steeper graph compared to the first dataset, indicating that the body shadowing effect is more significant in locations nearer to the receiver. When moving towards the receiver, with no obstacles between the beacon and the receiver, the mean RSSI values were higher when collected within 10 meters of the receiver.

Next, we present the results obtained from the experiments conducted to analyse the characteristics of the LoRa signal propagation in a dynamic motion, where the beacon was transported away and back towards the receiver. The beacon was moved 0.5 m after each data packet was sent, collecting 212 data points. Figure 4.5 depicts the RSSI data points that were gathered while traveling along the path, illustrating the alterations in RSSI along with the distance. Figure 4.6 to Figure 4.9 show the log-distance path loss model with the data points in Figure 4.5 in log scale and linear scale for moving away and moving towards the receiver.

Universiti Malaya

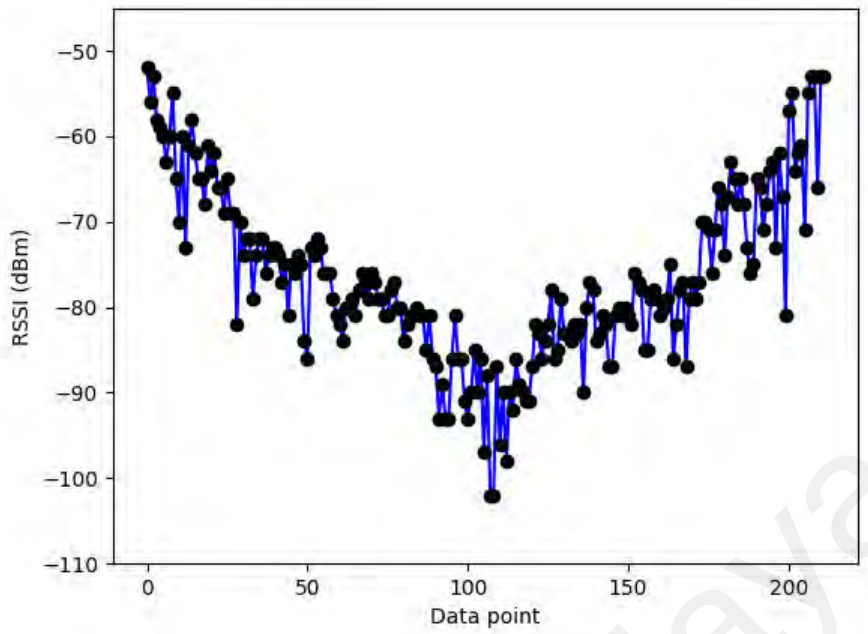

Figure 4.5: RSSI values collected by moving dynamically along the path

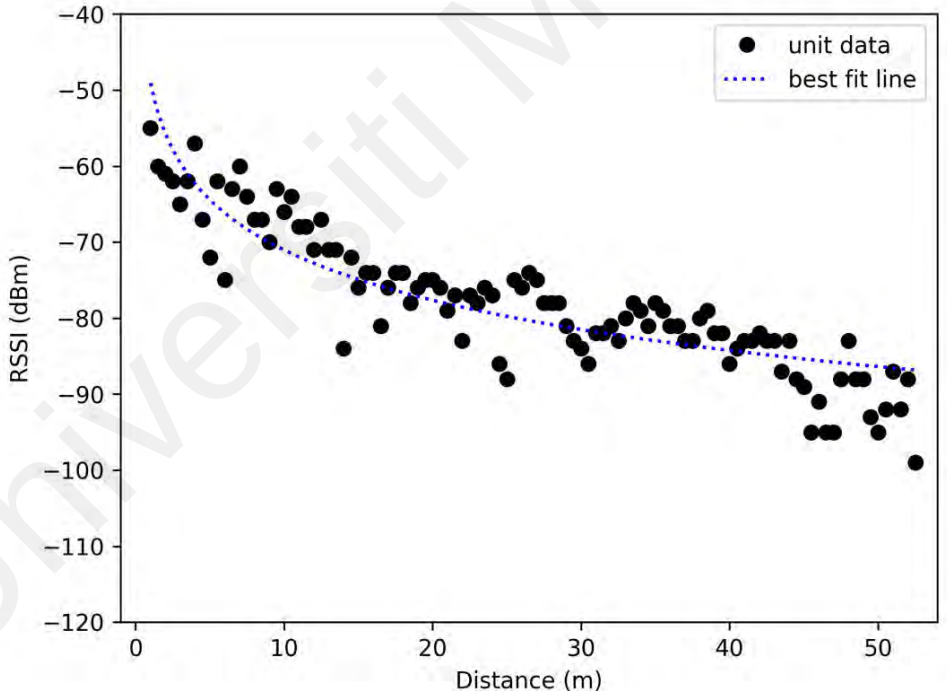

Figure 4.6: Log distance path loss model of the RSSI data collected in motion moving away from the receivercin linear scale

Universiti Malaya

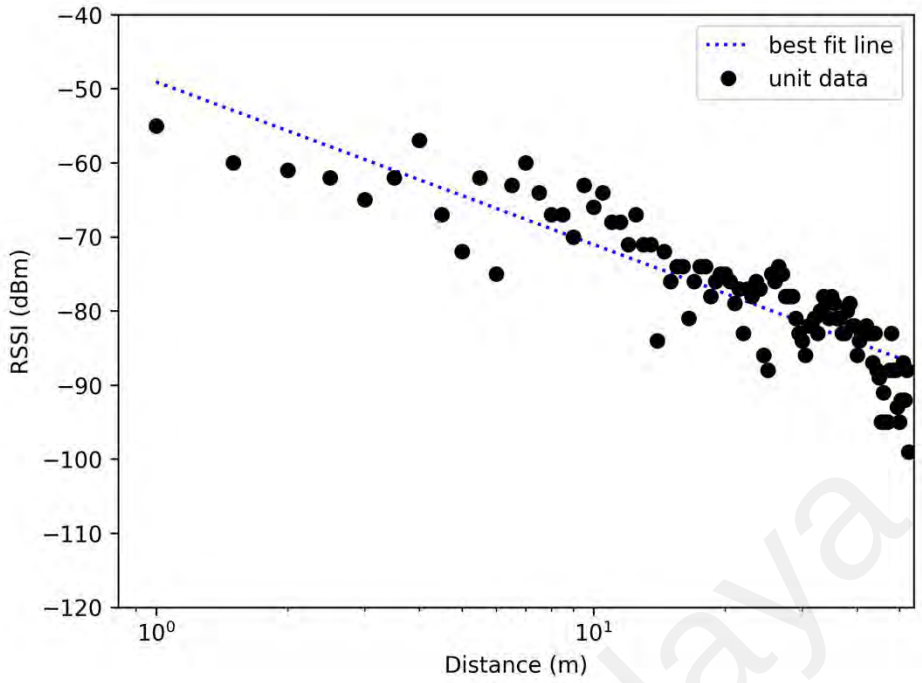

Figure 4.7: Log distance path loss model of the RSSI data collected in motion moving away from the receiver, with x-axis in logarithmic scale

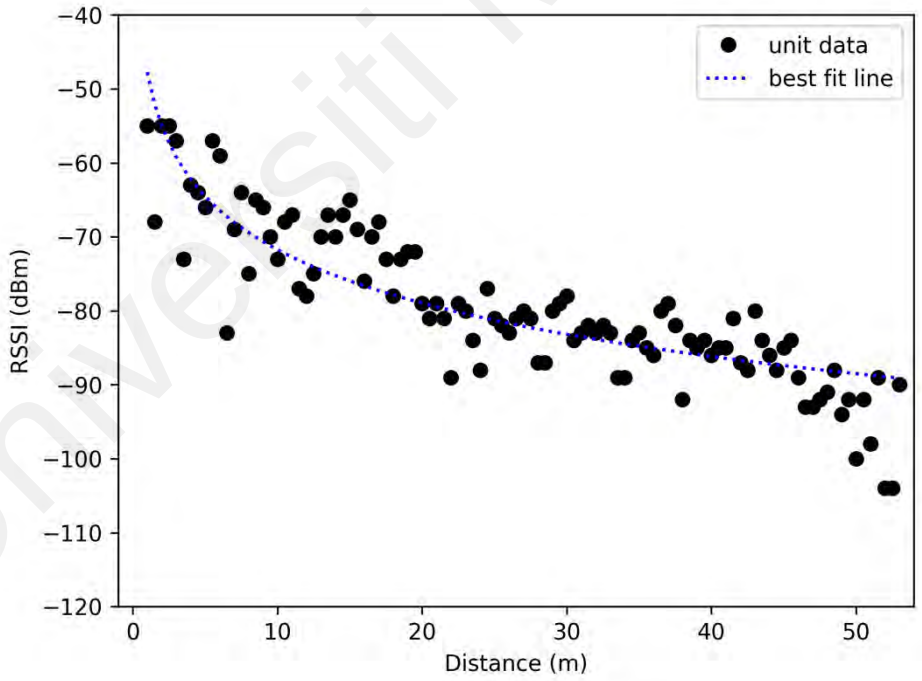

Figure 4.8: Log distance path loss model of the RSSI data collected in motion moving away from the receiver, with x-axis in linear scale

Universiti Malaya

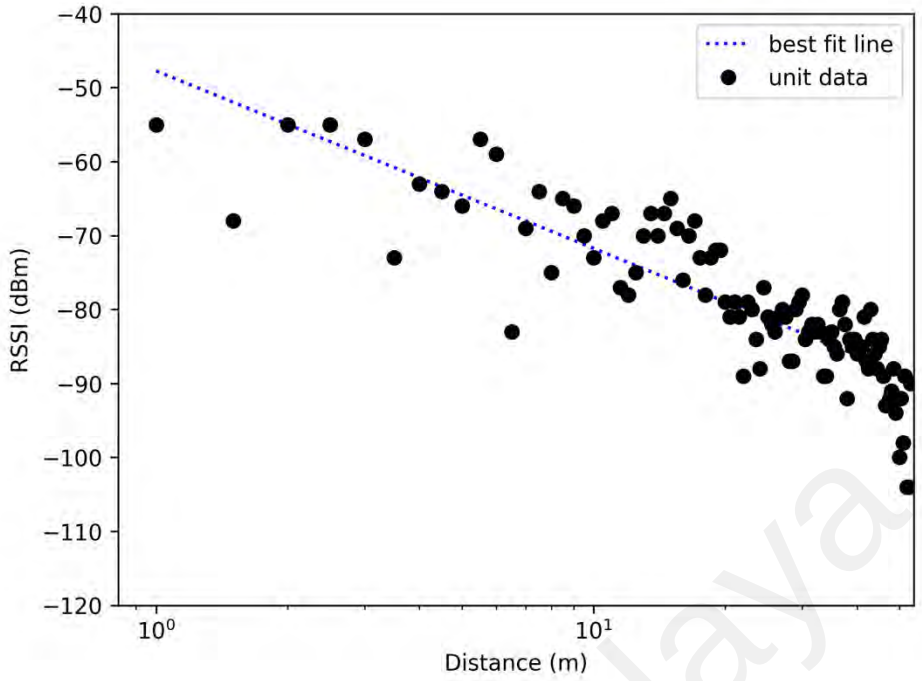

Figure 4.9: Log distance path loss model of the RSSI data collected in motion moving away from the receiver, with x-axis in logarithmic scale

From the graphs, we can observe a linear relationship between the RSSI values and the log of the distance, proving the log-distance path loss model. In Figure 4.6 and Figure 4.7, for the data points moving away from the receiver, the estimated path loss exponent was approximately 2.20 and the estimated path loss at 1m (d_0), was approximately 49.07 dB. In Figure 4.8 and Figure 4.9, for the data points with the beacon moving towards the receiver, the estimated path loss exponent was approximately 2.40 and the estimated path loss at 1m (d_0), was approximately 47.73 dB.

Similar to the log-distance experiment collected using static method, the estimated path loss at 1m was lower when moving towards the receiver compared to moving away from the receiver. This indicates that the body shadowing effect is more significant in locations nearer to the receiver.

To sum up, the observed path loss exponents in the experiments ranged from 2.20 to 2.75, which generally aligns with theoretical expectations for indoor environments.

Universiti Malaya

Typical values for indoor settings range from 1.6 to 3.6 (Al-Saman et al., 2021). The results fall within this range, indicating that the LoRa signal propagation in our test environment behaves similarly to other radio frequencies in indoor spaces. However, the variability in the observed exponents suggests that the data collection method, along with the structural characteristics of the test environment, such as walls, partitions, large industrial equipment, and dynamic obstacles, may influence signal propagation characteristics.

4.1.2 Multipath and Small-Scale Fading Effects

In this section, we present the results of our experimental analysis of multipath and small-scale fading effects on LoRa signal propagation in an indoor environment. The experiment was carried out in the same location as the preceding section.

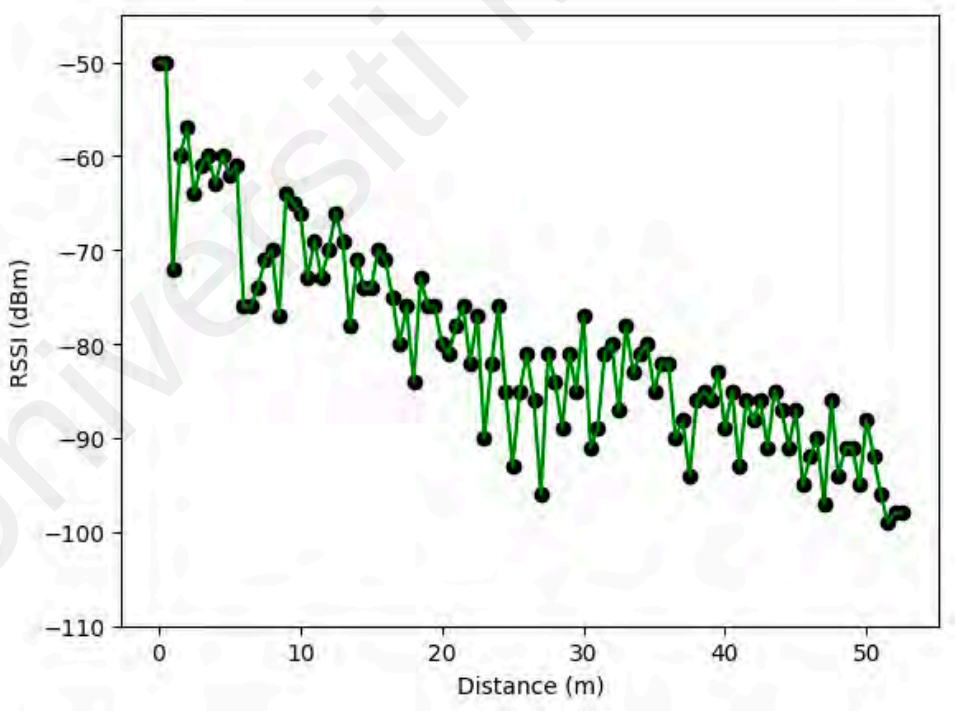

Figure 4.10: Plot of RSSI values against steps with increasing distance from receiver

Figure 4.10 illustrates the variation of RSSI values with increasing distance from the receiver. The overall trend of the graph shows that RSSI decreases when the distance

between the receiver and transmitter increases. However, when we focus on shorter distances, there was a non-monotonic pattern observed in the RSSI-distance relationship, where the RSSI values initially decrease with increasing distance, then increase at a certain point, and subsequently decrease again, suggesting the presence of multipath effects in the indoor environment.

Figure 4.11 depicts a scatter plot of the RSSI measurements collected within 1 meter or data collection point, with the first column representing 3.1 m, the second column representing 3.5 m, and the third column representing 3.9 m away from the receiver. These distances correspond to the start, middle, and end of a tile or data collection point, respectively.

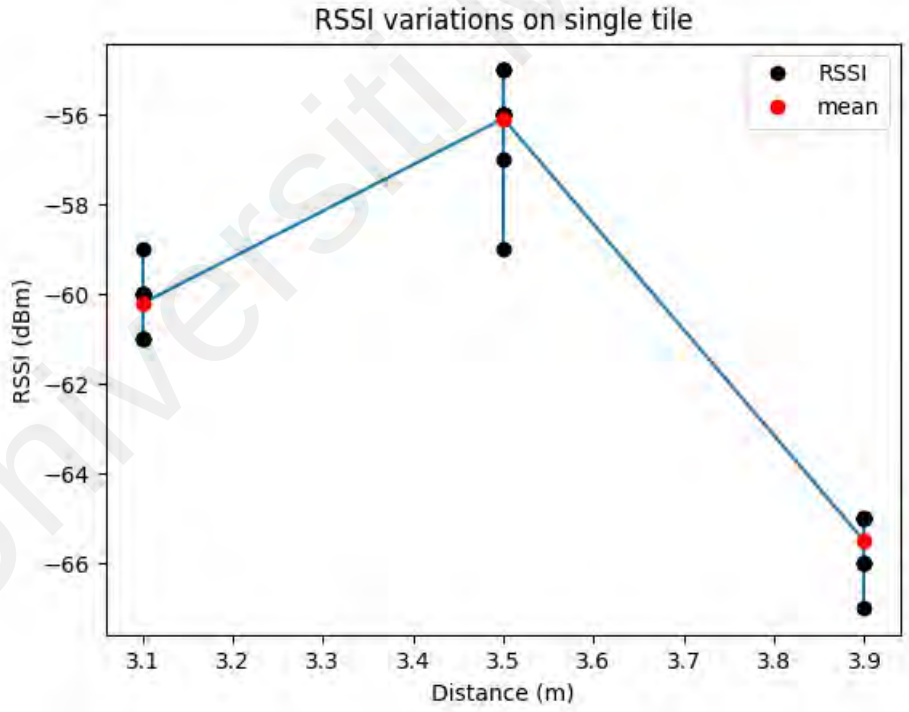

Figure 4.11: Scatter plot of RSSI values at the start, middle and end of a tile. The red dots represent the mean at each location.

The plot suggests the presence of multipath effects and signal attenuation over distance. The variations in RSSI values over different distances indicates the presence of multipath

Universiti Malaya

effects and signal attenuation. According to the large scale fading, the RSSI values decrease with increasing distance. However, in this instance, the data exhibits a distinct pattern. Contrary to the expected trend, the RSSI value at 3.5 m was the highest among the three measurements, reaching mean RSSI at -56.08 dB. In contrast, the mean RSSI values at 3.1 m (-60.2 dB) and 3.9 m (-65.5 dB) were lower, indicating signal attenuation as the distance from the transmitter increases. The observed RSSI variations within the 1-meter range are likely due to multipath effects, small-scale fading, and environmental reflections, which cause fluctuations in signal strength at different measurement points.

To quantify the variability in RSSI measurements, we calculated the standard deviation of RSSI values from the experiments from section 4.1.1. Figure 4.12 describes the standard deviation of RSSI values at each location.

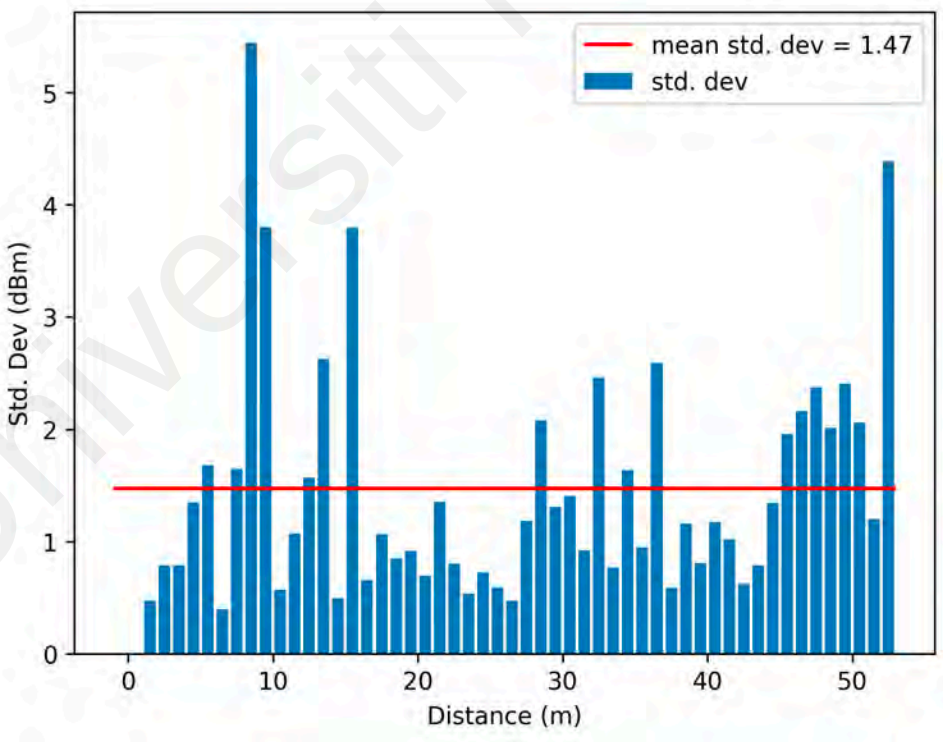

Figure 4.12: Standard deviation of RSSI values at different distances from the receiver

Figure 4.12 shows that there less correlation between distance and the standard deviation of RSSI values. However, it was observed that there were spikes at a few

locations where the standard deviation is much higher than the mean standard deviation. When these positions were projected into the real test environment, it was discovered that these positions are near to junctions to open areas such as lanes, doors and area for low workspaces meanwhile most of the tested area were resembling a tunnel like environment where machines are available at the left and right of the transmitter. Moreover, for some of the spikes in between range 30 m to 40 m, human and object movements near the transmitter were observed and noted manually during data collection.

Hence, this proves that the layout of the environment and nearby object movement may cause significant changes to the RSSI value. Furthermore, RSSI values collected in the same position are susceptible to temporal changes causing slight variations recorded values. This variability poses challenges for positioning accuracy, as it introduces uncertainty in distance estimation based on RSSI.

Conventional trilateration approaches for localization must account for the variable path loss exponent across different areas of the environment to accurately estimate distances from RSSI measurements. Fingerprinting methods may benefit from the distinct multipath patterns observed at different locations, potentially improving location discrimination. The observed small-scale fading effects suggest that positioning algorithms should incorporate temporal averaging or filtering to mitigate short-term RSSI fluctuations.

4.2 Machine Learning Methods for Single Point Estimation

In this section, the performance of various machine learning techniques for indoor positioning were evaluated. The machine learning methods investigated in this work can be broadly categorized into three classes: Classifier-based Methods, Regressor-based Methods, and Gaussian Process Regressor (GPR) Methods.

Universiti Malaya

To assess the performance of these machine learning techniques, we utilized two distinct datasets: the Motion Set and the Static Set. Within each dataset, we considered three different feature sets as described in section 3.2.1, to provide a thorough exploration of the impact of input data on the positioning accuracy. The feature sets included: (1) RSSI, Frequency Error, and SNR (All), (2) RSSI and SNR, (3) RSSI.

To quantify the positioning accuracy of the machine learning methods, we utilized the following performance metrics: Mean Absolute Error (MAE) and Root Mean Squared Error (RMSE). Performances of machine learning methods for each category will be described in detail in further subsections.

4.2.1 Classifier-based Methods for Indoor Positioning

First, we observe the performance of the classifier-based methods. Table 4.1 and Table 4.2 presents the MAE and RMSE results for the classifier-based methods, namely, Random Forest (RF), Decision Trees (DT), k-Nearest Neighbours (KNN), Weighted k-Nearest Neighbours (wKNN), Multilayer Perceptron (MLP), and Naive Bayes (NB) across the Motion and Static datasets, using the three different feature sets.

Table 4.1 and table 4.2 present the MAE and RMSE for the classifier category. For the static dataset with all features (RSSI, SNR & Frequency Error), the NB algorithm yielded the highest MAE and RMSE values 25.71725 m and 28.5481 m respectively. DT, MLP, KNN and wKNN algorithms present noticeable improvements in both MAE and RMSE values compared to the NB algorithm. Finally, the RF algorithm demonstrates the lowest error with MAE and RMSE values of 15.26747 m and 17.22313 m respectively.

Moving on to the static dataset with RSSI and SNR features, all algorithms show significant improvements in terms of accuracy compared to the static dataset with all features. The RF algorithm performs the best with MAE and RMSE values of 7.29921 m

Universiti Malaya

and 9.23356 m respectively. Followed by, MLP and wKNN with MAE of 8.26026 m and 8.26663 m and RMSE of 10.27202 m and 10.39511 m respectively.

Table 4.1: MAE values of various classifier models on the static and motion datasets

Dataset	Feature set	MAE (m)					
		RF	DT	KNN	wKNN	MLP	NB
Static	**All**	15.2675	21.6682	16.3969	16.2716	16.2385	25.7172
	RSSI & SNR	7.2992	11.1329	8.3278	8.2666	8.2603	11.3525
	RSSI	7.2867	11.0054	7.5618	7.5302	8.1239	11.2048
Motion	**All**	12.3557	13.7795	15.5437	15.4287	13.0594	16.9696
	RSSI & SNR	7.1242	8.2077	8.5046	7.6546	7.8079	8.4327
	RSSI	6.9330	8.3621	6.7764	6.9552	6.5849	6.2811

Table 4.2: RMSE values of various classifier models on the static and motion datasets

Dataset	Feature set	RMSE (m)					
		RF	DT	KNN	wKNN	MLP	NB
Static	**All**	17.2231	25.0820	18.0150	17.8998	18.6869	28.5481
	RSSI & SNR	9.2336	13.1406	10.4301	10.3951	10.2720	14.7586
	RSSI	9.3693	13.0476	9.4700	9.4545	10.2141	14.1974
Motion	**All**	14.5169	15.7116	17.4767	17.1254	15.1562	19.3589
	RSSI & SNR	9.1848	10.3641	10.4061	9.4642	9.8456	10.7937
	RSSI	8.9712	10.6624	8.5758	8.9235	8.6167	8.3063

For the static dataset with only RSSI, all classifier algorithms show an overall slight improvement in accuracy compared to datasets with more features. wKNN and KNN showed notable improvements of 8.91% and 9.19% in MAE and 9.05% and 9.20% in RMSE. The RF algorithm still performs the best among all algorithms with MAE and RMSE values of 7.28671 m and 9.36927 m, respectively, although the RMSE value was slightly higher than that of the static dataset with both RSSI and SNR features.

Overall, for the static dataset, the RF algorithm outperforms the other algorithms for all feature sets. The RSSI-only feature set has the highest overall accuracy, followed by RSSI & SNR, and then RSSI, SNR & Frequency error.

Universiti Malaya

For the motion dataset with all features (RSSI, SNR & Frequency Error), the NB algorithm again yielded the highest MAE and RMSE values of 16.96955 m and 19.35699 m, respectively. However, the other Classifier algorithms, such as DT, MLP, KNN, and wKNN, demonstrated significant improvements in accuracy, with MAE values ranging from 13.05941 m to 15.54375 m and RMSE values from 15.15616 m to 17.47666 m. Among the algorithms, RF still exhibits the lowest MAE and RMSE values, with 12.35570 m and 14.51688 m, respectively.

Focusing on the motion dataset with RSSI and SNR features, the RF algorithm again emerges as the top performer, with an MAE of 7.12415 m and an RMSE of 9.18478 m. When considering the motion dataset with only RSSI features, the Classifier algorithms generally demonstrated slightly lower errors compared to the motion dataset with RSSI and SNR features. While RF, typically regarded as a robust performer, did not exhibit the highest accuracy, the NB algorithm emerged as the best performer, with an MAE of 6.28115 m and RMSE of 8.30634 m, with MLP shows the second highest accuracy in terms of MAE (6.58493 m) and KNN in terms of RMSE (8.57576 m).

For the motion dataset, the NB classifier when used on RSSI only features the highest accuracy. In general, the classifier algorithms show better results when applied on Motion dataset than Static dataset. Also, better accuracy can be obtained when using only RSSI feature.

4.2.2 Regression-based Methods for Indoor Positioning

Table 4.3 and Table 4.4 presents the results for the regression-based methods, namely, RF, DT, wKNN, MLP and Linear Regression (LR) across the Motion and Static datasets, using the three different feature sets.

Universiti Malaya

Table 4.3: MAE values of various regression models on the static and motion datasets

Dataset	Feature set	MAE (m)				
		RF	DT	wKNN	MLP	LR
Static	**All**	18.21516	15.60140	16.26320	36.96480	18.57989
	RSSI & SNR	6.18885	7.80812	7.88411	7.24342	6.85376
	RSSI	5.85477	7.05994	7.09093	7.40290	7.07941
Motion	**All**	9.97450	11.13061	14.88617	18.06706	13.55468
	RSSI & SNR	5.67654	7.28150	6.54288	6.41449	6.99218
	RSSI	5.39553	6.13065	5.51865	5.70889	7.05318

Table 4.4: RMSE values of various regression models on the static and motion datasets

Dataset	Feature set	RMSE (m)				
		RF	DT	wKNN	MLP	LR
Static	**All**	20.35705	17.38273	17.89919	38.58354	19.77187
	RSSI & SNR	7.76168	9.87339	9.92101	8.48961	7.66823
	RSSI	7.41759	9.04934	9.01177	8.73742	7.86590
Motion	**All**	12.35449	13.57393	16.65390	19.58223	14.88372
	RSSI & SNR	6.73506	9.14580	7.94713	7.30727	7.71376
	RSSI	6.56478	6.61691	7.04710	6.69811	7.78369

Starting with the static dataset, the regressor models generally demonstrated higher accuracy compared to the classifier models. For the static dataset with all features, the DT algorithm achieved the lowest MAE of 15.60140 m and RMSE of 17.38273 m. Focusing on the static dataset with only RSSI and SNR features, the performance of the Regressor models improved significantly. The RF algorithm has the lowest MAE (6.18886 m) while LR has the lowest RMSE (7.66822 m). When considering the static dataset with only RSSI features, the Regressor models continued to demonstrate high accuracy. The RF algorithm achieved an MAE of 5.85477 m and an RMSE of 7.41759 m, outperforming the other Regression models, which was 17% more accurate than the second highest performing model for this feature set.

Universiti Malaya

Transitioning to the motion dataset, the Regression models exhibited slightly lower errors compared to the static dataset. For the motion dataset with all features, the RF algorithm demonstrated the best results, with an MAE of 9.97450 m and RMSE of 12.35448 m. Examining the motion dataset with RSSI and SNR features, the Regressor models showed further improvements in accuracy. The RF algorithm achieved an MAE of 5.67654 m and an RMSE of 6.73506 m, outperforming the other Regression models. When applying the Regression models on the motion dataset with only RSSI features, the RF algorithm maintained its position as the top performer, with an MAE of 5.39553 m and an RMSE of 6.56478 m. The RF algorithm with motion dataset with only RSSI features appears to have the highest accuracy among all regressors with all datasets and feature sets in the comparison.

Overall, the regression-based methods show a similar trend with the classifier-based methods where the RSSI only feature set displays better performance over the other two feature sets in both Motion and Static datasets. On top of that, the regressors show better accuracy with the Motion dataset than the Static dataset. However, regression-based methods show better accuracy when compared to classifier-based models, with a 14.1% (MAE) and 21.0% (RMSE) increase in accuracy.

4.2.3 Gaussian Process Regression (GPR) for Indoor Positioning

Table 4.5 and Table 4.6 presents the performance of the GPR models in estimating positioning error, using different kernel functions: Radial Basis Function (RBF), Matérn, the sum of RBF and Matérn, and the product of RBF and Matérn. The models were evaluated on the Static and Motion datasets with the feature sets: ALL, RSSI & SNR, and RSSI.

Universiti Malaya

Table 4.5: MAE values of GPR models using different kernel combinations

Dataset	Feature set	MAE (m)			
		RBF	**Matérn**	**Sum**	**Product**
Static	**All**	32.11951	51.20579	52.32647	51.36770
	RSSI & SNR	11.52446	6.96429	6.79526	6.96431
	RSSI	15.03679	6.45970	6.09794	6.45974
Motion	**All**	23.53539	15.54725	14.24731	15.54755
	RSSI & SNR	6.40863	6.04709	6.04315	6.04710
	RSSI	5.46437	5.25086	5.23723	5.25086

Table 4.6: RMSE values of GPR models using different kernel combinations

Dataset	Feature set	RMSE (m)			
		RBF	**Matérn**	**Sum**	**Product**
Static	**All**	34.43144	54.13059	55.27158	54.29538
	RSSI & SNR	15.51277	8.58881	8.08889	8.58886
	RSSI	19.61008	7.78767	7.32813	7.78772
Motion	**All**	26.01517	17.49776	15.36567	17.49814
	RSSI & SNR	7.21374	6.89329	6.90022	6.89329
	RSSI	6.39111	6.26103	6.25507	6.26103

Starting with the static dataset with all features, the GPR models underperform when compared to classifier-based methods and regression-based methods with MAE values ranging from 32.11951 m to 52.32647 m and RMSE values ranging from 34.43144 m to 55.27158 m. These results show that the GPR models with all features were highly inaccurate and most of the estimates lie outside of the test space.

Moving on to the static dataset with only RSSI and SNR features, all GPR models except for the GPR model with RBF kernel exhibits better accuracy than all classifiers and all regressors except for the RF regressor. With the GPR model with RBF kernel having the highest MAE and RMSE of 11.52446 m and 15.51276 m respectively while the GPR model using the sum of RBF and Matérn kernel having the lowest MAE and RMSE values of 6.79525 m and 8.08889 m respectively.

Universiti Malaya

When considering the static dataset with only RSSI features, the GPR model with the sum of RBF and Matérn kernels achieved the lowest MAE of 6.09794 m and RMSE of 7.32813 m, which outperform all classifiers and most regressors used in Table 4.1 and Table 4.2.

Transitioning to the motion dataset, the GPR models generally exhibited higher accuracy compared to the static dataset, similar to the observations from Table 4.1 and Table 4.2. For the motion dataset with all features, the GPR models have much higher accuracy compared to when used on the static dataset with all features with MAE ranging from 14.24731 m to 23.53539 m. However, they still exhibit higher errors compared to classifiers in Table 4.1 and regressors in Table 4.2.

Similarly to the static dataset with RSSI and SNR feature set, the GPR models with the motion dataset with RSSI and SNR features generally outperform all classifiers and most of the regressors except for the RF regressor. The GPR models with Matérn kernel, sum of RBF and Matérn kernels and product of RBF and Matérn kernels having similar MAE (6.04709 m, 6.04315 m, 6.04709 m) and RMSE (6.89329 m, 6.90022 m, 6.89329 m).

When considering the motion dataset with only RSSI feature, the GPR models generally surpassed the best results in Table 4.1 and Table 4.2. All GPR models except for the model using RBF kernel has higher MAE (5.46437 m) than the RF regressor model used on the motion dataset with only RSSI feature (5.39553 m), moreover, all GPR models have better RMSE, indicating that GPR was able to reduce larger errors. The GPR model with the sum of RBF and Matérn kernel achieved the best results, with an MAE of 5.23723 m and RMSE of 6.25507 m. The other 2 kernels (Matérn kernel and product of Matérn and RBF kernel) also have similar accuracy with the model with sum of RBF and Matérn kernels with only slight differences in error.

Universiti Malaya

Overall, the performance of GPR models were generally better compared to the Classifier and Regressor models, particularly when the number of features were less and used on the motion dataset. Besides, the usage of the Matérn kernel performs better than the RBF kernel. Combining Matérn and RBF kernels by either summing or multiplying them also proved effective.

To sum up, one key finding is that the motion dataset generally outperformed the static dataset in terms of positioning error estimation accuracy. By collecting data in motion, a more dynamic variation in the collected data is achieved. This dynamic variation leads to increased positioning accuracy with a reduced total number of data points needed. Another observation is that using only the RSSI feature, without the inclusion of SNR or frequency error, yielded the best results across the Classifier, Regressor, and GPR models. This indicates that the RSSI feature alone was the most informative and effective in representing the signal characteristics necessary for accurate positioning error estimation.

Regarding machine learning categories, by looking solely into the motion dataset with only RSSI feature, which exhibits better results, the NB classifier achieved the best accuracy among classification models, while the RF regressor exhibited superior performance among regression models. Generally, the regression-based methods outperformed the classifier-based methods in terms of both MAE and RMSE across most datasets and feature sets. This can be attributed to the fact that regression models directly predict continuous position coordinates, allowing for finer-grained localization compared to classifiers that assign discrete class labels.

Universiti Malaya

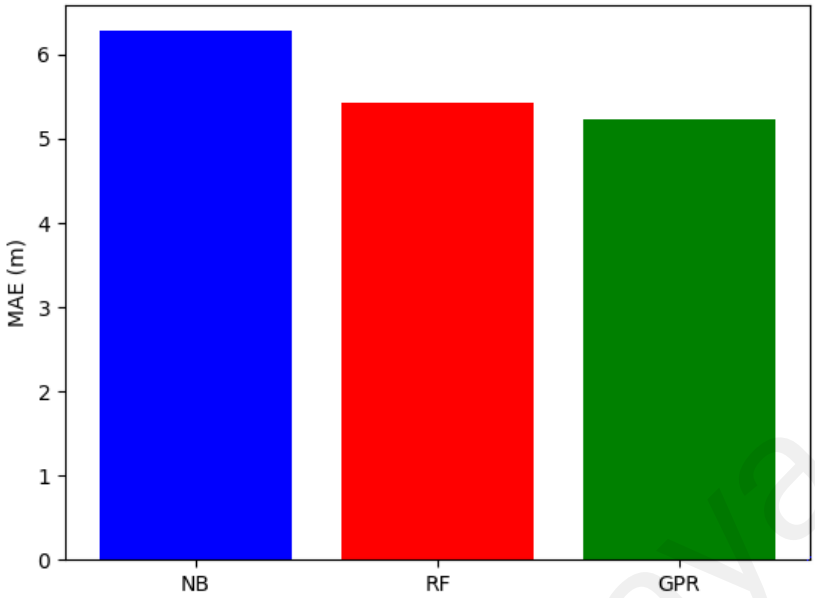

Figure 4.13: Comparison of MAE for the best machine learning models from Table 4.1, Table 4.3 and Table 4.5 respectively

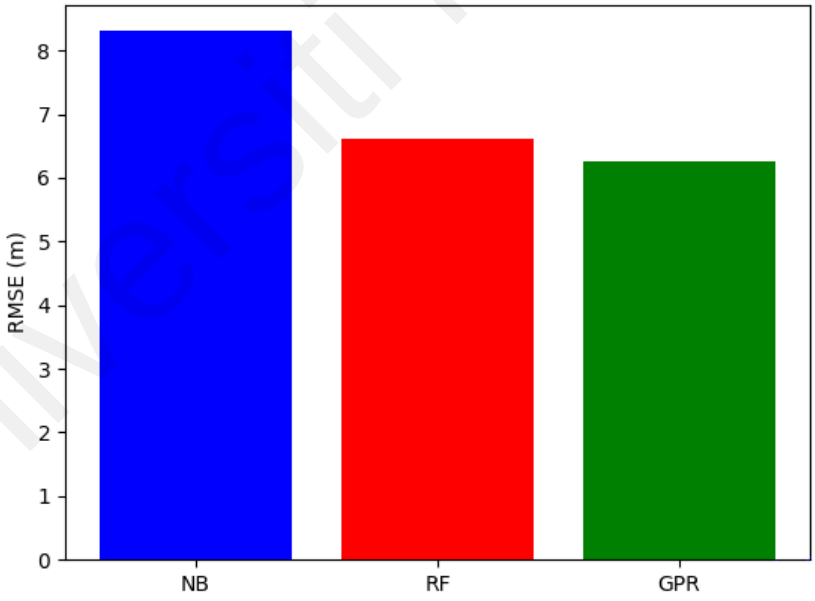

Figure 4.14: Comparison of RMSE for the best machine learning models from Table 4.2, Table 4.4 and Table 4.6 respectively

Universiti Malaya

The GPR models generally demonstrate the highest accuracy specifically when used on. Also, GPR models with motion dataset with only RSSI feature greatly reduced the RMSE values, suggesting the improvement of larger errors. The best performing GPR (with sum of Matérn and RBF kernels) achieved an increase in accuracy by 16.6% and 2.9% in MAE and 24.7% and 4.7% in RMSE in comparison to the NB classifier and RF regressor respectively.

4.3 DGP Regression

In this section, the results obtained from the DGP Regression model for single point estimation were presented. The system parameter selection process which includes kernel selection, selection of number of dimensions in the hidden layer and number of inducing points to identify the optimal model configuration were described. Subsequently, the performance of the DGP model were evaluated using various metrics and compare it with the results obtained from the previous sections.

4.3.1 System Parameter Selection

In selecting the kernel, we tested two types of kernel combinations: the sum and product of the RBF kernel and the Matérn kernel. We chose these kernel combinations because they outperformed a single kernel in section 4.2.3. Table 4.4 compares these kernel combinations.

Table 4.7: Comparison of Sum and Product of the RBF kernel and the Matérn kernel

Kernel name	MAE (m)	RMSE (m)	Training loss	Training time (s)
Sum	5.10877	6.19212	5.80792	183.48
Product	5.04566	6.14681	5.82745	185.00

The product of the RBF kernel and the Matérn kernel has slightly better performance in all aspects except training time when compared to the sum of the RBF kernel and the

Matérn kernel. The product of the RBF kernel and the Matérn kernel is chosen for further experiments.

For the number of dimensions in the hidden layer, 10 different numbers of dimensions were used ranging from 1 to 19. Figure 4.15 and Figure 4.16 show the MAE and RMSE at different numbers of dimensions. The MAE and RMSE exhibit similar trends. When the number of dimensions is 1, the MAE and RMSE were 7.15 m and 8.13 m respectively. The positioning error dropped and remained relatively low and stable for the dimensions ranging from 3 to 15 dimensions. The model with 3 dimensions has the lowest MAE of 4.98 m while the model with 15 dimensions has the lowest RMSE with 6.10 m. However, beyond 15 dimensions, there is a noticeable and substantial increase in both MAE and RMSE to approximately 9.94 m and 16.76 m. This indicates that the model performance deteriorates rapidly with an oversized number of dimensions.

The rapid performance deterioration observed beyond 15 dimensions in the hidden layer can be attributed to the curse of dimensionality. As the number of dimensions increases, the data becomes increasingly sparse in the high-dimensional space, making it more challenging for the model to generalize effectively. This sparsity can lead to overfitting, where the model captures noise in the training data rather than the underlying signal propagation patterns. This finding highlights the importance of careful dimensionality selection in DGP models for indoor positioning applications, balancing the need for expressive power with the risk of overfitting.

The training loss in Figure 4.17 also shows that it exhibits similar trends with the evaluation accuracy at different numbers of dimensions with the lowest training loss at 5 dimensions (5.83). Figure 4.18 shows the training time at each number of dimensions. As shown, the training times show an upward trend as number of dimensions increases.

Universiti Malaya

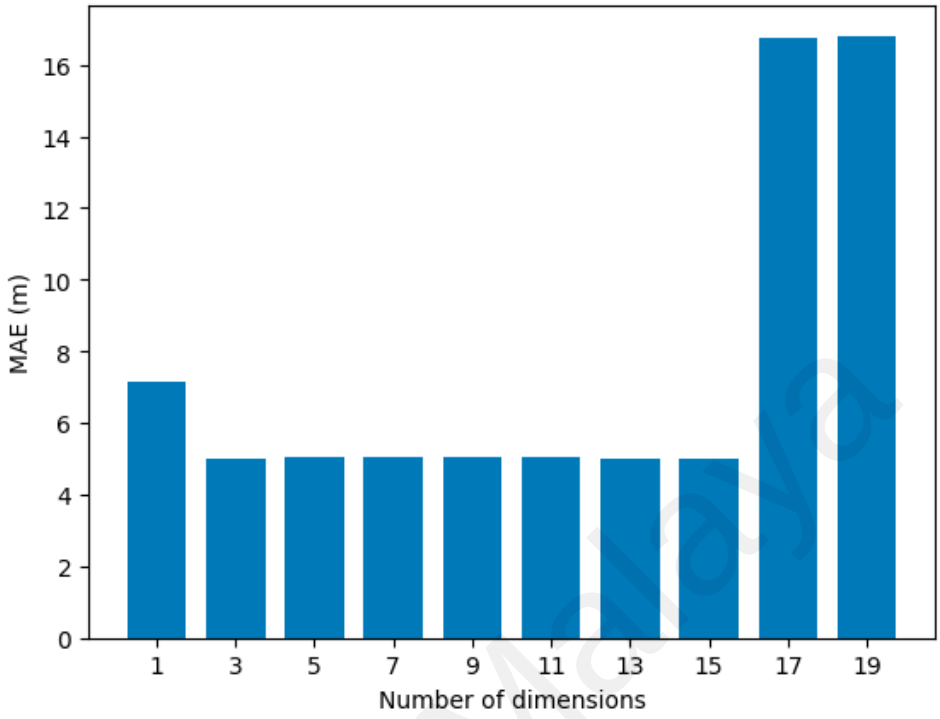

Figure 4.15: MAE of the DGP model on the Motion dataset with RSSI only feature set at different number of dimensions

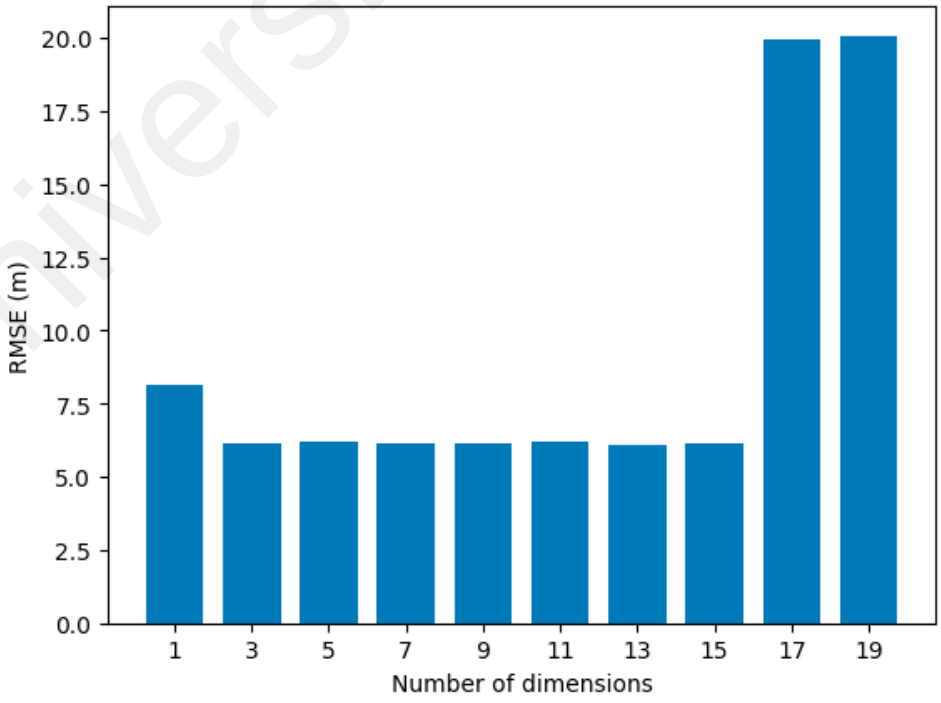

Figure 4.16: RMSE of the DGP model on the Motion dataset with RSSI only feature set at different number of dimensions

Universiti Malaya

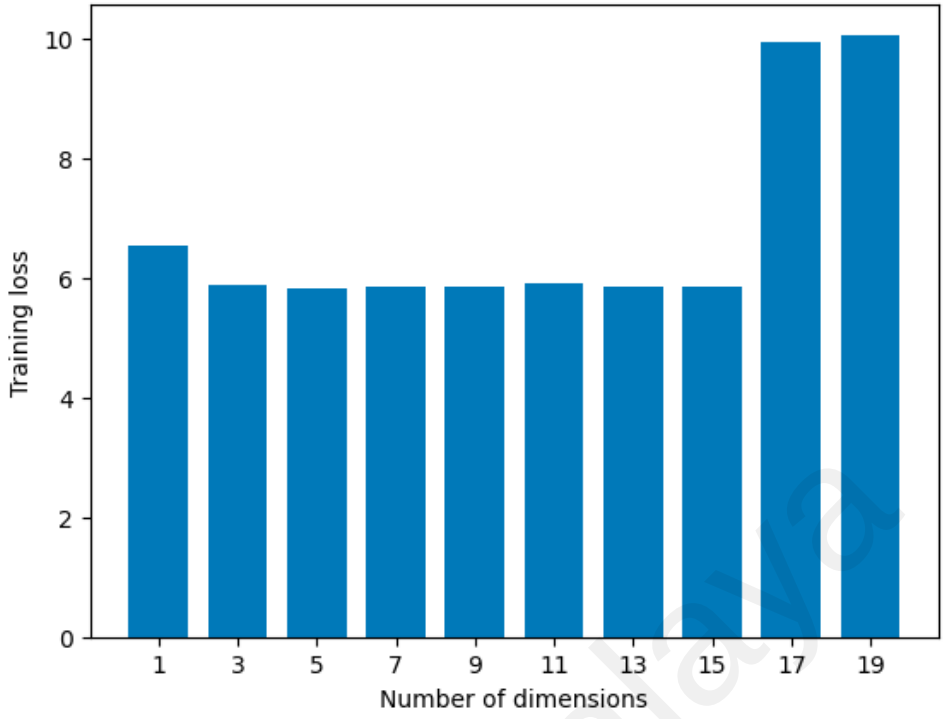

Figure 4.17: Training loss of the DGP model on the Motion dataset with RSSI only feature set at different number of dimensions

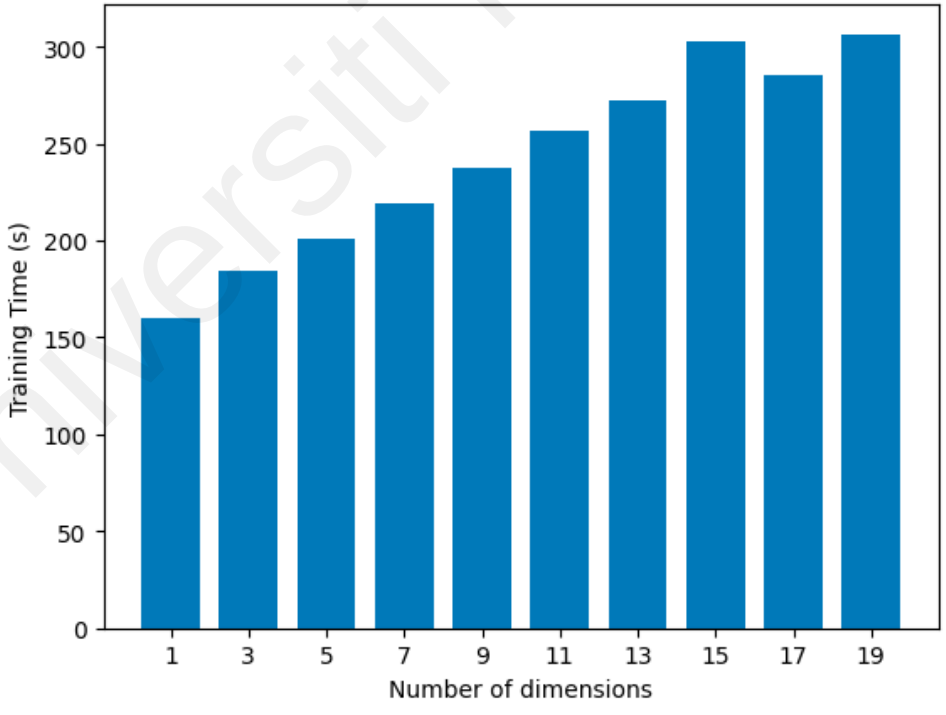

Figure 4.18: Training times of the DGP model on the Motion dataset with RSSI only feature set at different number of dimensions

Universiti Malaya

Figure 4.19 to Figure 4.22 shows the MAE, RMSE, training loss and training time for different numbers of inducing points. The MAE, RMSE and training loss is relatively constant across the range of number of inducing points. The MAE and RMSE exhibit a decreasing trend as the number of inducing points increases when ranging between 24 and 48 inducing points. Beyond 48 inducing points, the MAE and RMSE slowly increase as the number of inducing points increases. 48 inducing points produces the lowest MAE and RMSE at 4.95 m and 6.08 m respectively. Moreover, the training time of the models shows a general up trend as the number of inducing points increases. For our specific indoor positioning scenario, 48 inducing points provided the best balance between model expressiveness and generalization ability. This value is chosen for further experiments.

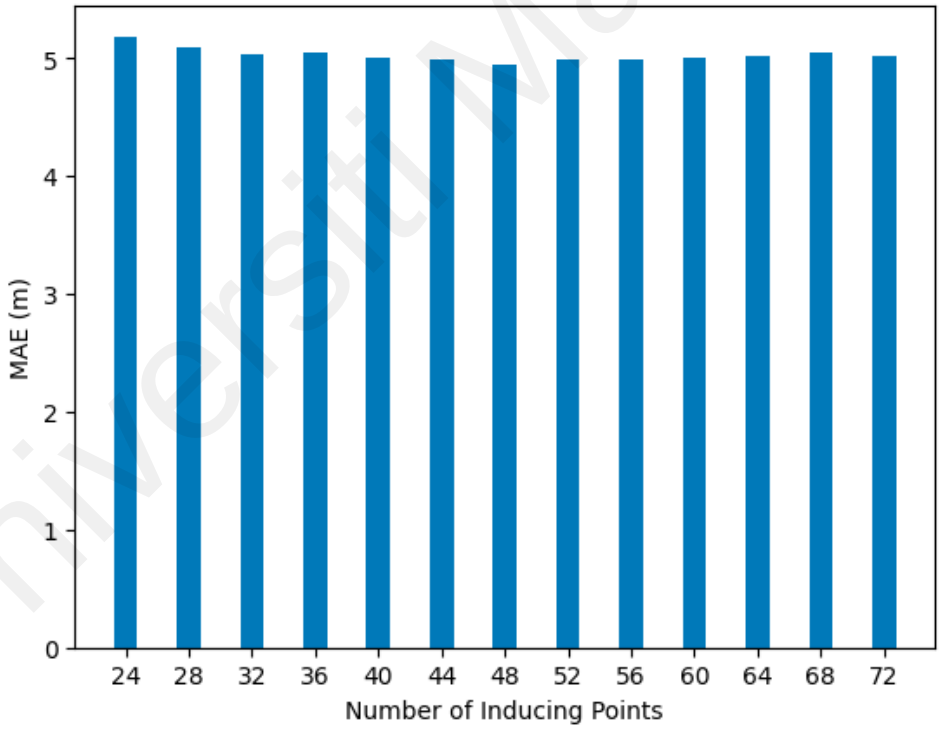

Figure 4.19: MAE of the DGP model on the Motion dataset with RSSI only feature set at different numbers of inducing points

Universiti Malaya

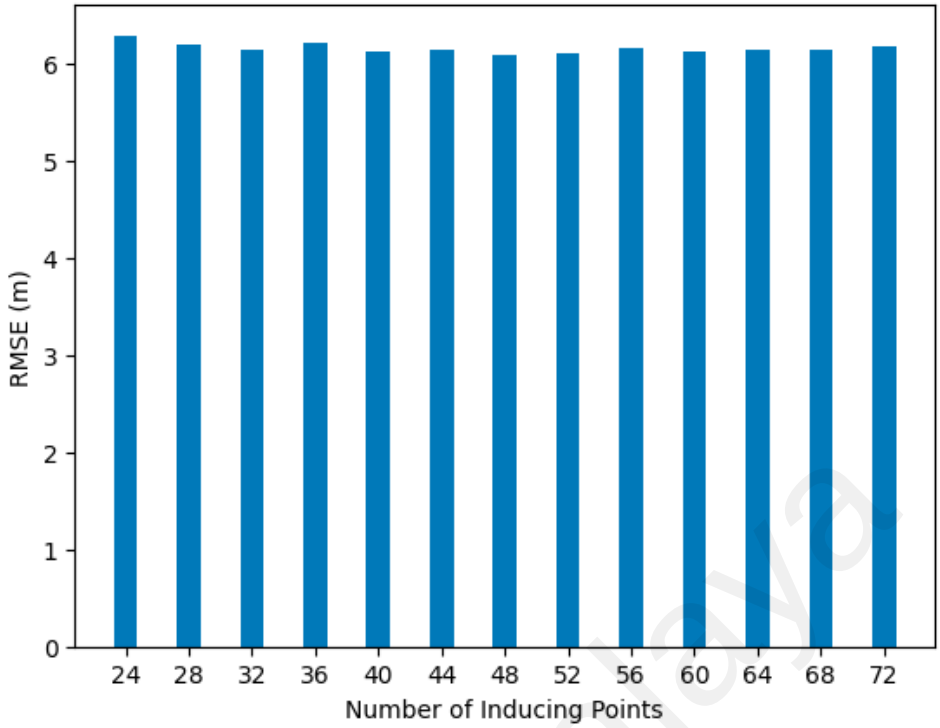

Figure 4.20: RMSE of the DGP model on the Motion dataset with RSSI only feature set at different numbers of inducing points

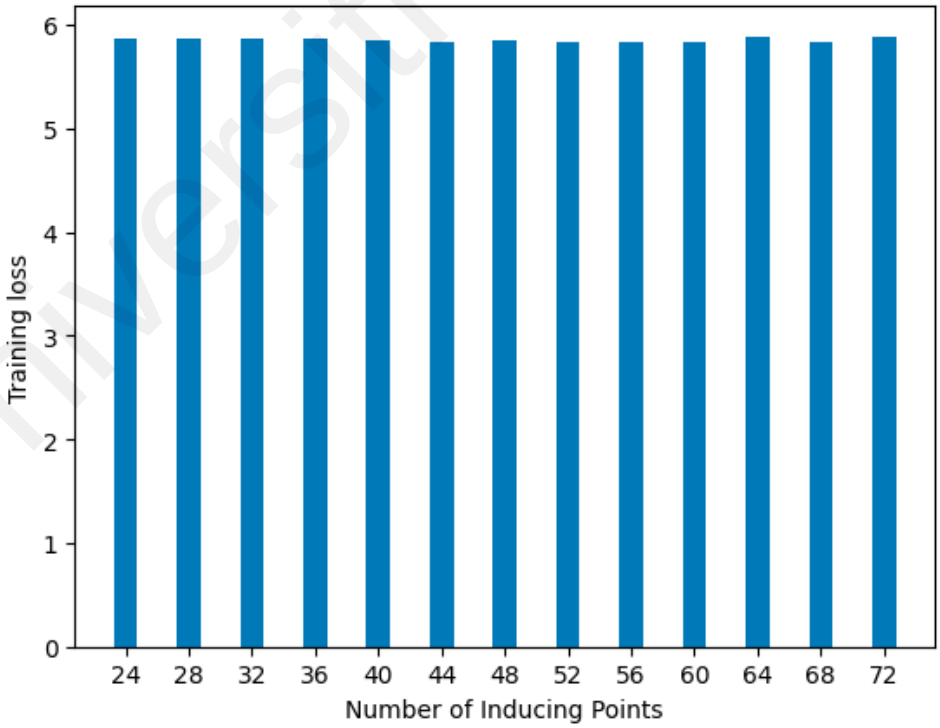

Figure 4.21: Training loss of the DGP model on the Motion dataset with RSSI only feature set at different number of inducing points

Universiti Malaya

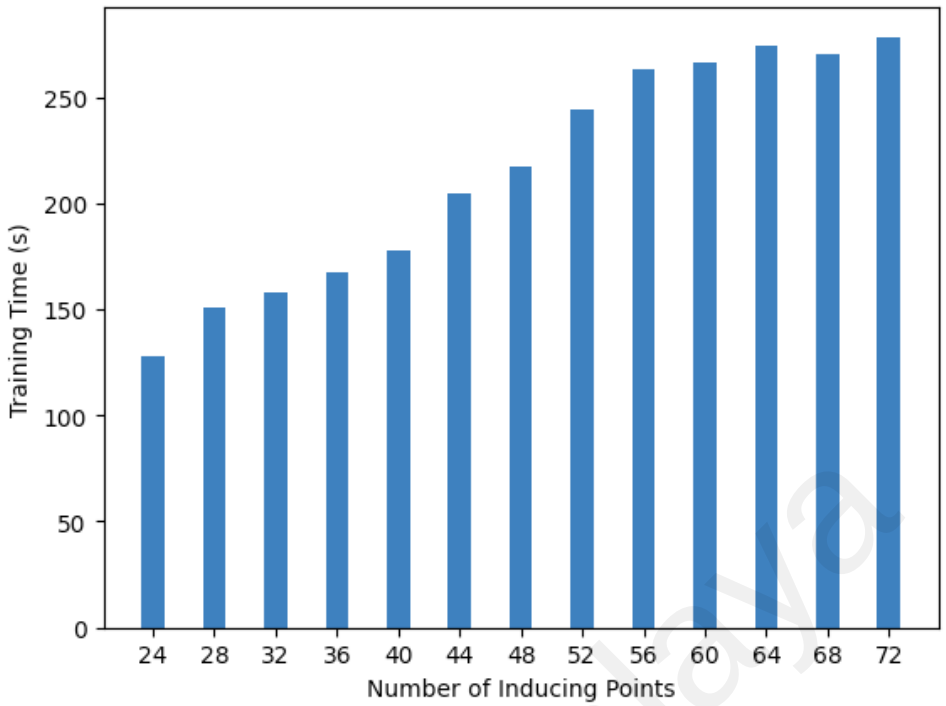

Figure 4.22: Training times of the DGP model on the Motion dataset with RSSI only feature set at different number of inducing points

4.3.2 Comparison with GPR

Taking the results with best accuracy, the model with 5 dimensions at the hidden layer and 48 inducing points were chosen. The model performance was compared to the best performing model in Section 4.3.1, GPR model with motion dataset. The DGP has an accuracy of MAE and RMSE of 4.94972 m and 6.07725 m while the GP's had MAE of 5.23723 m and RMSE of 6.25507 m. DGP showed an improvement of 5.5 % in terms of MAE and 2.8 % in terms of RMSE. Additionally, the median positioning error for the DGP was 4.27 m while the GPR has a positioning error of 4.55 m.

Figure 4.22 illustrates the cumulative distribution function (CDF) of positioning errors for the DGP and GPR method. From the figure, it can be observed that the DGP curve lies above the GPR curve for most of the distance error range. This is more obvious at lower positioning errors, between 1.5 m and 6.0 m. 56 % of the positioning errors are lower than 5 m for the GPR, whereas 59 % of the positioning errors are lower than 5 m with DGP. 29 % of the positioning errors are lower than 3 m for the GPR, whereas 36 %

Universiti Malaya

of the positioning errors are lower than 3 m with DGP. The positioning errors have less significant differences on larger distance errors when they are larger than 7 m. This indicates that both models struggle similarly in challenging areas, possibly due to severe fluctuations in RSSI readings in one or more BSs. Further improvements such as targeted improvements or hybrid approaches are needed to overcome these challenging areas.

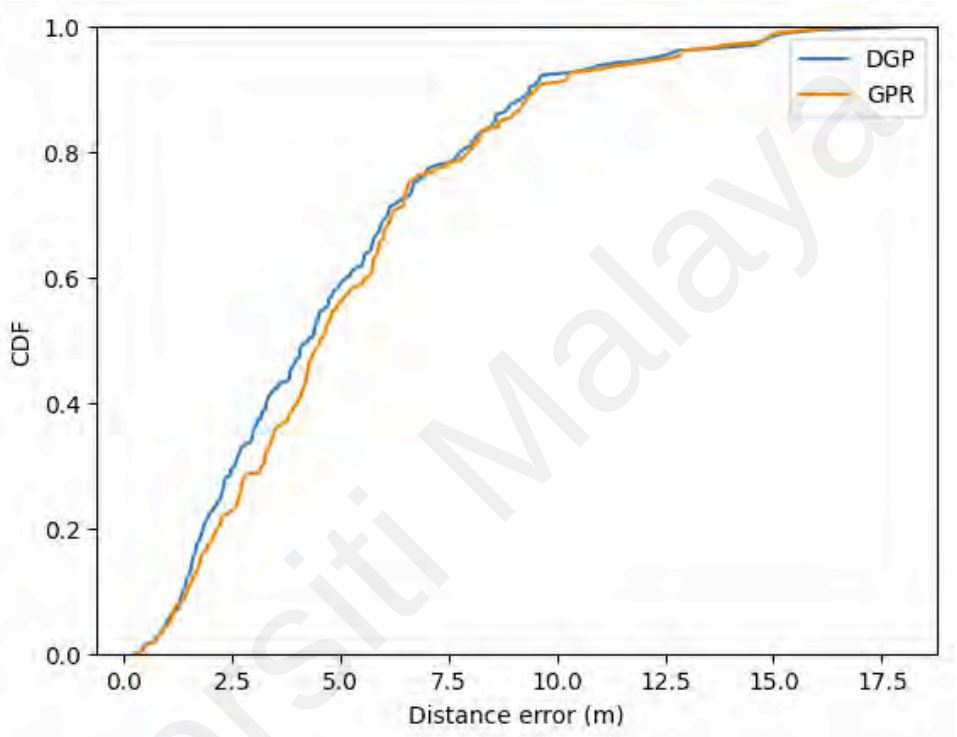

Figure 4.23: CDF of the positioning error for the DGP and GPR methods

4.4 Enhancing Single Point Estimation

This section analyses the impact and performance improvements achieved by incorporating the various techniques proposed in Section 3.5 to enhance the single point position estimates obtained from the machine learning models. The DGP regression model would be used as the baseline model for the experiments in this section.

4.4.1 Temporal-Weighted RSSI Averaging

The weighting factor λ in the Temporal-Weighted RSSI Averaging (TWA) scheme determines the relative importance given to recent samples compared to older samples.

Figure 4.24 show the positioning error distributions for different values of λ ranging from 0.1 to 0.9 with lag numbers of 1, 2, and 3.

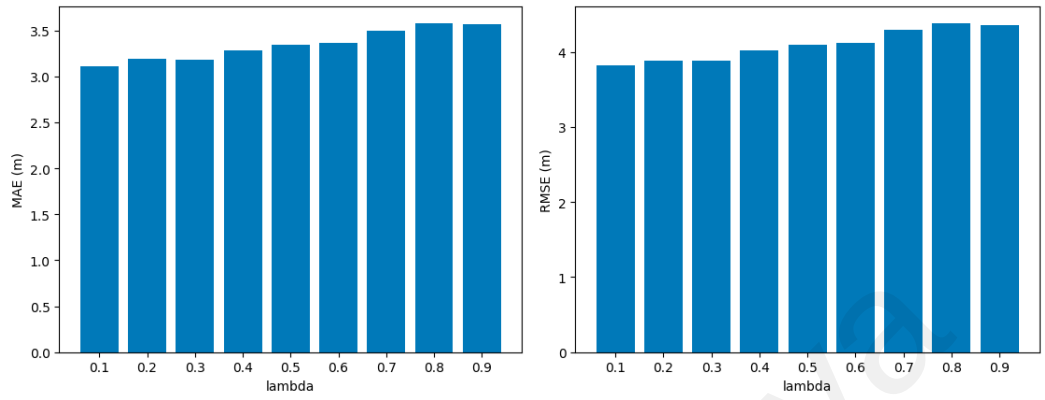

(a)

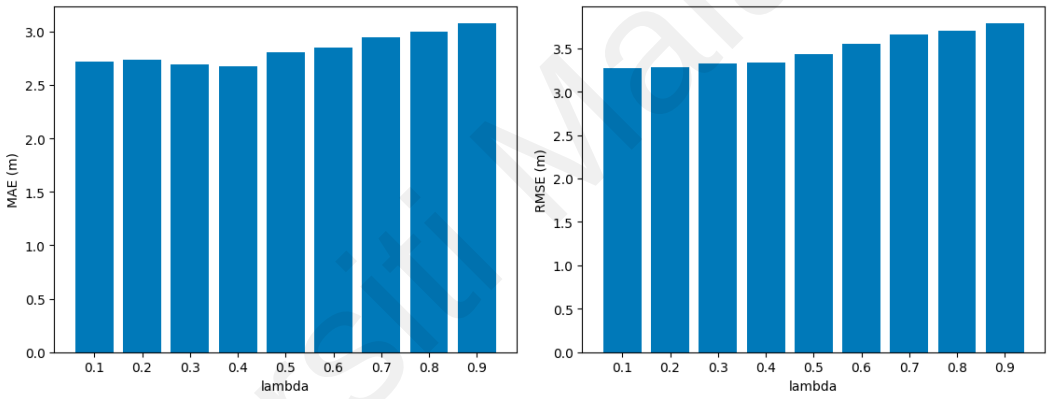

(b)

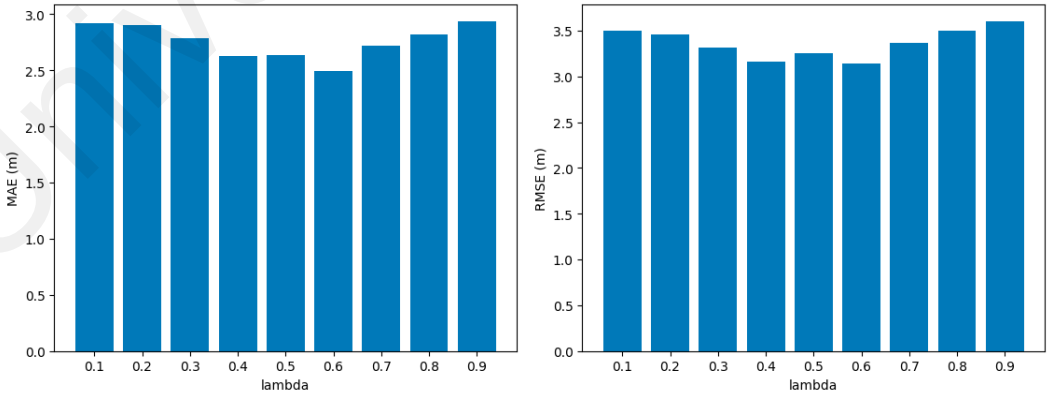

(c)

Figure 4.24: MAE and RMSE of the DGP model when using the TWA for lambda values ranging from 0.1 to 0.9 with a lag of (a) 1 (b) 2 (c) 3

Universiti Malaya

Figure 4.24 (a) shows the performance of TWA method with DGP regression with a lag of 1. The MAE values range from approximately 3.1 to 3.6 meters, with the lowest error occurring at lambda = 0.1. The higher lambda values result in increased errors showing that the historical value carries a crucial weightage to improving the positioning accuracy. Meanwhile in Figure 4.24 (b) shows the results with a lag of 2, The MAE values show a slight improvement, ranging from approximately 2.6 to 3.0 meters, while the RMSE values range from approximately 3.2 to 3.8 meters. The MAE has the lowest MAE occurring at lambda = 0.4 while the lowest RMSE was at lambda = 0.1. The lambda values between 0.1 to 0.4 show relatively close MAE and RMSE values but then showed an increasing trend starting lambda = 0.5. Furthermore, Figure 4.24 (c) illustrates the performance with a lag of 3. The MAE values exhibit the best performance, ranging from approximately 2.4 to 3.0 meters, while the RMSE values range from approximately 3.1 to 3.6 meters, with the lowest error at lambda = 0.6.

In conclusion, the TWA technique can largely increase the positioning accuracy by correlating the instantaneous RSSI value with its previous RSSI values. The lower lags generally show better performance with the use of lower lambda values. However, when the number of lags increases, a higher lambda value can be used for optimal results. Figure 4.25 shows the comparison of the histogram of errors between the DGP models with raw data and TWA technique, represented by DGP and TWA-DGP respectively. It can be observed that TWA-DGP significantly reduces the frequency of errors larger than 5 m and only one position estimate is larger than 10 m which is the first data point where it was unable to be smoothen by the weighting technique.

Universiti Malaya

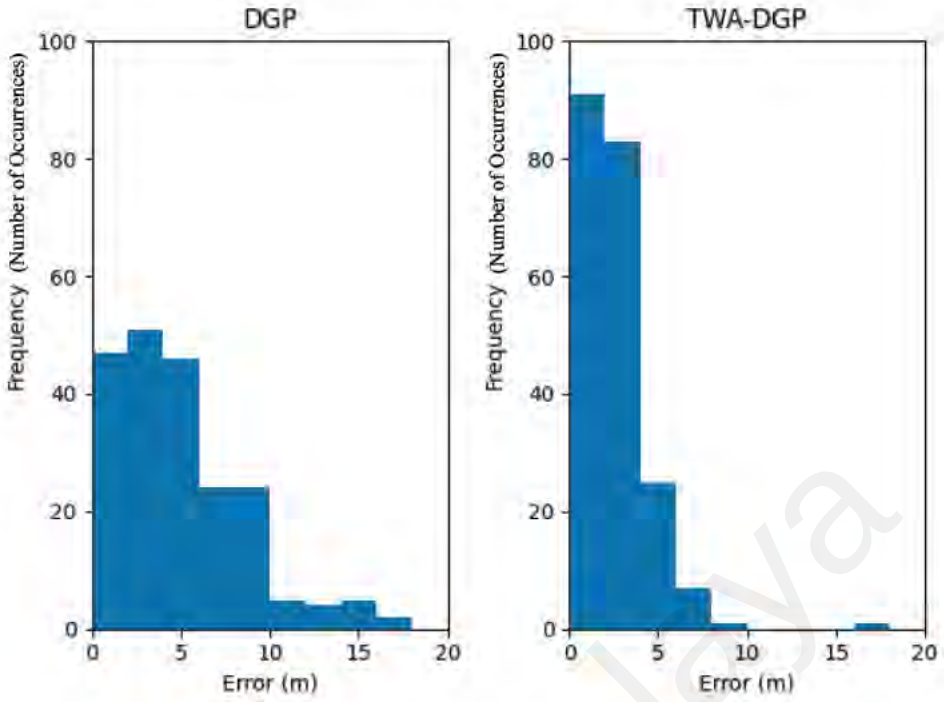

Figure 4.25: Comparison histograms representing error values of DGP and TWA-DGP

4.4.2 Kalman Filtering

The Kalman filter was applied to refine the position estimates obtained from the DGP model. The measurement noise covariance parameter R in the Kalman filter was tuned using a grid search approach, with values of 0.01, 0.1, 1, and 10 tested.

Table 4.8 presents the MAE and RMSE of the positioning system when using different R values for the Kalman filter, with DGP models trained on raw RSSI and Temporal-Weighted averaging RSSI, represented by DGP-KF and TWA-DGP-KF respectively.

When the DGP model was trained on raw RSSI values, the Kalman filter with R value equals to 1 yielded the lowest MAE of 2.86342 m, while the TWA-DGP model has the best MAE of 1.94439 m at R = 0.1. This shows that the noise in the output of the TWA-DGP is low compared to the output of the DGP, resulting in needing a lower noise measurement coefficient R.

Universiti Malaya

The differing optimal R values for the Kalman Filter when applied to raw DGP output (R = 1) versus TWA-DGP output (R = 0.1) provide insight into the noise characteristics of these estimates. The lower optimal R value for TWA-DGP suggests that the TWA technique effectively reduces noise in the position estimates, resulting in more reliable measurements that require less aggressive filtering.

This difference in optimal R values highlights the importance of properly tuning the Kalman Filter for each specific preprocessing technique. It also suggests that the TWA technique not only improves accuracy but also enhances the consistency of the estimates, allowing the Kalman Filter to place more trust in each measurement.

Table 4.8: MAE and RMSE values on the result4s of Kalman Filter with different R values used on output coordinates from DGP and TWA-DGP

	R value	**0.01**	**0.1**	**1**	**10**
DGP-KF	**MAE (m)**	3.95612	3.47434	2.86342	4.80262
	RMSE (m)	4.54630	3.99012	3.24485	5.23563
TWA-DGP-KF	**MAE (m)**	2.00502	1.94439	2.81333	6.38965
	RMSE (m)	2.33968	2.20489	3.08949	6.83976

The results show that Kalman Filtering can improve the positioning accuracy by smoothing the trajectory of the coordinate estimates and thus reduce the probability of obtaining large errors. The movement trajectory of the position estimates of DGP and TWA-DGP-KF were depicted in Figure 4.26 and Figure 4.27 respectively, the trajectory itself was represented by the blue lines.

In Figure 4.26, the trajectory appeared jagged and erratic, indicating significant noise or fluctuations in the position estimates. Instead of a smooth, continuous path, the trajectory exhibits abrupt changes in direction and numerous scattered points, suggesting that the DGP model alone may struggle to capture the underlying motion dynamics accurately. In contrast to this noisy trajectory, the application of the Kalman filter is

Universiti Malaya

expected to result in a much smoother and more realistic movement path. The Kalman filter can effectively smooth out the erratic fluctuations as observed in Figure 4.27.

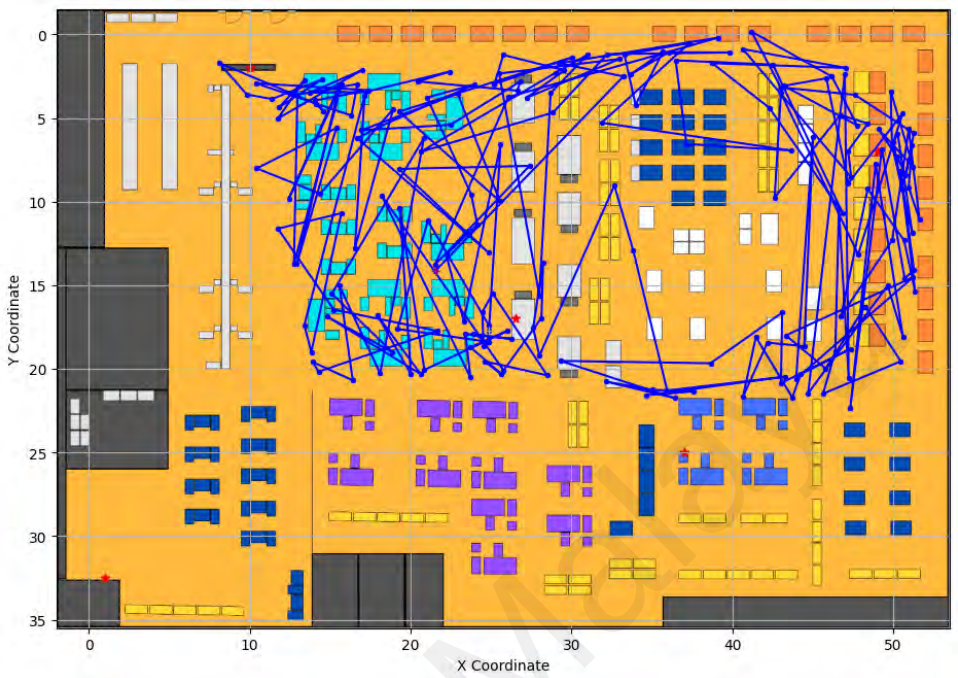

Figure 4.26: Movement trajectory of the DGP position estimates

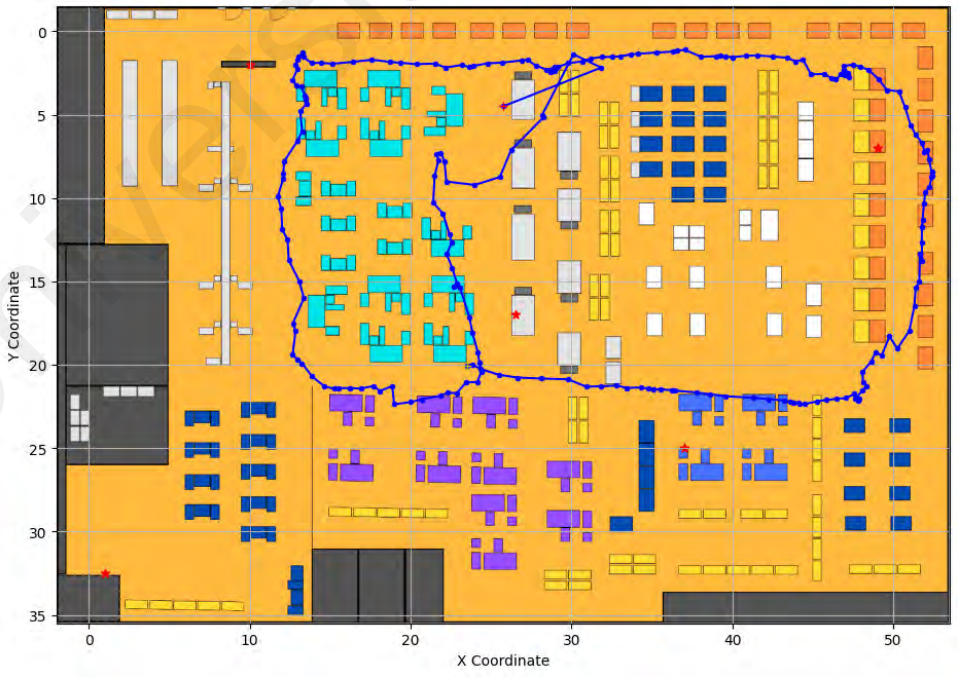

Figure 4.27: Movement trajectory of the TWA-DGP-KF position estimates

Universiti Malaya

4.4.3 Lane Constraint

The lane constraint method was applied to further refine the position estimates obtained from the positioning system, leveraging the known layout and traversable paths within the indoor environment. The building floor plan was segmented into a grid of tiles, and navigable lanes were defined as sequences of connected tile coordinates. Table 4.9 presents the MAE and RMSE for the positioning system with and without applying the lane constraint method, represented by DGP and DGP-LC.

Table 4.9: MAE and RMSE for the positioning system with and without applying the lane constraint method

	MAE (m)	**RMSE (m)**
DGP	4.94972	6.07725
DGP-LC	4.84624	6.42983

The application of lane constraints yielded improvements in the MAE metric, as position estimates with smaller errors were mapped onto the nearest lane coordinate, effectively enhancing their accuracy. However, this mapping process came at the cost of a slight increase in the RMSE. The RMSE deterioration indicates that lane constraints can exacerbate large errors. These erroneous estimates were effectively "dragged" onto the nearest feasible lane coordinate, potentially increasing the distance between the estimated and true positions.

Hence, the positioning accuracy, in terms of both MAE and RMSE, can be further improved by implementing techniques such as Temporal-Weighted RSSI averaging and Kalman filtering as mentioned in the previous subsections to remove larger errors before applying lane constraints. Table 4.10 shows the MAE and RMSE for the positioning system with and without applying the lane constraint method together with Temporal-Weighted RSSI Averaging and Kalman Filter and benchmarked by the pure DGP model.

Universiti Malaya

Table 4.10: MAE and RMSE for the positioning system with and without applying the lane constraint method together with TWA and KF

	MAE (m)	RMSE (m)
DGP	4.94972	6.07725
TWA-DGP-KF	1.94439	2.20489
TWA-DGP-KF-LC	1.57958	1.90308

The table indicates that augmenting the DGP model with TWA and Kalman Filtering significantly enhances the accuracy of position estimation under lane constraints. The further inclusion of lane constraints leads to the best results, showcasing the importance of leveraging contextual information to improve model performance.

4.4.4 Summary of Position Accuracy Enhancement Techniques

To comprehensively evaluate the effectiveness of the proposed position accuracy enhancement techniques, several configurations were explored by combining Temporal-Weighted RSSI Averaging (TWA), Kalman Filtering (KF), and Lane Constraints (LC). Table 4.11 presents a summary of the performance metrics, including the MAE and RMSE and the percentage improvement over the baseline DGP model.

Table 4.11: Performance of Position Accuracy Enhancement Techniques

Configuration	MAE (m)	MAE Improvement compared to DGP	RMSE (m)	RMSE Improvement compared to DGP
DGP	4.94972		6.07725	
DGP-LC	4.84624	2.09%	6.42983	-5.80%
DGP-KF	2.86342	42.15%	3.24485	46.61%
TWA-DGP	2.49319	49.63%	3.13971	48.34%
TWA-DGP-LC	2.19067	55.74%	2.96828	51.16%
TWA-DGP-KF	1.94439	60.72%	2.20489	63.72%
DGP-KF-LC	2.20631	55.43%	2.81086	53.75%
TWA-DGP-KF-LC	1.57958	68.09%	1.90308	68.69%

Universiti Malaya

The baseline DGP model, without any enhancement techniques, exhibited an MAE of 4.94972 meters and an RMSE of 6.07725 meters, serving as the reference for performance comparisons.

Applying Temporal-Weighted Averaging RSSI (TWA-DGP) led to improvements of 49.63 % in MAE and 48.34 % in RMSE compared to the baseline, demonstrating the effectiveness of this technique in mitigating noise and leveraging temporal dynamics in RSSI measurements.

The Kalman Filter (DGP-KF) provided more modest improvements, with a 42.15 % reduction in MAE and a 46.61 % reduction in RMSE, indicating its potential for incorporating motion models and further refining position estimates.

The combination of TWA and KF (TWA-DGP-KF) yielded significant enhancements, with an MAE improvement of 60.72 % and an RMSE improvement of 63.72 %, showcasing the synergistic effects of these complementary techniques.

Lane Constraints (TWA-DGP-LC and DGP-KF-LC) exhibited varying degrees of improvement, with the DGP-KF-LC configuration outperforming the TWA-DGP-LC configuration in terms of both MAE and RMSE. This highlights the importance of combining Lane Constraints with noise mitigation techniques and KF ability in reducing noise in the output coordinates.

However, the Lane Constraint method may introduce larger errors if the estimated points deviate significantly from the actual position. The Lane Constraint method is designed to improve positioning accuracy by restricting estimated locations to predefined paths or lanes. However, if the initial position estimation is inaccurate or if the constraints are too restrictive, the method can force the estimated position onto an incorrect path. This misalignment can lead to larger errors instead of improving accuracy.

Universiti Malaya

The configuration incorporating all three enhancement techniques (TWA-DGP-KF-LC) achieved the best overall performance, with a 68.09 % improvement in MAE and a 68.69 % improvement in RMSE compared to the baseline DGP model. This result underscores the effectiveness of integrating TWA, KF and LC in a comprehensive positioning system architecture as shown in Figure 4.28.

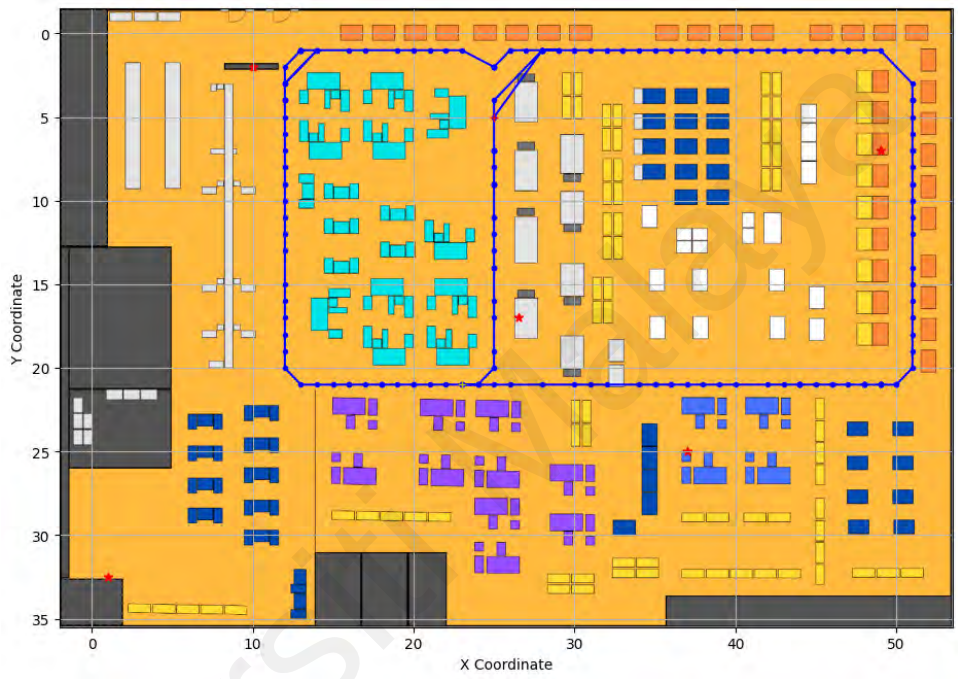

Figure 4.28: Movement trajectory of the TWA-DGP-KF-LC position estimates

In summary, the evaluation of various configurations demonstrates the potential for significantly enhancing position accuracy by leveraging the strengths of each proposed technique. This combination allows for a multi-layered approach to error reduction. The TWA and DGP provide a solid foundation of accurate position estimates, which are then refined by the KF to ensure temporal consistency. Finally, the LC step ensures that the estimates adhere to the physical layout of the environment.

University of Malaya

CHAPTER 5: CONCLUSION

This thesis has presented a comprehensive investigation into the development of a LoRa-based indoor positioning system tailored for the intricate and dynamic environments found in industrial production lines. The research objectives outlined in Chapter 1 have been systematically addressed, leading to the successful demonstration of the feasibility and effectiveness of utilizing LoRa technology for indoor positioning systems.

The research commenced with a thorough exploration of existing indoor positioning technologies and techniques, as detailed in Chapter 2. This review highlighted the limitations of traditional methods, particularly GPS, in indoor settings due to signal attenuation and multipath interference. The emergence of LoRa technology, with its long-range communication capabilities and robustness against interference, was identified as a promising candidate for addressing these challenges. The case studies of fingerprinting technique using machine learning were also studied.

The investigation into LoRa signal propagation characteristics revealed valuable insights into path loss, multipath fading, and small-scale fading effects. These findings, presented in Chapter 4, contributed to a deeper understanding of LoRa's behaviour in indoor environments and informed the development of effective positioning algorithms. The characterization of signal propagation provided a foundation for understanding the challenges and opportunities associated with LoRa-based positioning.

The methodology adopted in this research, as expounded in Chapter 3, involved a meticulous experimental setup within a real-world industrial production line. LoRa-enabled nodes were strategically deployed to collect radio signal data, which was then subjected to rigorous preprocessing to ensure data quality and consistency. A variety of

Universiti Malaya

machine learning algorithms, encompassing both classification and regression models, were employed to evaluate their performance in single-point estimation tasks.

The exploration of various machine learning techniques showcased the potential of these algorithms in mapping radio signal features to spatial coordinates. Notably, the evaluation of these methods across different datasets and feature sets provided valuable insights into their performance under varying conditions. The comparative analysis revealed the superior performance of Gaussian Process Regression (GPR) in achieving accurate and reliable position estimates.

Building upon the strengths of GPR, the thesis introduced Deep Gaussian Process (DGP) regression as a means of further enhancing positioning accuracy. The hierarchical nature of DGPs enabled the capture of complex non-linear relationships between radio signal parameters and location coordinates, leading to improved positioning accuracy and robustness. Through extensive experimentation and hyperparameter tuning, the DGP model was optimized to achieve improved accuracy compared to GPR.

To address the limitations of single-point estimation and further enhance precision, spatial-temporal techniques were used. Temporal-Weighted RSSI Averaging (TWA) and Kalman filtering were implemented to smooth out fluctuations in position estimates and provide a more continuous tracking experience. Additionally, a lane constraint method was introduced to refine the positioning of objects within predefined lanes, ensuring their accurate localization along production lines. These techniques effectively mitigated RSSI fluctuations, noise, and outliers, resulting in more accurate, stable, and contextually aware position estimates.

The culmination of these efforts was the successful implementation of a proof-of-concept system that integrated the DGP model with temporal filtering and lane constraints.

Universiti Malaya

This system demonstrated its ability to accurately track the movement of trolleys within the industrial production line, providing real-time location information that could be visualized through a user-friendly interface. This real-world demonstration showcased the potential of LoRa-based indoor positioning in industrial settings.

The findings of this research contribute significantly to the field of indoor positioning by showcasing the potential of LoRa technology in conjunction with advanced machine learning techniques. The integration of temporal filtering and lane constraints further enhances the system's robustness and practicality in real-world applications.

This research not only advances indoor positioning technologies but also opens new possibilities for various applications, including asset tracking, personnel monitoring, and navigation assistance. The developed methodologies and insights gained from this study pave the way for future advancements in the field and offer practical solutions for real-world challenges.

5.1 Future Works

Future work in this area presents several promising avenues for further research and development. The integration of additional sensor data, such as inertial measurement units (IMUs) or ambient light sensors, could significantly enhance positioning accuracy and reliability by providing complementary information to the LoRa signals. This multi-modal approach could help mitigate environmental factors that affect LoRa performance.

Implementation of active learning techniques could optimize the data collection process, allowing the system to intelligently select the most informative data points for model training, thereby improving efficiency and reducing the need for extensive manual data collection. Transfer learning methodologies could be explored to adapt pre-trained

Universiti Malaya

models to new environments or different types of indoor spaces, potentially reducing the setup time and effort required for deployment in diverse settings.

Traditional LoRa systems operate on a fixed frequency, which may suffer from interference and multipath fading in dense indoor environments. Future work could explore the potential of multi-frequency LoRa, where multiple frequency bands are utilized adaptively based on environmental conditions. By employing frequency-hopping techniques, the system could dynamically switch between different channels to avoid interference and maintain reliable communication. This approach would improve signal stability, reduce packet loss, and enhance overall positioning accuracy in challenging indoor scenarios.

The exploration of multi-sensor fusion techniques to combine LoRa with other complementary technologies, such as Ultra-Wideband (UWB) or Bluetooth Low Energy (BLE), could leverage the strengths of each technology to create a more robust and versatile positioning system.

Energy efficiency is a crucial factor in ensuring the long-term sustainability of IoT-based positioning systems, particularly for large-scale deployments. Future research could focus on optimizing the power consumption of LoRa nodes by implementing adaptive transmission power control and dynamic duty cycling. These techniques allow devices to intelligently adjust their transmission power and frequency based on environmental conditions and movement patterns, thereby reducing energy waste. Additionally, integrating energy-harvesting solutions, such as solar panels or kinetic energy systems, could extend the operational lifespan of deployed nodes and minimize maintenance costs.

Universiti Malaya

To improve the responsiveness and scalability of the positioning system, real-time data processing techniques need to be explored. One potential direction is the integration of edge computing, where lightweight deep learning models are deployed on edge devices such as microcontrollers or embedded systems. By processing localization data directly at the edge, latency can be reduced, and reliance on cloud-based computation minimized. Techniques such as model quantization and knowledge distillation can be leveraged to ensure that deep learning models remain computationally efficient while maintaining high accuracy.

As LoRa-based indoor positioning systems handle sensitive location data, ensuring security and privacy is essential. Future work could explore the implementation of robust encryption techniques to protect data transmissions from eavesdropping and unauthorized access. End-to-end encryption schemes, coupled with secure authentication mechanisms such as cryptographic key exchanges, can enhance the security of the system. Furthermore, privacy-preserving localization techniques, such as federated learning and homomorphic encryption, could be employed to allow collaborative model training while keeping raw location data private.

Finally, increasing the scalability of the system to accommodate other areas and more devices would be crucial for its widespread adoption. This could involve optimizing the network architecture, improving data processing algorithms, and developing more efficient communication protocols to handle increased data loads without compromising performance. These future directions aim to enhance the system's accuracy, adaptability, and practical applicability across various indoor positioning scenarios.

Universiti Malaya

REFERENCES

Abdelghani, B., & Qiang, G. (2017). Hybrid rss-based fingerprinting positioning method with segmentation and knn in cellular network. 2017 3rd IEEE International Conference on Control Science and Systems Engineering (ICCSSE),

Al-Saman, A., Cheffena, M., Elijah, O., Al-Gumaei, Y. A., Abdul Rahim, S. K., & Al-Hadhrami, T. (2021). Survey of Millimeter-Wave Propagation Measurements and Models in Indoor Environments. *Electronics*, *10*(14), 1653. https://www.mdpi.com/2079-9292/10/14/1653

Alhammadi, A., Alias, M. Y., Tan, S.-W., & Sapumohotti, C. (2017). An enhanced localisation system for indoor environment using clustering technique. *Int. J. Comput. Vis. Robotics*, *7*(1/2), 83-98.

Alraih, S., Alhammadi, A., Shayea, I., & Al-Samman, A. M. (2017). Improving accuracy in indoor localization system using fingerprinting technique. 2017 international conference on information and communication technology convergence (ICTC),

Anjum, M., Khan, M. A., Hassan, S. A., Mahmood, A., & Gidlund, M. (2019). Analysis of RSSI fingerprinting in LoRa networks. 2019 15th International Wireless Communications & Mobile Computing Conference (IWCMC),

Anjum, M., Khan, M. A., Hassan, S. A., Mahmood, A., Qureshi, H. K., & Gidlund, M. (2020). RSSI Fingerprinting-based Localization Using Machine Learning in LoRa Networks. *IEEE Internet of Things Magazine*, *3*(4), 53-59.

Azmi, N. A., Samsul, S., Yamada, Y., Yakub, M. F. M., Ismail, M. I. M., & Dziyauddin, R. A. (2018). A survey of localization using rssi and tdoa techniques in wireless sensor network: System architecture. 2018 2nd International Conference on Telematics and Future Generation Networks (TAFGEN),

Bahl, P., & Padmanabhan, V. N. (2000). RADAR: An in-building RF-based user location and tracking system. Proceedings IEEE INFOCOM 2000. Conference on computer communications. Nineteenth annual joint conference of the IEEE computer and communications societies (Cat. No. 00CH37064),

Barreto, L., Amaral, A., & Pereira, T. (2017). Industry 4.0 implications in logistics: an overview. *Procedia Manufacturing*, *13*, 1245-1252.

Batalla, J. M., Mavromoustakis, C. X., Mastorakis, G., Xiong, N. N., & Wozniak, J. (2020). Adaptive positioning systems based on multiple wireless interfaces for industrial IoT in harsh manufacturing environments. *IEEE Journal on Selected Areas in Communications*, *38*(5), 899-914.

Universiti Malaya

Belmonte-Hernández, A., Hernández-Peñaloza, G., Gutiérrez, D. M., & Alvarez, F. (2019). SWiBluX: Multi-Sensor Deep Learning Fingerprint for precise real-time indoor tracking. *IEEE Sensors Journal*, *19*(9), 3473-3486.

Bornholdt, L., Kaven, S., & Skwarek, V. (2021). Adaptive procedure for indoor localization using LoRa devices. 2021 International Conference on Indoor Positioning and Indoor Navigation (IPIN),

Chen, L., Li, B., Zhao, K., Rizos, C., & Zheng, Z. (2013). An improved algorithm to generate a Wi-Fi fingerprint database for indoor positioning. *Sensors*, *13*(8), 11085-11096.

Chen, M., Zhao, H., Shi, C., Chen, X., & Niu, D. (2023). Multi-scene LoRa positioning algorithm based on Kalman filter and its implementation on NS3. *Ad Hoc Networks*, *141*, 103097.

Committee, L. A. S. (2018). *LoRaWan Geolocation Whitepaper*. LoRa Alliance™ Strategy Committee. https://lora-alliance.org/wp-content/uploads/2020/11/geolocation_whitepaper.pdf

Dahlgren, E., & Mahmood, H. (2014). Evaluation of indoor positioning based on Bluetooth Smart technology.

Fang, S.-H., Hsu, Y.-T., & Kuo, W.-H. (2011). Dynamic fingerprinting combination for improved mobile localization. *IEEE Transactions on Wireless Communications*, *10*(12), 4018-4022.

Géron, A. (2019). *Hands-On Machine Learning with Scikit-Learn, Keras, and TensorFlow: Concepts, Tools, and Techniques to Build Intelligent Systems*. O'Reilly Media.

Gu, C., Jiang, L., & Tan, R. (2018). Lora-based localization: Opportunities and challenges. *arXiv preprint arXiv:1812.11481*.

Guan, R., Zhang, A., Li, M., & Wang, Y. (2021). Measuring uncertainty in signal fingerprinting with gaussian processes going deep. 2021 International Conference on Indoor Positioning and Indoor Navigation (IPIN),

Ha, G. Y., Seo, S. B., Oh, H. S., & Jeon, W. S. (2019). LoRa ToA-Based Localization Using Fingerprint Method. 2019 International Conference on Information and Communication Technology Convergence (ICTC),

Universiti Malaya

Hayward, S., van Lopik, K., Hinde, C., & West, A. A. (2022). A survey of indoor location technologies, techniques and applications in industry. *Internet of Things*, *20*, 100608.

Henriksson, R. (2016). *Indoor positioning in LoRaWAN networks*

Hoang, M. T., Yuen, B., Dong, X., Lu, T., Westendorp, R., & Reddy, K. (2019). Recurrent neural networks for accurate RSSI indoor localization. *IEEE Internet of Things Journal*, *6*(6), 10639-10651.

Holmström, J., Liotta, G., & Chaudhuri, A. (2017). Sustainability outcomes through direct digital manufacturing-based operational practices: A design theory approach. *Journal of Cleaner Production*, *167*, 951-961.

Hu, K., Gu, C., & Chen, J. (2022). LTrack: a LoRa-based indoor tracking system for mobile robots. *IEEE Transactions on Vehicular Technology*, *71*(4), 4264-4276.

Islam, B., Islam, M. T., Kaur, J., & Nirjon, S. (2019). Lorain: Making a case for lora in indoor localization. 2019 IEEE International Conference on Pervasive Computing and Communications Workshops (PerCom Workshops),

Islam, B., Islam, M. T., & Nirjon, S. (2017). Feasibility of LoRa for indoor localization. *online, from semanticscholar. org*, 1-11.

Ji, W., Zhao, K., Zheng, Z., Yu, C., & Huang, S. (2021). Multivariable fingerprints with random forest variable selection for indoor positioning system. *IEEE Sensors Journal*, *22*(6), 5398-5406.

Khan, F. U., Awais, M., Rasheed, M. B., Masood, B., & Ghadi, Y. (2021). A comparison of wireless standards in iot for indoor localization using loPy. *Ieee Access*, *9*, 65925-65933.

Kim Geok, T., Zar Aung, K., Sandar Aung, M., Thu Soe, M., Abdaziz, A., Pao Liew, C., Hossain, F., Tso, C. P., & Yong, W. H. (2020). Review of indoor positioning: Radio wave technology. *Applied Sciences*, *11*(1), 279.

Kim, K., Li, S., Heydariaan, M., Smaoui, N., Gnawali, O., Suh, W., Suh, M. J., & Kim, J. I. (2021). Feasibility of LoRa for smart home indoor localization. *Applied Sciences*, *11*(1), 415.

Kingma, D. P., & Ba, J. (2014). Adam: A method for stochastic optimization. *arXiv preprint arXiv:1412.6980*.

Universiti Malaya

Kirch, M., Poenicke, O., & Richter, K. (2017). RFID in logistics and production–Applications, research and visions for smart logistics zones. *Procedia Engineering*, *178*, 526-533.

Kodippili, N., & Dias, D. (2010). Integration of fingerprinting and trilateration techniques for improved indoor localization. 2010 Seventh International Conference on Wireless and Optical Communications Networks-(WOCN),

Kułakowski, P., Vales-Alonso, J., Egea-López, E., Ludwin, W., & García-Haro, J. (2010). Angle-of-arrival localization based on antenna arrays for wireless sensor networks. *Computers & Electrical Engineering*, *36*(6), 1181-1186.

Laaraiedh, M., Yu, L., Avrillon, S., & Uguen, B. (2011). Comparison of hybrid localization schemes using RSSI, TOA, and TDOA. 17th European Wireless 2011-Sustainable Wireless Technologies,

Lam, K.-H., Cheung, C.-C., & Lee, W.-C. (2019). Rssi-based lora localization systems for large-scale indoor and outdoor environments. *IEEE Transactions on Vehicular Technology*, *68*(12), 11778-11791.

Lazaro, A., Lazaro, M., & Villarino, R. (2021). Room-Level Localization System Based on LoRa Backscatters. *Ieee Access*, *9*, 16004-16018.

Li, C., Xu, Q., Gong, Z., & Zheng, R. (2017). TuRF: Fast data collection for fingerprint-based indoor localization. 2017 international conference on indoor positioning and indoor navigation (IPIN),

Li, Y., Zhuang, Y., Hu, X., Gao, Z., Hu, J., Chen, L., He, Z., Pei, L., Chen, K., & Wang, M. (2020). Toward location-enabled IoT (LE-IoT): IoT positioning techniques, error sources, and error mitigation. *IEEE Internet of Things Journal*, *8*(6), 4035-4062.

LILYGO®. (n.d., 2025). *LoRa32 V2.1_1.6*. LILYGO®.

Lu, W.-C., Cheng, Y.-C., & Fang, S.-H. (2016). A study of singular value decomposition for wireless LAN location fingerprinting. 2016 IEEE Second International Conference on Multimedia Big Data (BigMM),

Manzoni, P., Calafate, C. T., Cano, J.-C., & Hernández-Orallo, E. (2019). Indoor vehicles geolocalization using LoRaWAN. *Future Internet*, *11*(6), 124.

Marquez, L. E., Bahillo, A., Calle, M., & De Miguel, I. (2023). Effects of Body Shadowing in LoRa Localization Systems. *Ieee Access*, *11*, 9521-9528.

Universiti Malaya

Mendoza-Silva, G. M., Torres-Sospedra, J., & Huerta, J. (2019). A meta-review of indoor positioning systems. *Sensors*, *19*(20), 4507.

Molina, B., Olivares, E., Palau, C. E., & Esteve, M. (2018). A multimodal fingerprint-based indoor positioning system for airports. *Ieee Access*, *6*, 10092-10106.

Nabati, M., & Ghorashi, S. A. (2023). A real-time fingerprint-based indoor positioning using deep learning and preceding states. *Expert Systems with Applications*, *213*, 118889.

Ng, T. J., Kumar, N., & Othman, M. (2024). LoRa-Based Indoor Positioning in Dynamic Industrial Environments Using Deep Gaussian Process Regression and Temporal-Based Enhancements. *Ieee Access*, *12*, 165298-165313.

Nguyen, D. K., Duong, T. H., Nguyen, L. C., & Hoang, M. K. (2024). Performance Enhancement of Wi-Fi Fingerprinting-based Indoor Positioning using Truncated Singular Value Decomposition and LSTM Model [Article]. *International Journal of Advanced Computer Science and Applications*, *15*(5), 281-288,

Pichaimani, V., & Manjula, K. (2022). A machine-learning framework to improve wi-fi based indoor positioning. *Intelligent Automation & Soft Computing*, *33*(1), 383-397.

Podevijn, N., Plets, D., Trogh, J., Karaagac, A., Haxhibcqiri, J., Hoebeke, J., Martens, L., Suanet, P., & Joseph, W. (2018). Performance comparison of RSS algorithms for indoor localization in large open environments. 2018 International Conference on Indoor Positioning and Indoor Navigation (IPIN),

Qin, F., Zuo, T., & Wang, X. (2021). Ccpos: Wifi fingerprint indoor positioning system based on cdae-cnn. *Sensors*, *21*(4), 1114.

Sadowski, S., & Spachos, P. (2018). Rssi-based indoor localization with the internet of things. *Ieee Access*, *6*, 30149-30161.

Sahar, A., & Han, D. (2018). An LSTM-based indoor positioning method using Wi-Fi signals. Proceedings of the 2nd International Conference on Vision, Image and Signal Processing,

Sakpere, W., Adeyeye-Oshin, M., & Mlitwa, N. B. (2017). A state-of-the-art survey of indoor positioning and navigation systems and technologies. *South African Computer Journal*, *29*(3), 145-197.

Universiti Malaya

Savazzi, P., Goldoni, E., Vizziello, A., Favalli, L., & Gamba, P. (2019). A Wiener-based RSSI localization algorithm exploiting modulation diversity in LoRa networks. *IEEE Sensors Journal*, *19*(24), 12381-12388.

Silva, I., Pendão, C., & Moreira, A. (2021). Real-world deployment of low-cost indoor positioning systems for industrial applications. *IEEE Sensors Journal*, *22*(6), 5386-5397.

Simka, M., & Polak, L. (2022). On the RSSI-based indoor localization employing LoRa in the 2.4 GHz ISM band. *Radioengineering*, *31*(1), 135-143.

Tang, Z., Li, S., Kim, K. S., & Smith, J. (2022). Multi-output Gaussian process-based data augmentation for multi-building and multi-floor indoor localization. 2022 IEEE International Conference on Communications Workshops (ICC Workshops),

Teng, F., Tao, W., & Own, C.-M. (2018). Localization reliability improvement using deep Gaussian process regression model. *Sensors*, *18*(12), 4164.

Wang, J., & Park, J. G. (2020). A novel indoor ranging algorithm based on a received signal strength indicator and channel state information using an extended kalman filter. *Applied Sciences*, *10*(11), 3687.

Wang, L., Luo, H., Wang, Q., Shao, W., & Zhao, F. (2021). A Hierarchical LSTM-Based Indoor Geomagnetic Localization Algorithm. *IEEE Sensors Journal*, *22*(2), 1227-1237.

Wang, X., Wang, X., Mao, S., Zhang, J., Periaswamy, S. C., & Patton, J. (2020). Indoor radio map construction and localization with deep Gaussian processes. *IEEE Internet of Things Journal*, *7*(11), 11238-11249.

Xingli, G., Yaning, L., & Ruihui, Z. (2018). Indoor positioning technology based on deep neural networks. 2018 Ubiquitous Positioning, Indoor Navigation and Location-Based Services (UPINLBS),

Yılmaz Börekçi, D., Büyüksaatçı Kiriş, S., & Batmaca, S. (2020). Analysis of enterprise resource planning (ERP) system workarounds with a resilience perspective. *Continuity & Resilience Review*, *2*(2), 131-148.

Youssef, M., & Agrawala, A. (2005). The Horus WLAN location determination system. Proceedings of the 3rd international conference on Mobile systems, applications, and services,

Universiti Malaya

Zafari, F., Gkelias, A., & Leung, K. K. (2019). A survey of indoor localization systems and technologies. *IEEE Communications Surveys & Tutorials*, *21*(3), 2568-2599.

Universiti Malaya